2010

Preparation and physicochemical characterization of Eudragit RL100 nanosuspension with potential for ocular delivery of sulfacetamide

Bivash Mandal
The University of Toledo

A Thesis

entitled

Preparation and Physicochemical Characterization of Eudragit® RL100 Nanosuspension with potential for Ocular Delivery of Sulfacetamide

by

Bivash Mandal

Submitted to the Graduate Faculty as partial fulfillment of the requirements for
the Master of Science Degree in Pharmaceutical Sciences
with Industrial Pharmacy Option

_____
Kenneth S. Alexander, Ph.D., Committee Chair

_____
Jerry Nesamony, Ph.D., Committee Member

_____
Curtis D. Black, Pharm.D., Committee Member

_____
Patricia R. Komuniecki, Dean
College of Graduate Studies

The University of Toledo

May 2010

An Abstract of

Preparation and Physicochemical Characterization of Eudragit® RL100 Nanosuspension with potential for Ocular Delivery of Sulfacetamide

by

Bivash Mandal

As partial fulfillment of the requirements of the
Master of Science Degree in Pharmaceutical Sciences with Industrial Pharmacy Option

The University of Toledo
May 2010

Eudragit® nanoparticles appear to be a suitable inert carrier for ophthalmic drug delivery due to their capability to form nanodispersion with smaller particle size, positive surface charge, good stability, biocompatibility and absence of any irritant effect on the cornea, iris, and conjunctiva. Sulfacetamide loaded polymeric nanosuspension was prepared from an inert polymer resin (Eudragit® RL 100) with the aim of improving the availability of sulfacetamide at the intraocular level and thereby reducing the frequency of dosing for bacterial infections in the eye. Nanosuspensions were prepared by the solvent displacement method using acetone and 1% (w/v) Pluronic® F108 solution. Drug to polymer ratio was chosen at four levels: 10/100 (B1), 20/100 (B2), 30/100 (B3), 40/100 (B4) (by weight). Characterization of nanosupension was performed by measuring particle size, zeta potential, Fourier Transform infrared spectra (FTIR), Differential Scanning Calorimetry (DSC), Powder X-Ray Diffraction (PXRD), drug entrapment efficiency and in vitro release. In addition, freeze drying, redispersibility and short term stability study at room temperature and at 4^0C were performed. Spherical, uniform

particles (size below 500 nm) with polydispersity index range of 0.414 to 0.67 and positive zeta potential were obtained. Positive surface charge can allow a longer residence time of nanoparticles on the cornea surface, with a consequence slower drug release and higher drug concentrations in the aqueous humor, compared to classical eye drop. No significant drug polymer interaction was observed in the solid state characterization of freeze dried nanosuspension using DSC, PXRD, FTIR. Drug entrapment efficiency was found to be in the range of about 28% to about 35%. In order to increase drug entrapment efficiency, selected batch was chosen to study the effect of changing polymer content, pH of external media and incorporation of polymethyl methacrylate (PMMA) on drug entrapment efficiency. Changing the external phase pH and incorporation of PMMA significantly increased drug entrapment efficiency of nanoparticles. No significant change in average particle size was observed after storage at room temperature and at 4^0C. Freeze dried nanosuspesnions were easily redispersed after manual hand shaking. Both batch of B3 containing 5% sucrose and 5% mannitol as cryoprotectant exhibited good redispersibility in water. The results indicate that formulation of Sulfacetamide in Eudragit® RL 100 nanosuspension could be utilized as potential delivery system for treating ocular bacterial infections.

To my Baba, Maa, Bordi, Paltuda, Chotdi, Bimanda, Satyam, Sradha and Chandrima.

Acknowledgements

I would like to express my deepest gratitude and heartfelt thanks to my instructor and advisor, Dr. Kenneth Alexander for his constructive guidance, intellectual support and his inspiring words. Also, I would like to thank my co-advisor Dr. Alan Riga, for his thoughtful input and help in my research.

I owe special thanks to my committee members Dr. Nesamony and Dr. Black for their valuable advice and support. I express my heartiest gratitude to Mr. Buddhadev Layek for his help with DLS instrument. My appreciation goes to Dr. Burckel for helping me with the PXRD and SEM. I also convey thanks to Dr. Lawrence of CMSC for instrumental instruction with TEM. I express my gratitude to Dr Wall, Dr Server, Dr Slama, Dr Trendell for their help and support. Furthermore, I am also grateful to my lab mates: Ranajoy; Arpana; Girish; Niraja; Carrie; Ermias; Khushboo; Shikha; Sanjeev; Sriramya; Ishan; Meghavi; Priti and Prathyusha.

Most importantly, I would like to thank my family members for their support and care. Baba and Maa, I thank you for all your love and concern throughout these years. Thanks to my sisters, brothers-in-law for their constant encouragement.

Finally, I would like to thank Chandrima, my fiancée, for her love, encouragement and support throughout these two years of my graduate study.

Table of Contents

List of Tables

List of Figures

Chapter One

Introduction

An ideal drug therapy achieves effective concentration of drug at the target for a specified period of time in order to minimize general and local side effects. An exciting challenge for developing suitable drug delivery systems targeted for ocular diseases is one of today's major focuses of pharmaceutical scientists. Conventionally, most ocular diseases or disorders are treated with water-soluble drugs in aqueous solution while water-insoluble drugs in ointments or aqueous suspension (1). However, there are several disadvantages such as: frequent installation of highly concentrated solutions due to rapid tear turnover and precorneal loss (2); large volume of the instilled dose (20-50 µl vs 7-8 µl of the tear film (3); irritation caused by drug penetration; drug solubility and stability in the eye fluids, difficulty in passing the blood-corneal barrier (4). The precorneal half-life is considered to be 2-3 minutes after installation of an excess volume of fluid (5). Typically less than 5% of the topically applied drug penetrates the cornea and reaches the posterior segment of the eye (6). A major fraction of the instilled dose is absorbed systematically via the nasolachrymal duct. This may cause systemic adverse effects such as trachycardia, hypertension, bronchial asthama e.g. Timolol ophthalmic solution (7).

There are several new ophthalmic drug delivery systems under investigation such as: hydrogels (8); microparticles (9); nanoparticles (10); liposomes (11); collagen shields (12); ocular inserts/discs (13); dendrimers (14); and transcorneal iontophoresis (15). Nanoparticles have been found to be the most promising of all the formulations developed over the past 25 years of intense research in ocular therapeutics due to their sustained release and prolonged therapeutic benefit. Polymeric nanoparticles are also able to target diseases in the posterior segment of the eye such as age-related macular degeneration, cytomegalovirus retinitis, diabetic retinopathy, posterior uveitis and retinitis pigmentosa (16). Nanoparticles are solid, submicron, colloidal particles ranging in size from 10 to 1000 nm, in which drug can be dissolved, entrapped, adsorbed or covalently attached (17). These colloidal particles can be applied in the liquid form just like eye drops and reduce discomfort caused by application of semisolid ointments. They are patient friendly due to less frequent application, extended duration of retention in the extraocular portion without blurring vision.

Sulfacetamide is a sulfonamide antibiotic used to treat pink eye (conjunctivitis) (18), blepheritis (infection in the eye lid) (19), trachoma (leading cause of infectious blindness globally) (20), corneal ulcer (21) and other ocular diseased conditions (22). They are bacteriostatic in nature and inhibit bacterial synthesis of dihydrofolic acid by preventing condensation of pteridine with aminobenzoic acid through competitive inhibition of the enzyme dihydropteroate sunthetase (23). The drug is marketed as Ophthalmic solution of its sodium salt, in a USP concentration of 10% (w/v) under the brand name Bleph®-10.

The usual adult dose for conjunctivitis is 1 to 2 drops into the conjunctival sac every 2 to 3 hours for 7 to 10 days (24). The drug has an ionization constant of 5.4 and an elimination half-life of 7 to 13 hours (24).

Polymeric nanosuspensions, prepared from Eudragit® RL 100 and RS 100, have been investigated extensively for the ocular delivery of ibuprofen(25, 26), flurbiprofen (27, 28), cloriocromene (29), piroxicam(30), methyl prednisolone (31), and amphotericin B (32). They are cationic copolymers of methacrylate with 4-12% quaternary ammonium groups. They are inert polymer resins, insoluble at physiologic pH but have swelling properties. They are approved by USFDA as a excipient for controlled drug delivery. Due to their capability to form nanodispersions with smaller particle size, positive surface charge, good stability, absence of any irritant effect on the cornea, iris, and conjunctiva, Eudragit® nanoparticles appear to be a suitable inert carrier for ophthalmic drug delivery.

The most simple method to prepare drug loaded nanoparticles is the nanoprecipitation or solvent displacement method, developed by Fessi et al (33). The method is based on the interfacial deposition of a polymer following displacement of a semi-polar solvent miscible with water. The technique is easy, less complex, less energy consuming as well as widely applicable without any additives for the manufacturing of defined nanospheres (34). However, entrapment of hydrophilic drug substances is very difficult in this method due to the low affinity of the drug and polymer. Ideally, nanoparticles with high drug entrapment efficiency will reduce the quantity of carrier required for the administration of a sufficient amount of drug at the target site, as well as drug wastage during

manufacturing. There are several methods already reported in the literature to modify drug entrapment efficiency utilizing the nanoprecipitaion method. These include: changing the pH of the inner/external phase; addition of excipients (fatty acids, oligomers); replacing the salt form of the drug with the base form; and the addition of salt to the aqueous phase (35, 36).

Currently, no attempt has been made to encapsulate sulfacetamide inside a polymeric nanoparticulate carrier which could facilitate the drug delivery to the ocular surface. Sensoy et al (37) has recently reported effectiveness of the treatment of ocular keratis in rabbit eye using bioadhesive sulfacetamide sodium microspheres consisting of pectin, polycarbophil and hydroxypropylmethyl cellulose. The observed in vivo corneal uptake of drug loaded polymeric nanoparticles was reported to be higher compared to microparticles after topical application to the albino rabbit eye (38).

Therefore, an attempt was made to prepare and characterize Sulfacetamide loaded Eudragit® RL 100 nanosuspensions intended for the treatment of ocular infections. Nanosuspensions were prepared by the solvent displacement method using acetone and 1 % (w/v) Pluronic® F108 solution. Physicochemical characterization of the nanosuspension was performed by measuring particle size, zeta potential, drug entrapment efficiency and in vitro drug release. Solid state characterization of the freeze dried nanosuspension was performed by Fourier Transform InfraRed (FTIR), Differential Scanning Calorimetry (DSC) and Powder X-Ray Diffraction (PXRD). These techniques allow us to understand the thermal behavior, drug crystallinity and possible occurance of

drug polymer interaction for nanosuspension. The effect of changing polymer content, pH of the external media, addition of polymethyl methacrylate (PMMA) on drug entrapment efficiency was studied for the selected batch. Freeze drying and redispersibility of the lyophilized samples were performed. Short term stability for 1 month for the selected batch was performed. The delivery system was intended to enhance ocular availability without blurring vision and reducing the frequency of dosing in conjunctivitis leading to patience compliance. Positive surface charge of nanoparticles can allow longer residence time for the drug on the eye surface by increasing the interaction of nanoparticles with the glycoprotein of the cornea and conjunctiva. It can form a precorneal depot resulting in the prolonged release of the bound drug from nanoparticles.

Chapter Two

Nanoparticulate Drug Delivery System

2.1. Introduction

Nanoparticles have become one of the most active areas of research in the field of drug delivery due to their ability to deliver drugs to the right place, at appropriate times, and in the right dosage (1). They have received considerable attention over the past 20 years due to their advantages compared to other drug delivery systems. These advantages include: targeted delivery of drugs to the specific site to minimize toxicity; improved bioavailability by reducing fluctuations in therapeutic ranges; improved stability of drugs against enzymatic degradation; sustained and controlled release effect that reduces dosing frequency with improved patience compliance; and the ease of administering through various routes including oral, nasal, pulmonary, intraocular, parenteral and transdermal (2).

Nanotechnology focuses on synthesizing biocompatible nanocomposites such as nanoparticles, nanocapsules, micellar systems (3) and nanoconjugates (4) for delivering small molecular weight drug as well as macromolecular therapeutic agents. Nanoparticles

can be defined as solid, sub-micron, colloidal particles ranging in size from 10 nm to 1000 nm in diameter, generally but not necessarily made of natural or synthetic polymers, in which drugs can be adsorbed, entrapped, encapsulated or covalently attached and are produced by mechanical or chemical means (5). The term "Nanoparticles" includes – Nanocapsule (Reservoir device) in which the drug is confined to an aqueous or oily core surrounded by a shell-like wall and Nanosphere (Monolithic/matrix device) in which the drug is adsorbed, dissolved, or dispersed throughout the matrix (6) as seen in Figure 2.1. Depending on the type of material or carrier used, four broad classes of nanoparticles are recognized: Polymeric nanoparticles (2), Lipid based nanoparticles (7), Metal based nanoparticles (8) and Biological nanoparticles (9).

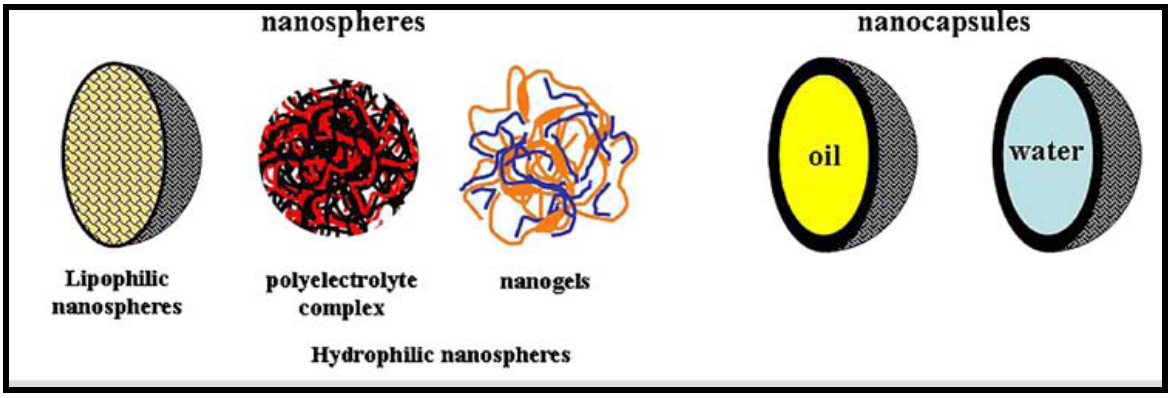

Figure 2.1: Structure of the polymeric nanospheres and nanocapsules (10)

2.1.1 Advantages over Microparticles

- They have higher intracellular uptake compared to micro particles. (1,11)

- They are better suited for I.V. delivery since the smallest blood capillaries in the body is about 5-6 μm.

2.1.2 Advantages over Liposomes (12)**:**

- They have better stability in biological fluids and during storage
- Their preparation is more amenable to scale up
- They have the unique ability to create a controlled release product

2.1.3 Materials used for preparation of nanoparticles

Nanoparticles can be prepared from a variety of materials such as metals (silver, gold, platinum, silicon) (8), as well as polymers (10) and lipids (7). Researchers have developed virus based nanoparticles for tissue-specific targeting and imaging agents *in vivo* (9). Potential improvements in the field of polymer chemistry have made polymers the most suitable carrier for delivering small and macromolecules. Polymeric materials can be classified broadly as natural polymers and synthetic polymers (Table 2.1).

The selection of materials for preparing nanoparticles depends upon consideration of the following factors (2):

- Size and surface characteristics of the particle desired.
- Aqueous solubility and stability of drugs or active ingredients.
- Degree of biodegradability, biocompatibility and toxicity.
- Drug release profile desired.
- Antigenicity of the polymers.

Table 2.1: Most widely used polymers for preparing nanoparticles in drug delivery (10)

Material	Full name	Abbreviation or commercial names*
Synthetic homopolymers	Poly (lactide)	PLA
	Poly (lactide-co-glycolide)	PLGA
	Poly (epsilon-caprolactone)	PCL
	Poly (isobutylcyanoacrylate)	PICBA
	Poly (isohexylcyanoacrylate)	PIHCA
	Poly (n-butylcyanoacrylate)	PBCA
	Poly (acrylate) and Poly(mathacrylate)	Eudragit*
Natural polymers	Chitosan	
	Alginate	
	Gelatin	
	albumin	
Copolymers	Poly (lactide)- poly (ethylene glycol)	PLA- PEG
	Poly (lactide-co-glycolide)- poly (ethylene glycol)	PLGA-PEG
	Poly (epsilon-caprolactone)- poly (ethylene glycol)	PCL-PEG
	Poly (hexadecylcyanoacrylate-co-poly (ethylene glycol) cyanoacrylate)	Poly (HDCA-PEGCA)
Colloid stabilisers	Dextran	
	Pluronic F68	F68
	Poly (vinyl alcohol)	PVA
	Co polymers (see above)	
	Tween®20 and Tween® 80	

2.2. Methods for the preparation of nanoparticles

2.2.1 Dispersion of preformed polymers

2.2.1.1. Emulsification-solvent evaporation

The emulsification-solvent evaporation method was the first method used to prepare biodegradable and injectable lattices by Gurny et al (13). Briefly, both the drug and polymer are dissolved in a volatile, water immiscible organic solvent such as dicholoro-

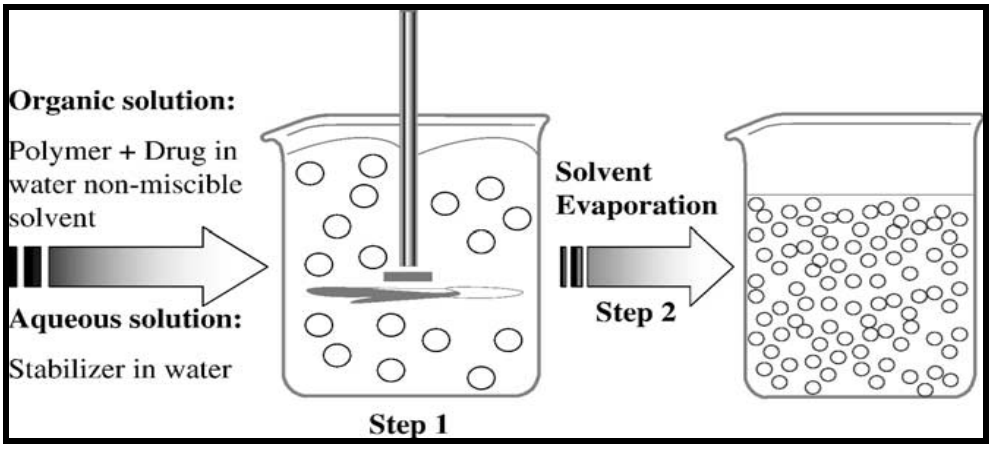

Figure 2.2: Schematic representation of the emulsification-solvent evaporation method (25)

-methane, chloroform or ethyl acetate. The organic phase is then emulsified as nanodroplets in an aqueous surfactant (such as Polyvinyl alcohol, Pluronic etc.) solution using high energy homogenizer or sonicator (14). The polymer precipitates as nanospheres and subsequently the organic phase is evaporated using a rotary evaporator or by continuous stirring (15) as represented in Figure 2.2. The parameters which affect

particle size are the stirring rate, type and amount of dispersing agent, viscosity of the organic and aqueous phases, and temperature (14). The method can also be applied to prepare amphiphilic copolymers including PEG-PLA, PEG-PLGA, PEG-PCL, PEG-PACA and polysaccharide-PCL without the need of any surfactant (16 - 18). Various lipophilic and hydrophilic drugs such as indomethacin (19), cyclosporine A (20), loperamide (21), praziquantel (22), tetanuous toxoid (23) and testosterone (24) have been encapsulated in polymeric nanoparticles using this method.

2.2.1.2 Solvent displacement and interfacial deposition method

One of the easiest and reproducible techniques for preparing nanospheres was the solvent displacement (also called nanoprecipitation) method developed by Fessi et al (26) and has been widely used to prepare nanoparticles (27 - 29). The method is based on the precipitation of preformed polymer following displacement of a semipolar solvent miscible with water in the presence or absence of surfactant (26). The basic principle of this technique is similar to spontaneous emulsification of the organic phase containing drug and polymer into the external aqueous phase. Three basic ingredients are needed for this method: polymer, polymer solvent and non-solvent for the polymer. In brief, both the polymer and drug are dissolved in a water miscible organic solvent (polymer solvent phase) of intermediate polarity (e.g. acetone and ethanol). The resulting organic phase is injected into a stirred aqueous phase (non-solvent phase) containing a surfactant as stabilizer. The nanoparticles are formed instantaneously during the rapid diffusion of the

organic phase into the aqueous phase as shown in Figure 2.3. Two important parameters affecting the physicochemical properties of the prepared nanoparticles include (30):

- Miscibility of the organic solvent with the nonsolvent;
- Nature of the polymer solvent interactions; and
- Concentration of the polymer in the organic phase.

Interfacial deposition is an emulsification/solidification technique which allows production of nanocapsules when nontoxic oil (such as benzyl benzoate) is incorporated into the organic phase (31). The polymer deposition occurs at the interface between the water and finely dispersed oil phase forming nanocapsules with a shell-like wall (32 - 33). The method has been adapted to various polymeric materials such as PLA (34), PLGA (35), PCL (36), peptides (37), cyclodextrins (38) and various drugs (39 - 40).

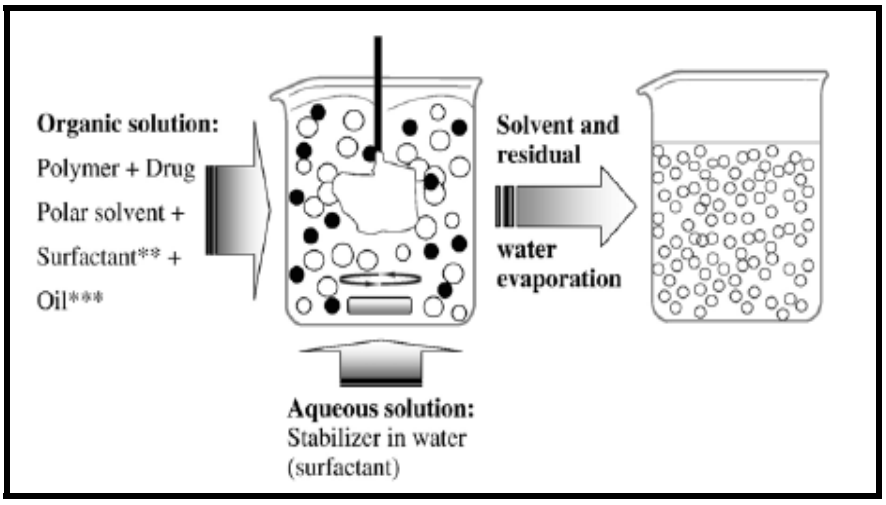

Figure 2.3: Schematic representation of the solvent displacement technique (25)

2.2.1.3 Emulsification–solvent diffusion

The emulsification solvent diffusion or emulsification-solvent displacement method is the widely used method for preparing nanoparticles due to several advantages. These include high drug entrapment efficiency for poorly water soluble drugs, narrow particle size distribution, high batch-to-batch reproducibility, no homogenization required, simplicity, ease of scale up and rapid organic solvent extraction (41). The drug and polymer usually PLA, PLGA, PCL or Eudragit are dissolved in a partially water soluble solvent. Commonly used solvents are propylene carbonate, benzyl alcohol, ethyl acetate, isopropyl acetate, methyl acetate, methyl ethyl ketone, butyl lactate or isovaleric acid (42). The organic phase is saturated with water to ensure the initial thermodynamic equilibrium. It is then diluted with an extensive amount of pure water to facilitate diffusion of the organic solvent from the organic phase droplets leading to the precipitation of the polymer as presented in Figure 2.4. The aqueous phase may contain surfactants such as Pluronic, PVA and sodium taurocholate while the organic phase sometimes contains soy lecithin as the emulsifier (42). Finally, the solvent is eliminated by evaporation or filtration, depending upon the boiling point. Several parameters can affect the size of the nanoparticles such as miscibility of the water with the organic solvent (43), stirring rate, concentration of the surfactant(s) and concentration of the polymer is the organic phase (44, 45). Nanocapsules are successfully prepared by this method when a small amount of oil is incorporated into the organic phase (46). The disadvantages of this method include: long time required to remove the high volume of water and leakage of water soluble drugs during processing.

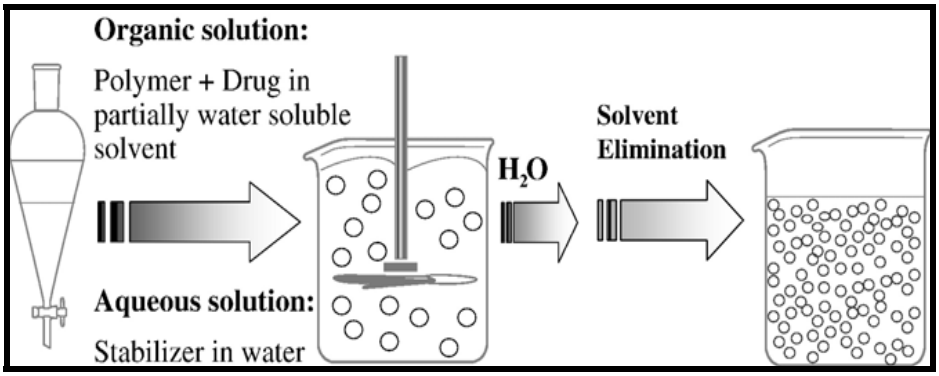

Figure 2.4: Schematic representation of the emulsification-solvent diffusion method (25)

2.2.1.4 Salting out method

The salting-out procedure can be considered as a modification of the emulsification/solvent diffusion method. The separation of a water miscible solvent from aqueous solution is achieved via a salting-out effect (Figure 2.5). Briefly, a water miscible organic solvent, usually acetone, containing polymer and drug is added drop wise to an aqueous phase saturated with an electrolyte or non-electrolyte (such as magnesium chloride, calcium chloride or sucrose) with a colloidal stabilizer (such as polyvinyl pyrrolidone) under agitation to form an o/w emulsion (47). A sufficient volume of water is added to enhance the diffusion of acetone to the water phase and nanospheres are thus obtained (48). The technique offers advantages such as the avoidance of chlorinated solvents and surfactants, minimization of stress for protein encapsulants (49), useful for heat-sensitive substances (50), high encapsulation efficiency and easy scaling up. The method is not popular because of the extensive washing steps required to achieve

purity of the nanoparticles (51) and the possibility of incompatibility between drugs and salts.

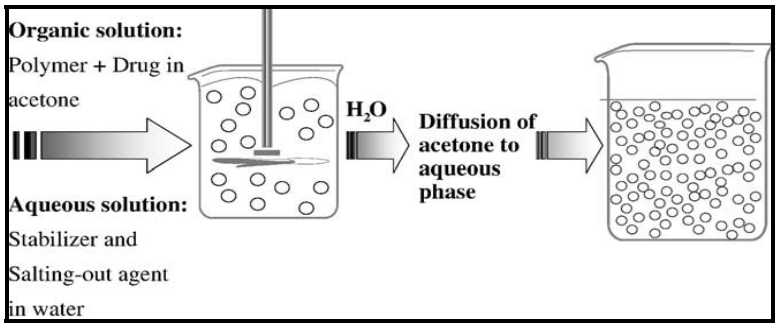

Figure 2.5: Schematic presentation of salting out method of preparing nanospheres (25)

2.2.2 Polymerization method

In the polymerization method, monomers are polymerized to form nanoparticles in aqueous solution. The polymerization method can be classified into emulsion and interfacial polymerization. The emulsion polymerization method is the fastest and scalable method of producing nanoparticles (52). It can be classified into two categories; continuous organic phase or continuous aqueous phase methodology depending on the use of the continuous phase. In general, the monomer is dissolved into an organic or aqueous continuous phase. Additional monomer molecules are then emulsified into the emulsion droplets that are stabilized by surfactant. The polymerization is started by chemical initiation, pH shift or by irradiation of gamma, ultraviolet or visible rays. In the continuous phase, chain growth starts when the initiated monomer ion or monomer radical collide with each other and forms aggregates which are stabilized by polymeric emulsifier particles. This mechanism is known as anionic polymerization (53). Several

materials are used to produce nanoparticles such as polyacrylamide (54), poly(methylmethacrylate) (55), polybutylcyanoacrylate (56), poly(hexylcyanoacrylate) (57) and poly(dialkylmethylidene malonate) (58).

The interfactial polymerization method is generally used to prepare nanocapsules using oily components such as benzyl benzoate or migliol (59) along with an organic solvent. In this case, polymerization occurs at the interface between the oily and aqueous phase to produce nanocapsules spontaneously. The nanocpsules are stabilized with the help of surfactant added in the aqueous phase. The technique is advantageous from the standpoint of producing nanocapsules with high drug entrapment efficiency with hydrophilic insulin (60). This process was used to produce nanoparticles of polyethylcyanoacrylate (61), poly (isobutylcyanoacrylate) (62) and poly (isohexylcyanoacrylate) (63).

Interfacial polycondensation is another method by which lipophilic monomer, such as phtaloyldichloride, and hydrophilic monomer, such as diethylenetriamine, is condensed to prepare nanocapsules in the presence or absence of surfactant (64). It is a spontaneous emulsification technique in which the organic phase contains a water miscile solvent, lipophilic polymer and the oil, whereas the aqueous phase contains hydrophilic monomer and surfactant. The polycondensation reaction occurs at the interface of the oil droplets to form an oil-in water emulsion and subsequently nanocapsules (65). By using the modified interfacial polycondensation method, encapsulation and stability of an oily

drug, alpha-tocopherol, was improved by the use of polyurethane and poly (etherurethane) (66).

2.2.3 Coacervation and ionic gelation method

Much research has been focused on preparing nanoparticles from natural hydrophilic polymers such as chitosan (67 - 69), albumin (70), gelatin (71), sodium alginate (72), agarose (73) and gliadin (74). Coacervation is a process during which is a homogenous solution of charged macromolecules undergo liquid-liquid phase separation producing a separated phase of polymer rich particles (75). In the ionic gelation method, the positive or negative charge of the hydrophilic polymer is complexed with a multivalent cationic (calcium chloride) or polyanionic (sodium tripolyphosphate) to form highly viscous gel particles with a size in the range of a nanometer. Calvo et al developed a method for preparing chitosan nanoparticles by this method (76).

2.2.4 Production of nanoparticles using supercritical fluid technology

Recently, supercritical or compressed fluids have been utilized as an alternative way to prepare biodegradable nanoparticles (77). This new technique obviates the use of toxic organic solvents associated with conventional methods. Two techniques are most commonly used for preparing nanoparticles – Supercritical anti-solvent (SAS) and Rapid Expansion of Critical Solution (RESS). In the SAS method, solutes are dissolved in methanol which is completely miscible with supercritical fluids. The extraction of methanol by the supercritical fluids leads to an instantaneous precipitation of the nanoparticles (78). Dexamethasone phosphate nanoparticles were prepared by this

method. In the RESS method, solutes are dissolved in the supercritical fluid and the solution is expanded through a small nozzle into a region of lower pressure (79). The solutes eventually precipitate as nanoparticles. Insulin loaded PEG/PLA nanoparticles were prepared by this method (80). The technique is very expensive and requires elaborate recycling measures.

2.3. Separation and purification techniques of nanoparticles

Depending on the method of preparation, potentially toxic impurities can be present in the nanoparticulate suspensions. These impurities are organic solvents, surfactants, residual monomers, polymerization initiators and large polymer aggregates (81). Separation of the drug entrapped nanoparticles from free polymer and unentrapped drugs is a very critical step in producing pure nanoparticles. The separation can be achieved by using Ultracentrifugation (82), crossflow microfiltration (83), Gel filtration (84), Dialysis (85) and Diafiltration (86).

2.4. Stability of nanoparticles

There are several physical and chemical factors that play a major role in the instability of prepared nanoparticles. The overall stability can be classified into two types: Physical and chemical stability.

2.4.1. Physical Stability

The colloidal submicron particles in homogenous suspension do not sediment due to the continuous thermal motion of the particles known as Brownian motion. Gravitational forces which cause the particles to sediment are opposed by Brownian motion. At

colloidal size range, the particles tend to remain suspended since Brownian motion dominates over gravitational forces (87). Random collision of suspended particles of various surface charge content and shape often lead to agglomeration and subsequent settling of the particles. In order to avoid this phenomenon, a suitable stabilizer such as PVA, DMAB, Pluronic or phospholipids is used. Magneheim et al investigated the PLA particle aggregation due to the absorption of nifedipine molecules which displaces a part of the steric stabilized surface layer (88). Charged stabilized particles are often reported to coagulate when counter ions are absorbed within the electrical double layer (89).

2.4.2. Chemical Stability

There are several factors which contribute to chemical instability of nanoparticles such as storage conditions including temperature and pH, chemical stability of entrapped drugs as well as the type and molecular weight of the polymer used. Biodegradable polymeric nanoparticles are generally stored at 4-5^{0}C for improving stability (90). Polymer degradation by hydrolysis was observed at extreme conditions of pH and temperature which the best stability was observed when the aqueous medium pH was adjusted to physiological pH (91). The overall stability of a nanoparticle formulation also depends on the chemical stability of the entrapped drugs. Most of the drugs have a pH dependent degradation profile and sometimes show photo degradation. Therefore, to reduce drug degradation and improve the stability of the nanoparticle formulation, freeze drying is most commonly used.

2.5. Freeze drying of nanoparticles

In order to remove the water from the nanoparticle system, freeze drying, also known as lyophilization is most commonly used. The basic principle of freeze drying is to remove water from a frozen sample by sublimation and desorption under vacuum (92 - 93). However, the process could generate various stresses which could cause instability of particles. In order to protect the particles from freezing and dessication stresses, cryoprotectants and lyoprotectants are incorporated into the formulation before freeze drying. Besides using these agents, other several excipients are commonly incorporated into the formulation for various purposes, as shown in Table 2.2.

Most commonly used cryoprotectants include sugars such as trehalose, sucrose, glucose, amnnitol, fructose, lactose and maltose (95 - 98). These saccharides act as a spacing matrix to prevent particle agglomeration. Freeze drying is generally carried out below the Tg′ temperature or T_{eu} temperature (eutectic crystallization temperature) so that nanoparticles can be immobilized within the glassy matrix of the cryoprotectants (99).

2.6. Physicochemical properties of nanoparticles

2.6.1. Particle size

Nanoparticles have relatively higher intracellular uptake as compared to microparticles (100). They were able to penetrate throughout the submucosal layers while the larger size microparticles localized in the epithelial lining (101). Nanoparticles are also reported to cross the blood brain barrier following the opening of the tight junctions by hyperosmotic barrier (103). Drug release and polymer degradation are alos affected by

Table 2.2: Excipients used in freeze drying of nanoparticle suspension (94)

Type	Function	Substance
Bulking agents	Provide bulk to the formulation specially when the concentration of the product to freeze dry is very low	Hydroxymethyl stach, trehalose, mannitol, lactose and glycine
Buffers	Adjust pH changes during freezing	Phosphate, Tris HCl, citrate and histidine
Stabalizers	Protect the product during freeze drying against the freezing and the drying stresses	Sucrose, lactose, glucose, trehalose, glycerol, mannitol, sorbitol, glycine, alanine, lysine, poly ethylene glycol, dextran and PVP.
Tonicity adjusters	Yield an isotonic solution and control osmotic pressure.	Mannitol, sucrose, glycine, glycerol and sodium chloride.
Collapse temperature modifiers	Increase collapse temparature of the product to get higher drying temperature	Dextran, hydroxypropyl-β-cyclodextrin, PEG, poly (vinyl pyrrolidone).

the size distribution of nanoparticles. Larger particles allow more drug to encapsulate inside the hyperosmotic mannitol for sustained delivery of drugs to brain tumors (102). Polysorbate 80 coated nanoparticles were also reported to enhance drug delivery across blood-brain core and slowly diffuse the drug molecules (104). The rate of polymer degradation of PLGA nanoparticles was increased with increasing the particles size (105).

2.6.2. Surface charge

An important characteristic of nanoparticles is the surface charge which determines the physical stability in the formulation, in vivo distribution and targeting ability of nanoparticles. The zeta potential is the measure of the amount of charge on the particle and represents an index of particle stability. A physically stable nanosuspension stabilized by electrostatic repulsion should have a minimum zeta potential value of ± 30 mV (106). The stability is increased when negative zeta potential is lowered by the addition of PEG (107). The zeta potential also indicates whether the charged active material is encapsulated within the center or adsorbed onto the surface of the nanoparticles. Thus consideration of the zeta potential is important in preventing aggregation of the particles.

2.6.3. Surface hydrophobicity

Following intravenous administration, hydrophobic nanoparticles are easily recognized by the mononuclear phagocytic system. Thus, they are rapidly opsonized and massively cleared by macrophages of the liver, spleen, lungs and bone marrow (108). Thus in order

to minimize opsonization and prolong blood circulation of nanoparticles in vivo, the surface of the hydrophilic nanoparticles must be modified. There are two general approaches employed for this purpose. One is the surface coating of nanoparticles with hydrophilic polymers such as polyethylene glycol (PEG), chitosan (109) or surfactants such as poloxamers or poloxamines (110). The second approach is the use of biodegradable copolymers having hydrophilic segments such as PLA-PEG (111). PEG functionalized nanoparticles are not taken up by the body and often called as "stealth nanoparticles" (112).

2.6.4. Drug loading

Loading of the drug inside nanoparticles can be achieved by two methods: the incorporation method and the adsorption/absorption method. There are several factors which can affect drug loading and entrapment efficiency of nanoparticles such as drug solubility in the polymer matrix, molecular weight, drug polymer interaction and presence of end carboxylic groups (113 - 115). Ideally a nanoparticulate system should have high drug loading capacity in order to reduce the quantity of polymer required.

2.6.5. Drug release

One of the most important applications of polymeric nanoparticles is the sustained and controlled delivery of drugs. Various factors such as solubility of drug, desorption, drug diffusion, particle matrix degradation or erosion can affect drug release. Smaller particles have higher initial burst release caused by poorly entrapped drug or drug adsorbed onto the surface of the nanoparticles (116). Larger particles have longer sustained release with

smaller initial burst release. It is also possible to alter the release rate from PLA-PEG-PLA copolymer by changing the amount of PEG or the molecular weight of the polymer (117). Various methods can be used to study the in vitro release of drug from nanoparticles such as diffusion cell, dialysis bag diffusion, agitation followed by ultracentrifugation or ultra filtration.

2.7. Application of Nanoparticles in Drug Delivery Systems

Association of anticancer drugs or cytotoxic agents with nanoparticles has resulted in efficient drug penetration, cell internalization, controlled release, and reversion of multidrug resistance and protection from premature inactivation during transport, reduction of toxicity to healthy cells or tissues (118). Nanoparticles fight against cancer by the indirect mechanism by the uptake in neighbouring cancer cells via the enhanced permeation and retention effect or active targeting with ligand decorated nanoparticles (119).

Stealth nanoparticles which are invisible to macrophages have prolonged blood circulation time. They can easily gain access to most tumors located outside the MPS system. Thus coating of nanoparticles with hydrophilic polymers such as poloxamers or polysorbates provides a dynamic cloud of polymer chains at the particle surface (120). These coated particles evade the MPS system by resisting the binding of plasma proteins required in opsonization. Coadministrations of P-glycoprotein inhibitors such as verapamil and antitumor drugs in nanoparticles have proven to be effective in the treatment of multidrug resistant tumors (121).

Nanoparticles are utilized as drug delivery vehicles to deliver drugs and therapeutic peptides across the blood brain barrier to treat brain tumors, Alzheimers disease, prion disease and other neurological disorders. Receptor mediated transcytosis is the most probable mechanism for the brain uptake of naoparticles (122). Polysorbate 80-coated nanoparticles have been shown to increase permeation of several agents across the blood brain barrier including the polar hexapeptide dalargin (123), tubocurarine (124), loperamide (125) and doxorubicin (126).

Pulmonary delivery of drugs and biotherapeutics including Insulin contained within nanoparticles are attractive for noninvasive and sustained targeted delivery for both local and systemic application. Most commonly chitosan, alginate and PLGA are the nanocarrier materials used for pulmonary delivery of Insulin (127), antitubercular drugs (128) and antifungal drugs (129).

In order to overcome the various problems associated with ocular administration of drugs such as rapid precorneal loss, poor drug absorption into the posterior segment of the eye, rapid tear turnover etc, nanoparticulate drug delivery systems have been investigated as a novel approach to enhance ocular availability of drugs and therapeutic agents (130 - 132). Several drugs including amikacin, betaxolol, indomethacin, ibuprofen, flurbirpofen, pilocarpine, hydrocortisone and timolol were encapculated inside polymeric nanocarriers for ocular administration.

Nanoparticles containing absorbed antigens have been investigated as strategy for oral immunization for systemic and mucosal immunity. Biodegradable nanoparticles

containing staphylococcal enterotoxin B toxoid and tetaneous toxoid have shown to have long lasting immune response in animals (133 - 134).

Sustained release of DNA from nanoparticles intracellularly would be effective in achieving gene expression to the target tissue in conditions such as cardiac and limb ischeamia, angiogenesis and bone regeneration (135). Plasmid DNA loaded nanoparticles has been shown to protect enzymatic degradation of nucleotides from nucleases due to rapid endolysosomal escape into the cytosolic compartment (136).

Chapter Three

Laser Light Scattering

3.1 Introduction

Laser Light scattering is the alteration of the direction and intensity of a laser light beam that strikes an object (1). This is caused by the combined effects of reflection, refraction and diffraction. The samples may be solid particles suspended in a liquid, solid particles or liquid particles suspended in a gaseous media (aerosols). Two different laser light scattering techniques are used to determine the particle size distribution of solid liquid dispersions: Static laser light scattering and Dynamic light scattering.

3.2 Static Laser Light scattering

3.2.1 Introduction

This technique is also known as “Laser diffraction”, “Rayleigh” scattering, low-angle laser light scattering (LALLS), Fraunhofer diffraction. Measurement of particle size and distribution using laser diffraction has become preferred choice for wide range of samples (2,3).

3.2.2 Basic Principle

The interaction of laser light with particles produces a scattering pattern due to reflection, refraction and/or diffraction phenomena (Figure 3.1). The basic assumption of laser diffraction, when determining particle size, is based on the fact that a particle passing through a laser beam will scatter light at an angle based on their size and the refractive index of the material under study. The intensity of the scattered light can be affected by particle size, refractive index, number of particles, angle of observation as well as the wavelength of light. The higher the refractive index of the particles relative to the medium, the more light that will be scattered. Scattering intensity will be high for larger particles at narrow angles, whereas intensity will be low and isotropic for smaller particles at wider angles. The instrument reports the volume fraction of a given size range rather than the number of particles since the scattering intensity is proportional to the cross section (D^2) of the particles.

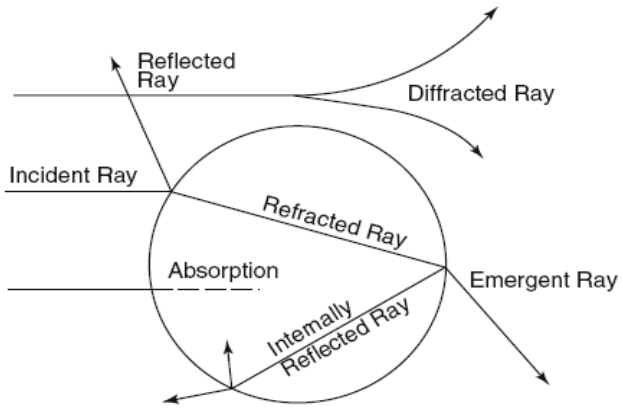

Figure 3.1: Interaction of light with particles (1)

Two different optical models are used to calculate the particle size distribution for laser light scattering experiments: the Fraunhofer Approximation (4,5) and Mie Theory (6). The Fraunhofer approximation assumes the particles are opaque, two dimentional, large circular discs and describes light scattering from the edges of an object. The Mie theory is a powerful tool to calculate size distribution based on refractive index differences between the particles and dispersion medium. The Mie theory holds true for spherical, isotropic particles illuminated by monochromatic light.

3.2.3 Instrumentation

The major components of a typical Laser Diffraction instrument are shown in Figure 3.2. A laser source along with beam expander is used to produce an extended, parallel, monochromatic beam of light. The light is then passed through the particle field (sample). The scattered light is collected by a Fourier lens and focused onto a series of detector elements at an angle. The scattering light intensity is converted into electrical signal and processed into a computer to calculate particle size distribution (1).

3.2.4 Sample preparation

Particulate materials dispersed in a gas or liquid, including aerosols, sprays and gas bubbles in a liquid can be measured using the Laser diffraction technique. Typically, the range of concentration for solid particles in a liquid should be about 0.001 to 1% w/v (1). No sample preparation is needed except dilution. The dispersion medium should be transparent with a refractive index difference from the particulate materials.

3.2.5 Application

The advantages for the Laser Diffraction technique are; its large flexibility to different

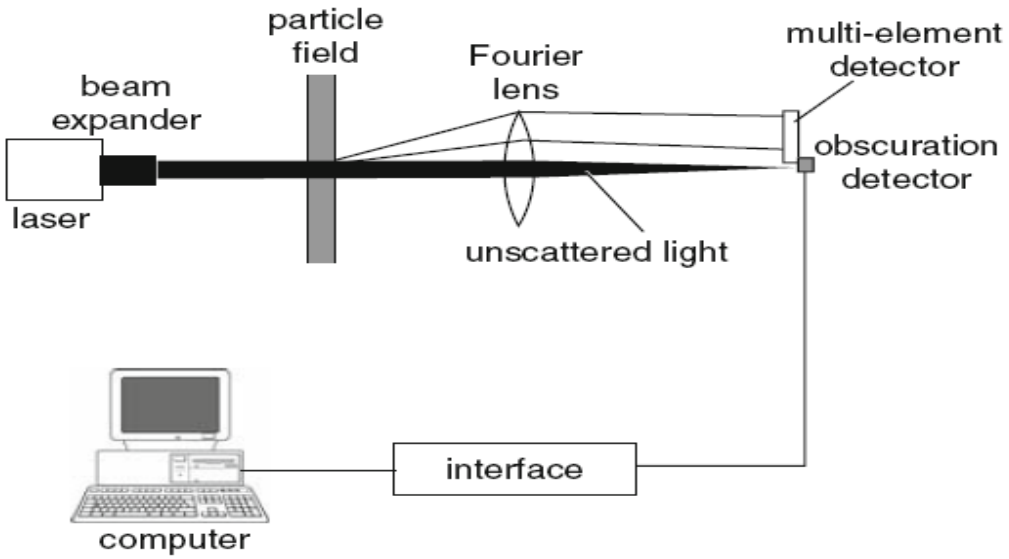

Figure 3.2: Schematic of the components of a laser diffraction instrument (1)

sample types; wide size range; rapidity; and high precision. There are few limitations with these instruments. At a given particle concentration, multiple scattering can affect the results when using a single scattering model. Nonspherical particles show widening of particle size distribution due to their differences in cross sections of a single particle (1).

3.3 Dynamic Light Scattering (DLS)

3.3.1 Introduction

DLS is also known as Photon Correlation Spectroscopy, Quasi-elastic Light Scattering,

and Diffusing Wave Spectroscopy (7). It is used to determine the particle size, and size distribution. It can also measure the polydispersity index of various types of samples including nanoparticles, colloids, gels, emulsions, pigments, liquid crystals, DNA, polymers and proteins (8). It can measure submicron particles in the range of 0.6 nm to 6 μm (9).

3.3.2 Basic Principle

In PCS, the temporal fluctuation in intensity of scattered laser light (in microseconds or milliseconds) by the particles (scatterers) in solution or suspension (medium), is processed with the auto-correlation function. This provides information about the particle size distribution, particle motion in the medium, and the dynamics of the dispersed particles. This autocorrelation function corresponds to decay constants and diffusion coefficients of the particles. Assuming particles are spherical without interparticulate interactions, the Stokes-Einstein equation is used to convert the diffusion coefficients into particle size. The DLS technique gives particle size as a hydrodynamic diameter while particle size distribution is based on scattering intensities. The scattered light undergoes either construction or destructive interference by the surrounding particles. This fluctuation in intensity of scattered light at a given scattering angle (usually 90^0C) is due to particle movement rising from the Brownian motion (10). The lower size limit of detection with this instrument depends on differences in refractive index between the particles and the medium, experimental noise (arising from electronic noise as well as

temperature fluctuations, and environmental disturbances). Medium viscosity and density of the materials determines upper size limit of detection.

The semi-classical light scattering theory is based on two assumptions: One is that particles are in random Brownian motion and the second is that all the particles are spherical in diameter. The probability density function for the Brownian motion of a given particle with a radius (d) and diffusion coefficient of (D) can be expressed as (11):

$$P(d,t|0,0)=(4\pi Dt)-3/2 \exp (- d2\ 4Dt) \qquad \text{(Equation 3.1)}$$

Assuming the spherical shape of the particle with no interparticulate interaction, the hydrodynamic radio of a particle is calculated using the Stokes-Einstein equation based onto translational diffusion coefficient. The equation is given as follows:

$$d (H)= k T/3\pi\eta D \qquad \text{(Equation 3.2)}$$

Where (D) is the diffusion coefficient, (d(H)) is the hydrodynamic radius of particles, (k) is the Boltzmann constant, (T) is the temperature in Kelvin degrees and (η) is the viscosity of the medium.

DLS provides three types of diameters of samples such as Z-average diameter, number mean diameter, volume mean diameter etc. Z-average diameter is the mean diameter based of laser scattering intensity. It is obtained from an exponential fit.

The polydispersity index (PDI) can also be measured from Dynamic light scattering instruments. PDI is an index of width or spread or variation within the particle size distribution. Monodisperse samples have a lower PDI value, whereas higher value of PDI

indicates a wider particle size distribution and the polydisperse nature of the sample. PDI can be calculated by the following equation as follows (12):

$$PDI = \Delta d/d_{avg} \qquad \text{(Equation 3.3)}$$

Where (Δd) is the standard deviation of particle size and (d_{avg}) is the average particle size. The usual range of PDI values is; 0-0.05 (monodisperse standard), 0.05-0.08 (nearly monodisperse), 0.08-0.7 (mid range polydispersity), > 0.7 (very polydisperse).

3.3.3 Instrumentation

A schematic diagram of a conventional DLS instruments is depicted in Fig 3.3. A beam of monochromatic, vertically polarized, coherent laser light from the He-Ne laser of 2-5 mW and 633 nm is generally used as the light source. A focusing lens is used to direct the

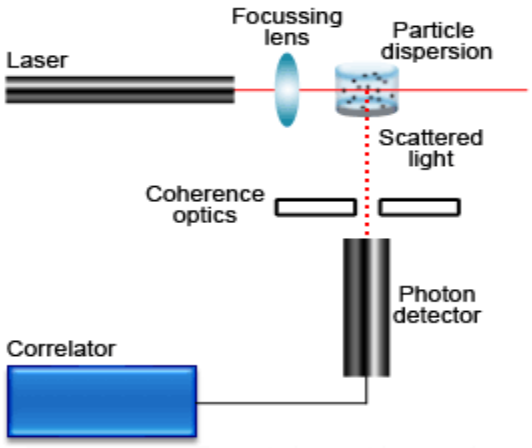

Figure 3.2: Schematic of a Dynamic Light Scattering instrument (9)

beam into a measurement zone of the sample cuvette. To obtain spatial resolution, small size of the measurement zone is used. The scattering angle can be changed to fit the range of 30^0 to 150^0 using a goniometer or by optical fiber. The intensity of the scattered light is converted into an electrical signal using an avalanche photodiode detector or photomultiplier tube. A computer is used to analyze the signal into a digital autocorrelation function. The decay of this correlation function is then converted into a diffusion coefficient and then particle size (7).

3.3.4 Sample Preparation

For data evaluation, several parameters for the sample can affect the analysis of DLS, such as solvent viscosity, solvent refractive index and sample temperature (12). Samples are liquid dispersions such as an emulsion or suspension. Samples should be diluted to suppress interparticulate interactions. The scattering intensity depends on mass or size of the particles, solute particle concentration and refractive index differences between the solute and solvent. The solute-solvent interaction forming the aggregates or micelles should be avoided. In order to avoid a Coulombic interaction between charged systems (Polyelectrolytes), a low concentration of salt such as NaCl, KBr or NaBr are recommended for aqueous systems. For organic solvents, Tetrahydrofuran (THF), dimethyl formamide (DMF) and chloroform are used. In addition to these factors, sample purification is another critical step in order to obtain reliable data. Air bubbles are removed by ultrasonication while dust particles are removed by filtration or by centrifugation. The sample cell should be cleaned with acetone and dried under a dust free special hood.

3.3.5 Application

There are several advantages for using the DLS method such as non-destructive, non-invasive technique, no need for calibration, small volume of sample (9). It also doesn't require extensive sample preparation, has a short analysis time, and modest development costs. Particle size, size distribution (including the polydisperisity index) can be measured for various systems such as proteins, polymers, micelles, carbohydrates, nanoparticles, colloidal dispersions, emulsions and microemulsions (13).

Chapter Four

Laser Doppler Electrophoresis

4.1 Introduction

Laser Doppler Electrophoresis (LDE) combines the principles of Laser Doppler Anemometry (LDA) and electrophoresis (1). Laser Doppler Anemometry is the technique used to measure the speed of moving particles taking into account the Doppler shift of scattered light by particles in motion. It is the most widely used technique to determine electrophoretic mobility, particle surface charge or zeta potential for colloidal dispersions including nanoparticles (2), biological cells, bacteria (3-6).

4.1.1 Electrophoresis

The motion of the charged colloidal particles, relative to the liquid, under the influence of an electric field is known as electrophoresis (7,8). The positively charged particles migrate to the cathode while negatively charged particles move towards the anode. In 1807, Reuss first observed this electrokinetic phenomenon when clay particles in water migrated upon the application of a constant electric field (9).

4.1.2 Zeta potential

There are three ways by which a solid particle (colloid) dispersed in a liquid media can acquire a surface charge (10). First, by the adsorption of ions present in the solution. Second, by the ionization of functional groups on the particle's surface. Third, due to the difference in dielectric constant between the particle and the medium. Attention should be paid to the formation of electric double layer at the solid-liquid interface. The zeta

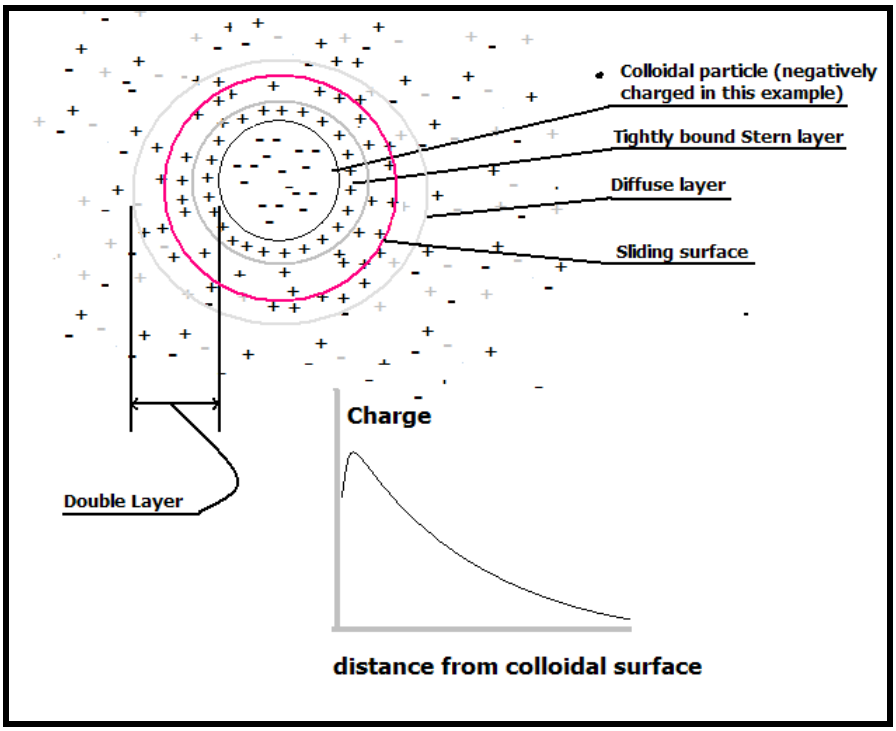

Figure 4.1: Schematic of the formation of electric double layer (11)

Potential is defined as the difference in potential between the surface of the tightly bound layer (shear plane) and the electro-neutral region of the solution (10). The potential

gradually decreases as the distance from the surface increases. As the concentration of electrolyte increases in the medium, the zeta potential falls off rapidly due to the screening effect of the counterions (Figure 4.1).

The zeta potential cannot be measured directly; however, it can be calculated using theoretical models and from experimentally determined electrophoretic mobility data. The most widely-used theory for calculating zeta potential was developed by Smoluchowski in 1903 (12). The theory is based on electrophoresis and can be expressed as:

$$\mu = \zeta\varepsilon/\eta \qquad \text{(Equation 4.1)}$$

where (μ) is the electrophoretic mobility, (ε) is the electric permittivity of the liquid, (η) is the viscosity and (ζ) us the zeta potential.

Table 4.1: Zeta potential for colloids in water and their stability (14)

Zeta Potential [mV]	**Stability behavior of the colloid**
0 to ±5	Rapid coagulation or flocculation
from ±10 to ±30	Incipient instability
from ±30 to ±40	Moderate stability
from ±40 to ±60	Good stability
more than ±61	Excellent stability

There are few limitations when applying of the above equation. The equation is only valid when the thin double layer (Debye length) is much smaller than the particle radius. For nano-colloids, the equation is not valid when the ionic strength approaches to that of pure water. The theory doesn't take into account the surface conductivity of the colloidal particles (13). ASTM provides a table (Table 4.1) from which the stability of the colloidal dispersions cab be predicted based on the zeta potential (14).

4.2 Basic principle and Instrumentation

Laser Doppler Electrophoresis (LDE) is based on the combination of electrophoresis andLaser Doppler Anemometry (LDA). It is used to measure velocities and thereby zeta potential of colloid particles. The technique is based on the measurement of light scattering to the determine particle size for diluted dispersions or suspensions when particles flow through a series of interference fringes. For concentrated dispersions, acustophoresis is the preferred method to analyze particle velocities (15).

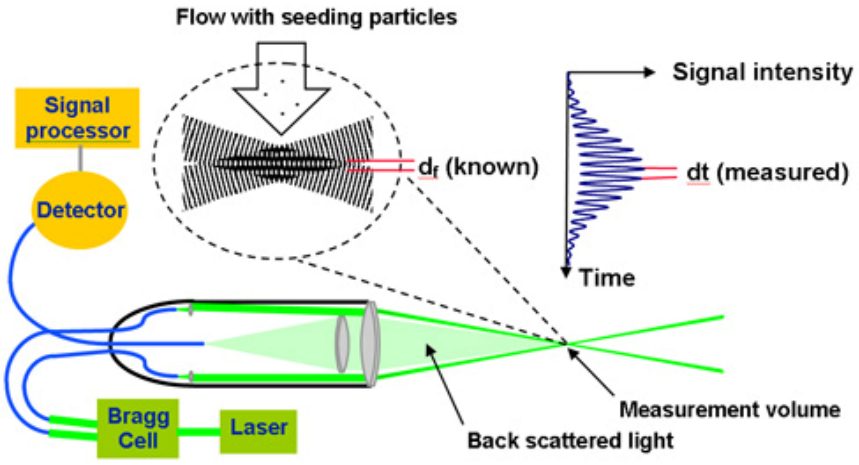

Figure 4.2: Schematic of a Laser Doppler Electrophoresis instrument (16)

An electric field voltage is applied across the liquid dispersion juncture containing particles which will migrate towards either electrode depending on their magnitude and sign of charge. The higher the velocity of the particle, higher the zeta potential it carries. The velocity of the particle is measured by the Laser Doppler Anemometry (LDA) technique and converted to zeta potential using Smoluchowski equation as given above.

The LDA measures the frequency or phase shift of an incident laser beam. A typical dual beam LDA consists of the following major components inlcude: a laser source; transmission optics (e.g. Bragg cell, lenses, fiber optics, beam expanders, beam splitter, mirrors, prisms), receiving optics (e.g. pin holes, interference filter, photomultiplier); traversing system, signal processor (e.g. spectral analysis, photon-correlation) and computer as seen in Figure 4.3 (17). The monochromatic, coherent laser beam is divided into two beams of equal intensities. These two beams are focused to cross each other using lenses, the Bragg cell and fiber optics. The crossing point is known as the the "measurement volume". Actually the crossing beams form equally spaced bands of dark and light interference fringes. The velocity of moving particles is measured at the point where the laser beams cross each other. When particles move through the measurement volume, according to the Mie theory, they scatter light at a frequency of proportional to velocity of the particles. If the movement of the particle is perpendicular to the fringes, the relation between this frequency (f_d), and the velocity (V_x) is determined by the angle (2θ) between the two intersecting laser beams and the wavelength (λ_0) of the laser light as follows:

$$fd \approx 2 \sin \theta \, (V_x / \lambda_0) \qquad \text{(Equation 4.2)}$$

By measuring the Doppler frequency-shift of the scattered light, the velocity of the moving particles can be determined by measuring time (dt) and travelled distance (df). The Doppler Effect is the change in frequency of a wave for an observer moving relative to the source of the wave. The scattered light is detected by a photomultiplier tube or other type of photodetector. The electronic signal can be split into two parts: a low frequency part known as the "pedestral" and a high frequency part known as the "Doppler". Signal processors use digital technology to determine the frequency using autocorrelation or Fourier transformation. Thus, calculating the velocity component of the Smoluchowski equation, the zeta potential is given as an output signal.

4.4 Application

There are several advantages for using LDE. LDE is a very rapid and accurate technique which can measure in few seconds. Wide range of particle concentration and solution containing high concentration of salts such as alkali halides can be measured. Small value of electrophoretic mobility can be detected accurately. Heating of sample and polarization of electrodes are greatly reduced. Typical applications are in the formulation of particulate dispersions. Most widely used instrument available is Zetasizer® with standard cell (18).

Chapter Five

Electron Microscopy

5.1 Scanning Electron Microscopy (SEM)

5.1.1 Introduction

The scanning electron microscope (SEM) is one of the most versatile instruments widely applied to surface microstructure imaging (1). SEM is a type of electron microscopy that images the sample surface of a solid specimen by using a focused beam of high-energy electrons. The signal contains information about surface topography, external morphology, chemical composition (3), crystallographic information (2), and electrical conductivity (4).

5.1.2 Fundamental principles

The Scanning process and image formation in SEM depends on signals produced from elastic and inelastic interactions between the high energy electron beam and the specimen surface (Figure 5.1). When the primary electron beam bombards on sample surface, energetic electrons penetrate into the sample surface forming an excitation zone, known as the interaction volume before they collide with the specimen atom (Figure 5.2). The shape and size of the interaction volume depends on the accelerating voltage and atomic

number. In the process, the electrons also lose energy by repeated, random scattering. Elastic scattering occurs from the deflection of incident electrons by the atomic nucleus or outer shell electrons (1). This accounts for the negligible energy loss and produces backscattered electrons (BSE) at an angle of more than 90^0. Inelastic scattering transfers substantial amounts of energy to emit secondary electrons. In addition to those signals, a number of other signals such as Auger electrons, characteristic X-rays, cathodoluminescence, transmitted electrons, and specimen currents are emitted (Figure 5.3). Electronic amplifiers are used to amplify the signal and cathode ray tube scans the surface. The image is captured by photography or digitally and displayed on computer monitor.

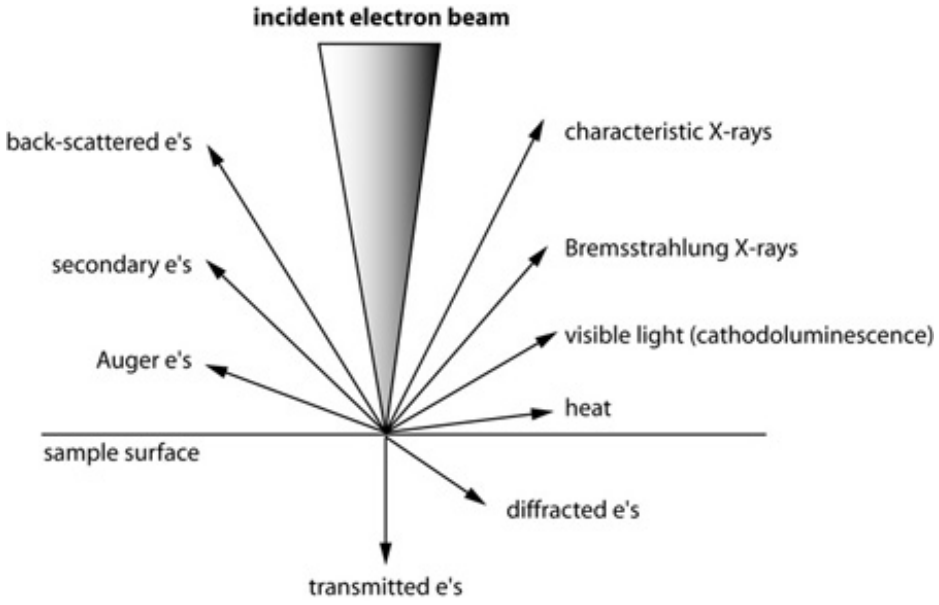

Figure 5.1: Schematic of signals generated by the electron beam–specimen interaction in the scanning electron microscope (10)

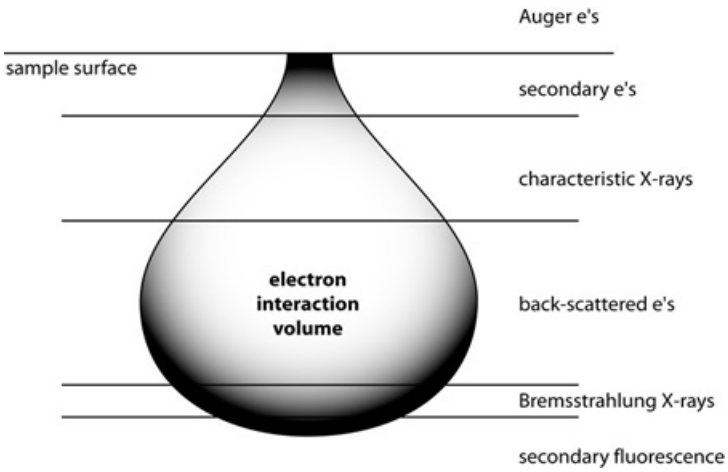

Figure 5.2: Electron interaction volume within a sample (10)

5.1.3 Instrumentation

The major components of an SEM include the electron gun, electron lenses, sample stage, detectors, data output devices, and the vacuum system (1). Figure 1 shows a structure of a conventional SEM. The Electron gun produces a high current, small spot size, stable electron beam and accelerates at an energy level of about 0.1-0.3 keV. Tungesten, lanthanum hexaboride, and field emission are the types of electron guns widely used (6). . The electron beams can be focused by electromagnets or electron lens and aperture. There are two types of electron lenses: condenser lenses and objective lenses. Condenser lens converges and collimates the diverging electron beams into parallel beams. Objective lenses demagnify the electron beam into a probe point at the specimen surface

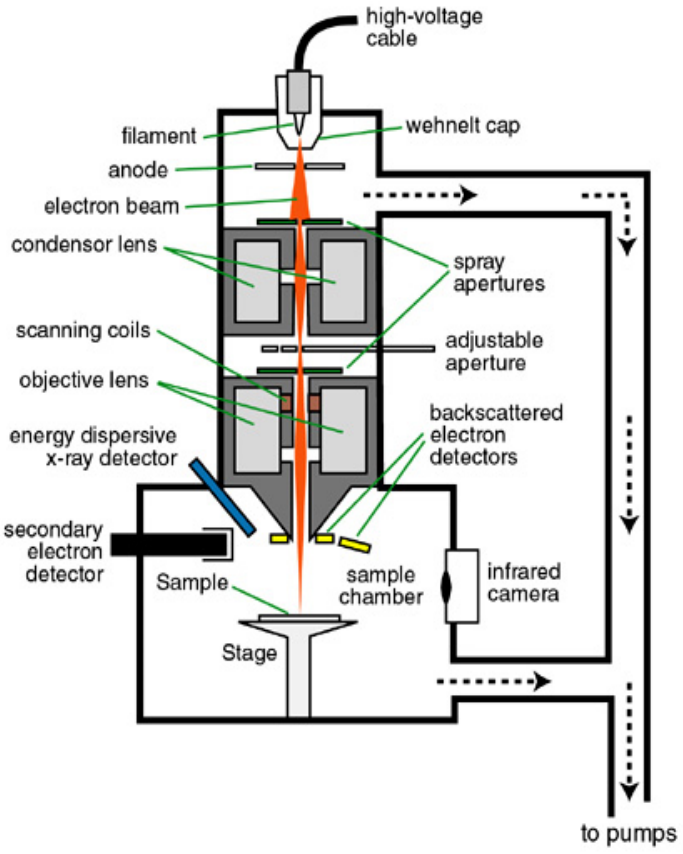

Figure 5.3: Schematic diagram of a scanning electron microscope (5)

A stigmator consists of a series of coils surrounding the electron beam. It can be used to correct astigmatism and achieve an image with higher resolution. Interaction of the focused electrons on the specimen surface produces secondary electrons, back scattered electrons (BES), transmitted electrons, characteristic X-rays, and auger electrons which are collected by detectors, processed and displayed in the output device. In order to avoid scattering of electrons by air molecules, and the contamination of the electron guns and other components, a ultrahigh vacuum system is maintained using mechanical, diffusion, ion or turbo pumps.

5.1.4 Sample preparation

Depending on the type of sample and image required, sample preparation can be elaborate or minimal for SEM analysis. For conductive materials, the surface can be visualized directly by loading the sample onto carbon tape. For nonconductive organic materials and biological samples, a thin layer of conductive materials such as carbon, gold, silver, platinum are coated by low vacuum sputter coating or high vacuum evaporation to make the surface conductive, increase signal and surface resolution, and prevent accumulation of static electric charge on the specimen. An alternative method for coating biological samples is to use OTO (Osmium Thiocarbohydrazie Osmium) stain (7). Uncoated nonconductive materials can also be visualized using specialized instruments such as the Environmental SEM (ESEM) (9) and Field Emission SEM (FESEM) (1) at low voltage. Solvated biological and organic samples can be visualized without solvent removal by using a new technique known as Cryo-HRSEM at low temperature (8).

5.1.5 Application

Combination of large depth of field, high resolution, high magnification, minimal sample preparation, easy sample observation, and rapid data acquisition makes SEM one of the widely used instruments in a variety of research areas (11). SEM is routinely used to analyze shapes and surface topography of samples. It is used to analyze spatial variation in chemical compositions by using elemental maps, and spot chemical analysis. It is also used to identify the microfabric and crystalline orientation of materials (1, 11). Though there are few limitations associated with SEM such as its applicability only for solid

sample which are stable under vacuum, inability to detect very light elements (H, He, Li), and extensive sample preparation for nonconductive materials.

5.2 Transmission Electron Microscopy (TEM)

5.2.1 Introduction

Transmission Electron Microscope (TEM) is a type of microscopy technique which operates on the same basic principle as the light microscope except TEM uses a beam of electrons, instead of light. The image is formed by the interaction of the sample specimen when electron beams are transmitted through it. Due to the small de Broglie wavelength of electrons, it is possible to get significantly higher resolution down to 0.1 nm in TEM over light microscopy (12). Visualization of small details in the cell or materials down to near atomic levels makes it a viable tool in medical, biological, material science, and environmental geochemistry research (13, 14).

5.2.2 Fundamental principles

Image formation by TEM is based on the interaction of an electron beam with the object using various electron scattering mechanisms, illumination conditions, as well as the action of objective lens and arranged apertures (16). The TEM image contrast is due to elastic scattering of electrons. There are various contrast modes to improve the image quality. These modes include: bright and dark field; diffraction contrast; and phase contrast (17). Bright and dark field mode is based on the occlusion and absorption of electrons in the sample. For amorphous materials, a thicker region of the sample or region with high atomic number would appear dark in the image due to higher elastic scattering.

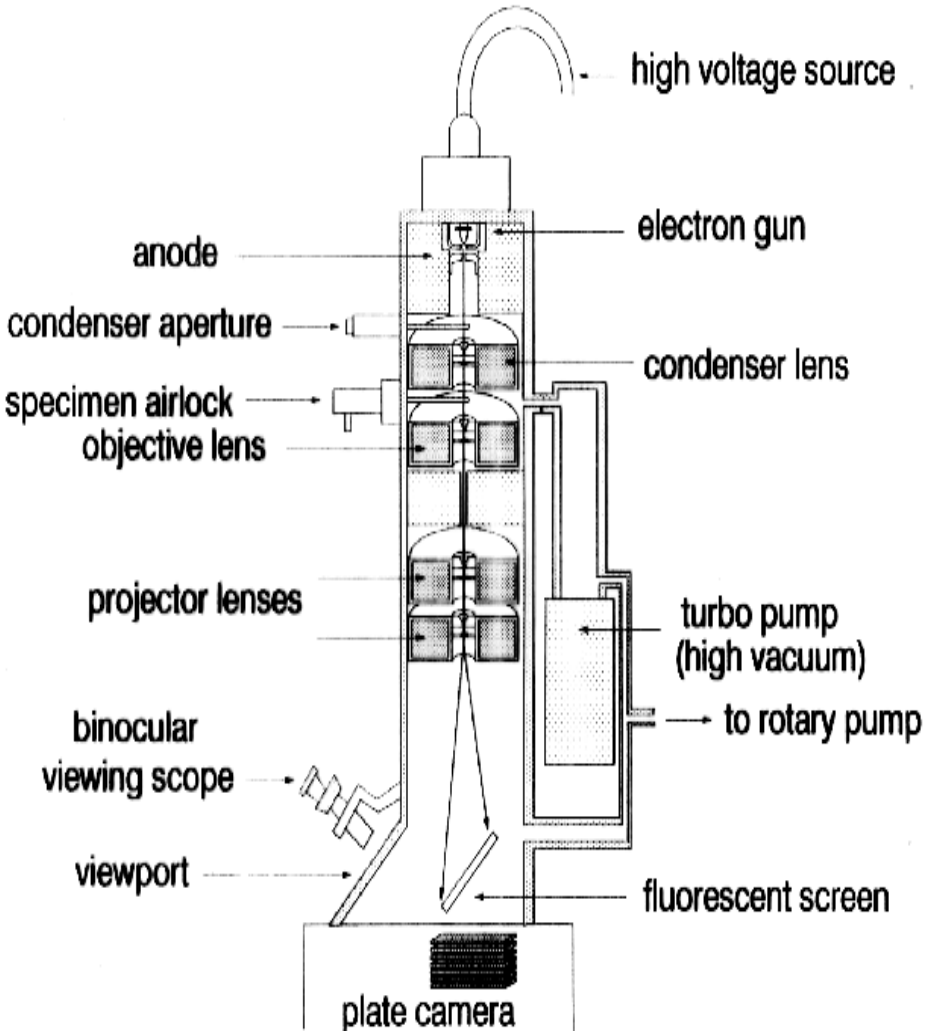

Figure 5.4: Schematic diagram of the cross section of a Transmission Electron Microscope (15)

The contrast is greater at low accelerating voltage and smaller aperture diameters. To study the crystalline structures, the diffraction contrast mode is used. Using selecting Bragg scattering, sharp spots can be visualized. In phase contrast mode, scattered electrons are allowed to recombine with unscattered electrons to form the image.

5.2.3 Instrumentation

The schematic diagram for a conventional TEM with its major components is depicted in Figure 5.4. In TEM, the emission source of electrons is a tungsten filament or lanthanum hexaboride source (18). They are also known as electron gun. Electromagnetic lenses are used to accelerate and focus the electrons into a very thin beam by varying the magnetic field of electromagnetic lenses. The interior of the microscope is evacuated to low pressure typically 10^{-4} Pa in order to minimize scattering of the electrons by air molecules and to increase the mean free path of the electron gas interaction. Depending on the density of the sample specimen used, some of the electrons will be scattered while some will be unscattered and hit at the bottom on to a fluorescent screen or on a layer of photographic film. The image can be detected by a sensor such as a CCD camera (13).

5.2.4 Preparation of sample

Preparation of samples for TEM analysis is specific to the material under study (17). For pharmaceutical and material sciences, the powder in the solid state is dissolved or dispersed in solvent and deposited onto a support mesh known as “grid”. Usually a grid is 2.5 – 3 mm in diameter, with a 50-400 mesh and made up of copper, molybdenum, gold or platinum. Biological samples can be fixed onto the grid using a negative staining material such as uranyl acetate or by plastic embedding. Cells may be affixed to a thin electron transparent film and stained using heavy metals such as uranium, osmium, or lead which scatters the electron beam resulting in dark images.

5.2.5 Application

Combined with good spatial resolution, ultra high magnification, TEM is widely used to obtain structural and compositional information of various materials. Inelastic scattering of electrons can be used for energy dispersive X-ray analysis (EDX), electron energy loss spectroscopy (EELS), or energy filtered TEM (EFTEM) (19-21). Recently, High resolution TEM (HRTEM) has been used to obtain a resolution of 0.2 nm (13). Another improved technique is Scanning TEM (STEM) which focuses at the electron beam into a narrow spot that scans the sample in a raster (22).

Chapter Six

Fourier Transform Infrared Spectroscopy (FTIR)

6.1 Introduction

Infrared Spectrometry (IR) is a widely used technique in both research and industry. It is a simple and reliable technique for the identification of unknown materials, determination of the amount of components in a mixture as well as for quality control of materials (1). Infrared (IR) spectroscopy gives molecular structural information using the frequencies

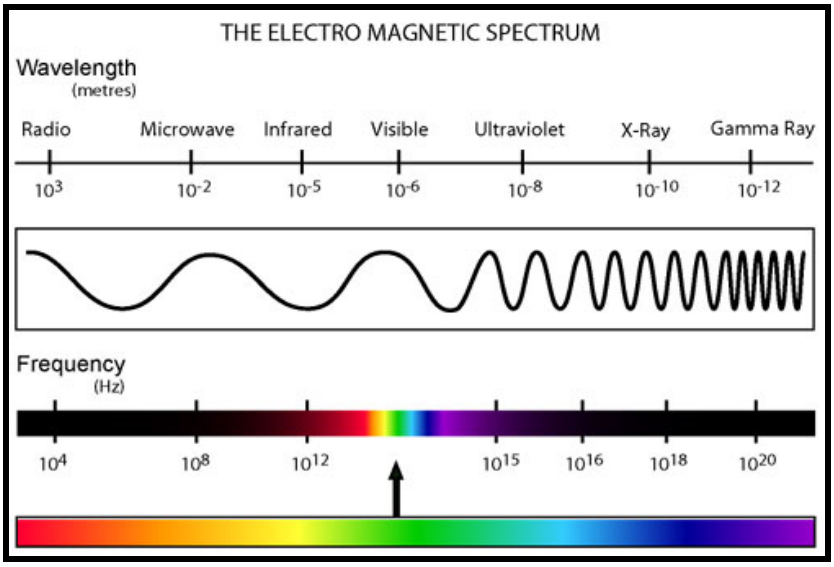

Figure 6.1: Various regions of the electromagnetic spectrum (3)

of the vibrational modes for a compound (2). IR is a type of energy absorption spectroscopy that uses the infrared region of the electromagnetic spectrum (Figure 6.1). Fourier Transform Infra Red (FTIR) spectroscopy is a measurement technique whereby IR spectra are collected by using a time domain measurement. The original IR spectrometers are of the dispersive or filter types. They measure the amount of energy at each frequency of the IR spectra with the aid of a prism or grating. FTIR uses an interferometer which measures the signal and performs a Fourier transform on the data to provide an IR spectrum (1). There are several advantages for FTIR over dispersive IR methods such as (1):

- The measurement time is faster
- Simultaneous measurement can be performed
- It is a non-destructive technique
- It requires no external calibration
- It is inexpensive
- It provides improved sensitivity and resolution
- It has mechanical simplicity

6.2 Basic Principle

A normal vibrational mode is one in which each atom oscillates about its equilibrium position, e.g. simple harmonic motion. When the frequency of the IR radiation is the

same as the vibrational frequency of a bond in a functional group, absorption of IR energy occurs (2). The absorption intensity depends on how efficiently the energy of an electromagnetic wave can be transferred to the atoms involved in the vibration. The greater the change in dipole moment during a vibration, the higher the intensity of absorption. Atoms in a functional group can vibrate in various ways, such as symmetrical and anti-symmetrical stretching, scissoring, rocking, wagging and twisting. An IR spectrum is obtained when a sample absorbs energy which causes a transition between two vibrational energy levels, from ground state to excited state.

Three typical spectral regions for IR spectroscopy can be distinguished based on their wavelength.

- Near-IR: It has the range of 14000–4000 cm^{-1}. It excites overtones or harmonics of fundamental vibrations (multiple level transition).
- Mid-IR: It excites the fundamental vibrations (single level transition). It has the wavenumber range of 4000–400 cm^{-1}. This region is the most widely used for IR spectroscopy, because it generates spectral fingerprints in which most of the organic molecules are IR active.
- Far-IR: It has the range of 400–10 cm^{-1}. It excites low-energy vibrations and higher energy rotations. Far IR detects very strong bonds such as metal-metal bonds or metal-ligand interactions (4). Today, it is used in the medical field (5,6).

The IR spectrum is obtained by recording transmitted light which shows how much energy was absorbed at each wavelength when a beam of infrared light was passed

through the sample. Thus, a transmittance or absorbance spectrum can be produced, showing the IR wavelength region where absorption occurred. Because of the unique patterns and complexity of IR spectra in the 1450 to 600 cm^{-1}, it is often called the fingerprint region. Absorption bands in the 4000 to 1450 cm^{-1} region are usually due to stretching vibrations of diatomic units, and known as the group frequency region. The details about the molecular structure of the sample can be obtained by analyzing the spectrum with standard reference frequencies.

6.3 Instrumentation

A basic FTIR spectrophotometer consists of an IR radiation source, the interferometer and the detector (Figure 6.2). Typically, an IR radiation source includes one of the following: Nernst glower; Glowbar source; Incandescent wire source; Mercury arc; Tungsten filament lamp; carbon dioxide laser (1). Interferometer works on the principle of superposition to combine separate waves together to have some meaningful property (8). One widely used interferometer is the Michelson interferometer (Figure 6.3). The monochromatic light is split into two beams which recombine to form a visible pattern of areas of constructive and destructive interference of bright and dark fringes (Figure 6.4). Typical IR detectors which are used include: Thermocouple; Bolometer; Pyroelectric detector; or a Photoconducting detector (1). The measured signal is transferred to the computer where the Fourier transformation of the data takes place and the typical percentage transmissions versus wave number plots are obtained. Various vibrational modes of the functional groups and atoms in organic compounds exhibit characteristic IR

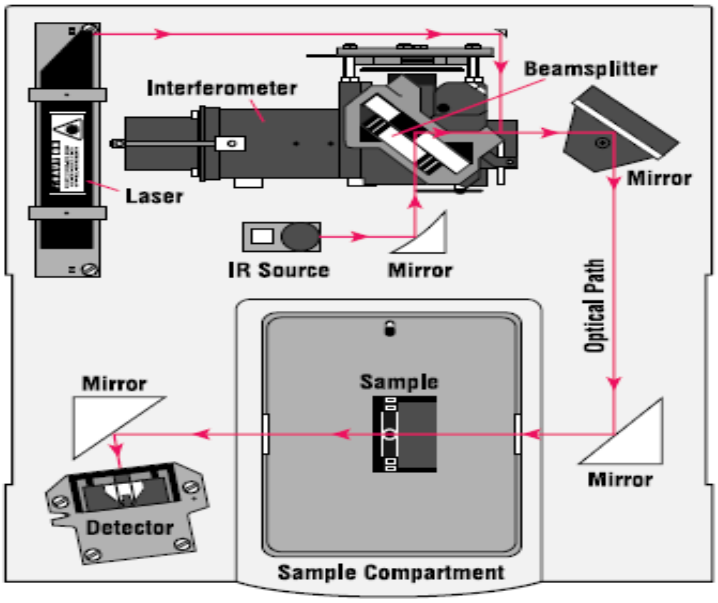

Figure 6.2: Schematic presentation of a FTIR spectrophotometer (7)

\

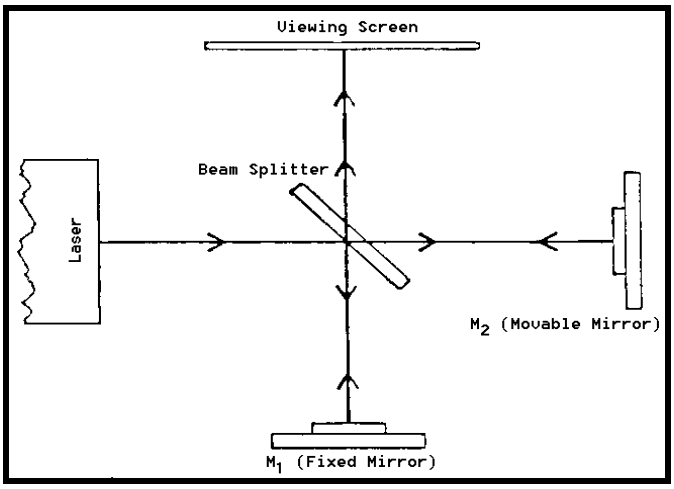

Figure 6.3: A schematic diagram of Michelson interferometer (9)

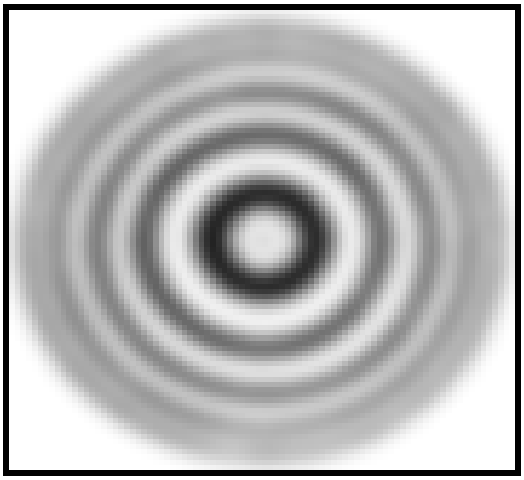

Figure 6.4: A typical interference pattern (7)

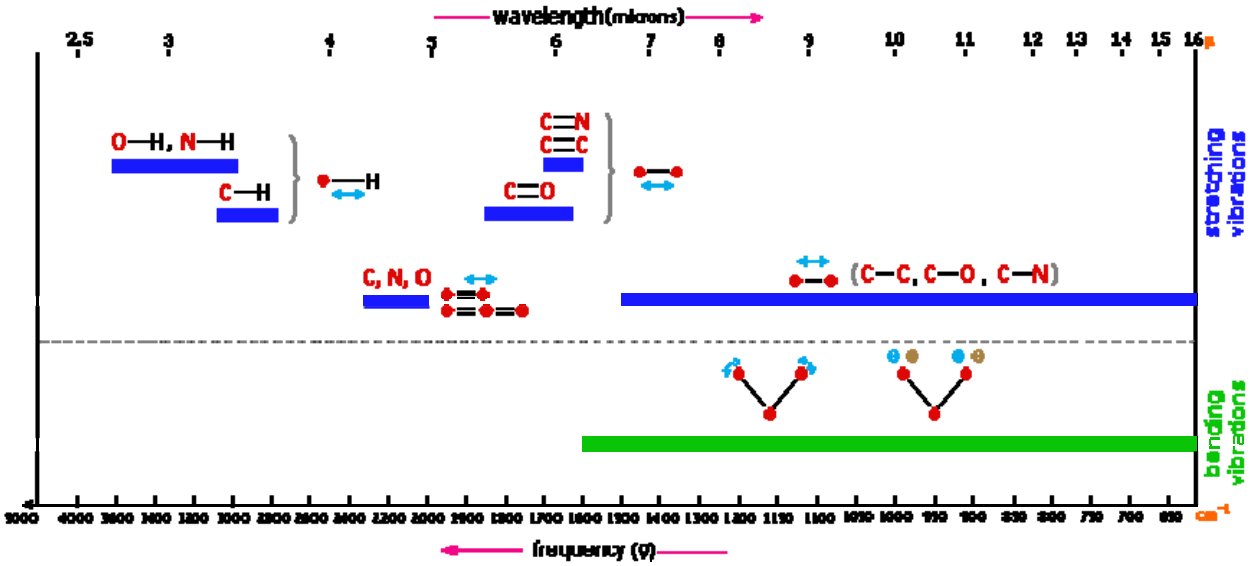

Figure 6.5: General regions of IR spectrum showing various types of vibrational bands (10)

absorption peaks at a specified wave number range (Figure 6.5). This helps to identify the nature of the functional groups and atoms present in a molecule.

6.4 Sample Preparation

FTIR is very widely used for gases, liquids and solid samples. For gaseous samples, sample cells of sodium chloride (NaCl) or potassium bromide (KBr) are used. Liquids can be sandwitched between two IR transparent plates made up of NaCl or KBr (11). Solid samples can be prepared by four different methods (12). First, the sample is mixed with a mulling agent such as Nujol and applied onto salt plates. Second, the sample is mixed with potassium bromide and crushed in a mortar with a pestle. The mixture is then compacted to form a translucent pellet with the aid of a mechanical die press. The third method is the cast film method in which a sample is dissolved in a non-hygroscopic solvent and a drop of the solution is deposited on the surface of NaCl or KBr plates; which is then evaporated to form a uniform thin film. The fourth method is microtomy in which thin films are cut from the solid sample.

6.5 Application

Advancements in computing techniques have enabled FTIR to become a popular tool to characterize various types of materials including polymers (13). FTIR is used for both qualitative and quantitative purposes (14). Molecular reaction mechanisms of biomolecules have been studied using time resolved FTIR (15). In Pharmaceutical research, FTIR is used to identify and analyze structure of drugs (16), excipients, polymorphism (17) and dissolution (18). Drug polymer interaction studies can be performed using this technique in dosage forms containing nanoparticles (19-21).

Chapter Seven

Powder X-Ray Diffraction Analysis

7.1 Introduction

X-ray diffraction is one of the most important characterization tools used in solid state chemistry (1,2) and materials science (3-6). X-rays are electromagnetic radiation having a wavelength of about 1 Å (10-10 m), which is about the same size as an atom (7). One of the major applications for this technique after the discovery of X-rays by WC Roentgen in 1895, was in the field of Crystallography to probe the crystalline structure at the atomic level. Each crystalline material has its own unique characteristic PXRD pattern known as a "fingerprint' (7). Some of the common applications for X-ray powder diffraction can be summarized below (8):

- Identification of single-phase materials
- Identification of multiple phases in microcrystalline mixtures
- Determination of the crystal structure of identified materials
- Identification and structural analysis of clay minerals
- Recognition of amorphous materials in partially crystalline mixtures

7.2 Fundamental Principles

The three-dimensional structure of any crystalline compound is depicted by regular, repeating planes of atoms that form a lattice (Figure 7.1). When a collimated beam of monochromatic X-ray impinges with these planes of atoms, part of the beam is diffracted in various directions. Depending on the arrangement of atoms in the crystal lattice, each material would produce different patterns of diffraction. Thus, we can measure the distances between the planes of the atoms by applying Bragg's Law (9). Bragg's law states that diffraction occurs only when the distance traveled by the rays reflected from successive planes differs by a complete number (*n)* of wavelengths.

Thus, for a monochromatic X-ray beam with wavelength λ (lambda) is projected onto a crystalline material at an angle (θ) (theta), Bragg's Law states that:

$$n \lambda = 2 d \sin \theta \qquad \text{(Equation 7.1)}$$

Where the integer (n) is the order of the diffracted beam, (d) is the distance between adjacent planes of atoms (the d-spacings). The characteristic set of *d*-spacings generated in a typical X-ray scan provides a unique "fingerprint" for the sample. When properly interpreted, by comparison with standard reference patterns and measurements, this "fingerprint" allows for identification of the material.

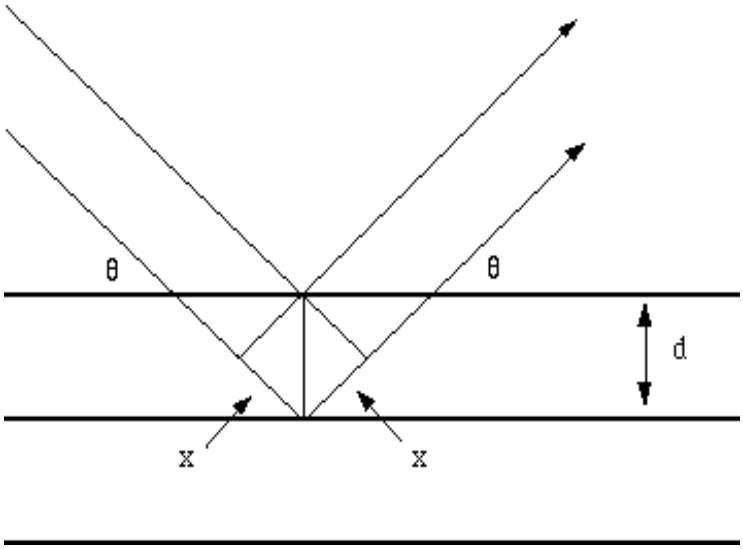

Figure 7.1: Diagram of reflection of X-rays from two planes of atoms in a solid (10)

7.3 Instrumentation

A typical X-Ray diffractometer consists of three basic elements; X-Ray tube (generator), sample holder and X-Ray detector as shown in Figure 6.2 (7, 11, 12). X-rays are generated in a cathode ray tube where a filament is heated to produce electrons. These electrons are then accelerated toward a target by applying a high voltage and, subsequently the target material (anode) is bombarded with accelerated electrons to produce an X-Ray. The most commonly used laboratory X-ray tube uses Copper as the target material, however Cobalt, Molybdenum are also popular. The radiation consists of several components, the most common being K_α and K_β. For example, the wavelength of the strongest Cu radiation (Kα) is approximately 1.54 Å. By using foils or crystal monochromators, the desired wavelength for diffraction can be produced. These X-rays are collimated and directed onto the sample, which has been ground to a fine powder at

an angle of (θ). As the sample and detector are rotated (at an angle of 2θ) using a goniometer, the intensity of the reflected X-rays is recorded. For typical power diffraction experiments, data can be collected at a wide angle (2θ from ~5° to 70°), however small

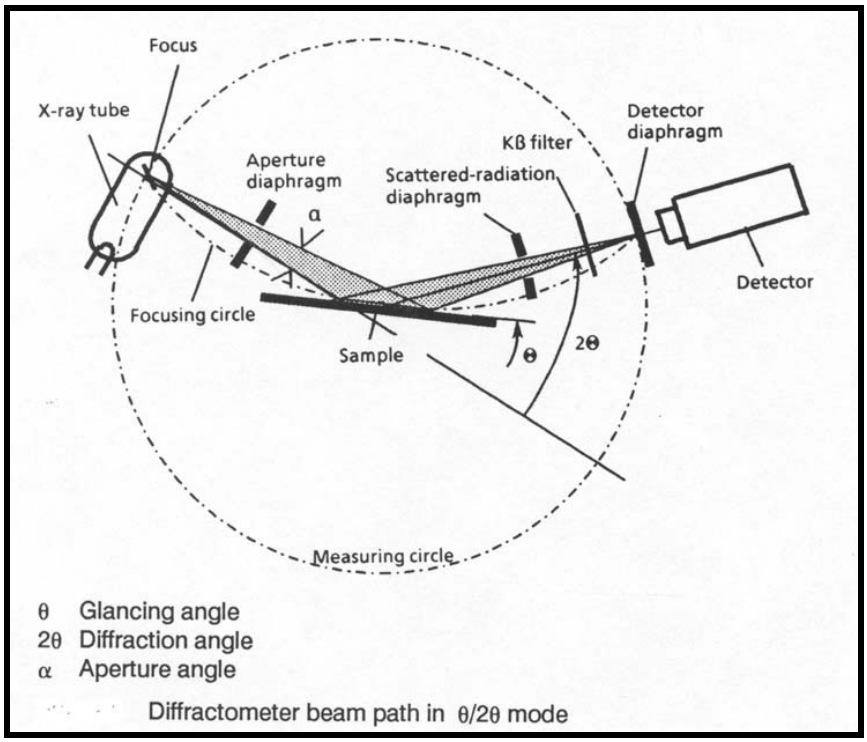

Figure 7.2: Schematic diagram of a powder diffractometer (8)

angle (2θ closer to 0°) can be used for probing the structure in the nanometer to micrometer range (13). The commonly used laboratory diffractometer uses a scintillation counter as the detector. The detector detects, then processes the signal either by a microprocessor or electronically and converts the signal to a count rate which is then sent to an output a device, such as a computer.

7.4 Nonambient powder diffractometry

The polymorphic transformations, thermal expansion, changes in Bragg peaks of materials can be studied under nonambinet conditions maintained within the instrument (14). The most common thermodynamic parameters varied are temperature and pressure. For temperature controlled PXRD, the sample is enclosed with a vacuum tight enclosure made from low X-Ray absorbing materials such as Mylar®. A furnace is used for high temperatures whereas a cryostat is used for low temperature experiments. The temperature is controlled using fully automated temperature controllers. For pressure controlled PXRD, the sample is mixed with a pressure standard and kept inside diamond anvil cell. The cell can be coupled with temperature controlled environment.

7.5 Preparation of the sample

Depending on the capacity of the sample holder, a few tenths of a gram (or more) of the material is required. The sample material should be ground into a fine powder (~10 μm or 200-mesh). The sample is smeared uniformly onto the sampling block and then packed. The upper surface of the sample must be flat to achieve random distribution of the lattice orientation.

7.6 Application

There are several advantages associated with the PXRD analysis such as: fast measurement; non-destructive analysis of multi-component mixtures; no need for extensive sample preparation; and relatively straightforward data interpretation (15). PXRD can be used for analysis of a variety of transformations during pharmaceutical processing and storage such as: polymorphic transformations; alterations in crystallinity;

changes in state; and degree of hydration. There are relatively few limitations of the PXRD technique (16, 17). Small impurities are not detected. For identification of unknown materials, the sample must be homogenous and pure. Standard reference compounds with known d-spacings should be available (7). A gram of material is required for analysis with detection limit of about 2% for mixed materials. Indexing pattern for non-isomeric crystal systems is complicated. Peak overlay may occur and worsen at high angle reflections.

Chapter Eight

Differential Scanning Calorimetry

8.1 Introduction

DSC is a thermoanalytical technique in which the difference in heat flow between a sample and reference material is measured as a function of time or temperature when they are subjected to the same heating rate in a controlled atmosphere (1). It is used to study thermal transitions involving energy or heat capacity changes, such as melting, glass transitions, recrystallization, mesomorphic transition temperature, corresponding entropy and enthalpy changes, and exothermic decompositions of various materials with great sensitivity (2). The technique was first developed by E.S. Watson and M.J. O'Neill in 1960 (3).

8.2 Basic principle and Instrumentation

Calorimetry is generally based on the following relationship:

$$\delta Q = C.\ \Delta T = c.m.\ \Delta T \qquad \text{(Equation 8.1)}$$

Assuming that time is independent of sample mass and specific heat capacity, the differential form can be presented as:

$$\frac{\delta Q}{\delta t} = \Phi = C. \frac{dT}{dt} = c.m.\beta \qquad \text{(Equation 8.2)}$$

where (δQ) is the heat exchanged; (ΔT) is the temperature change; (Φ) is the heat flow rate; (C)is the heat capacity, (c=C/m) is the specific heat capacity, m is the sample mass and β is the scan rate. In most differential scanning calorimeters, there are two sample positions:

In most Differential Scanning Calorimeters, there are two sample positions; sample pan or a crucible containing material under investigation and the reference pan (empty crucible or sometimes containing inert material). The crucibles are generally made of a nonreactive materials such as aluminum, quartz glass, platinum, stainless stell, nickel, etc (4). The crucibles are either crimped: with a lid; kept open; or with a pinhole on top of the lid, depending upon the study. Both pans are maintained at temperatures predetermined by isothermal or gradient programming. The sample and reference pans are heated electrically by a heater to maintain the programmed temperature at a specific heating rate in an inert atmosphere of nitrogen gas purge at constant pressure. The amount of heat or energy to be supplied or withdrawn to maintain a zero temperature differential between sample and reference is recorded and displayed in the thermogram. Thus, any change in specific heat produces discontinuity in power signal and produces exothermic or endothermic peaks in the thermogram. The area under the curve is proportional to the total enthalpic change (5).

DSCs are generally operated by two modes depending on the heating rate; constant heating rate and variable heating rate (5). Constant heating rate mode follows the time law as given below:

$$T(t) = T_0 + \beta_0.t \qquad \text{(Equation 8.3)}$$

Where (T_0) is the starting temperature, (β_0) is the heating or cooling rate and (t) is the time. The equation gives the linear relationship between temperature and time. The constant heating rate mode is of two types: isothermal mode and scanning mode. In the isothermal mode, the heating rate (β_0) is zero i.e. (T_0) is kept constant. In the scanning mode, the temperature changes linearly with time and heat flow rate may be represented as follows:

$$\Phi (T,t) = \Phi_0 (T) + \Phi cp (T) + \Phi r (T,t) \qquad \text{(Equation 8.4)}$$

Where (Φ_0) (T) is caused by asymmetry of the DSC, (Φcp) (T) is caused by difference in heat capacity between the sample and reference, wherease (Φr) (T,t) is caused by latent heat changes occuring in the sample.

The variable heating rate (Modulated temperature) employs a modulation term in the temperature-time function as follows (6):

$$T(t) = T_0 + \beta_0.t + T_A. \text{Sin } (\omega t) \qquad \text{(Equation 8.5)}$$

Where (T_A) is the amplitude and (ω) is the angular frequency of modulation. There are various types of modulated temperature modes, such as the quasi-iosthermal mode,

heating-cooling mode, heating only mode, heating-iso mode, sawtooth mode and stop scan mode (7).

There are two basic types of Differential Scanning Calorimeter units that are recognized: a) Heat Flux DCS and b) Power Compensated DSC

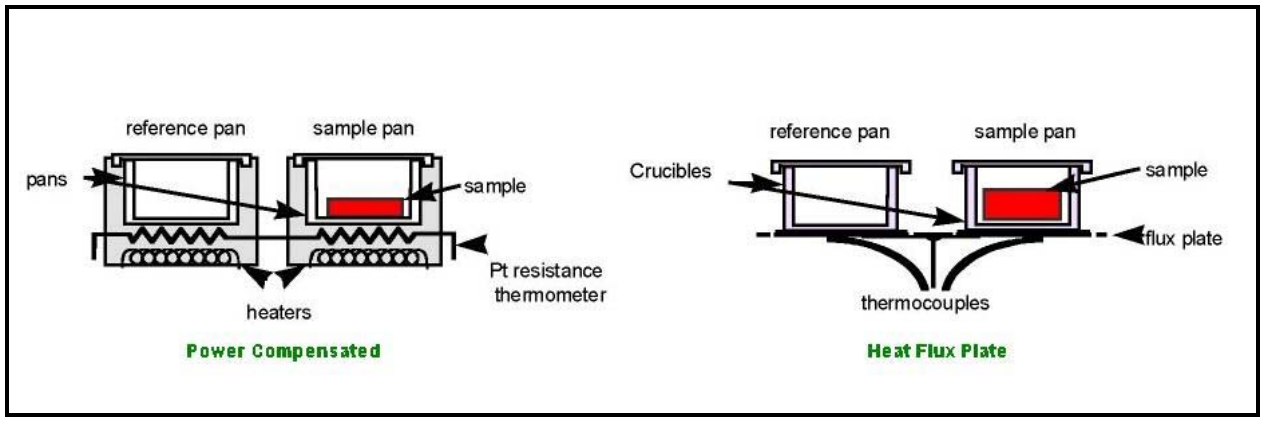

Figure 8.1: Schematic diagram of the Power compensated and the Heat Flux DSC (8)

The heat flux DSC belongs to the class of heat-exchanging calorimeters in which sample and reference pans are placed in a single furnace (9). A Platinum resistance thermometer or thermocouple is used to measure the temperature differential which is converted to energy flow via a mathematical equation. There are three major types of measuring systems used in heat flux DSC: disc type, turret type and cylinder type (10).

Power compensated DSC belongs to the class of heat compensating calorimeters in which the heat to be measured is compensated with electric energy. The system is maintained in

a thermal null state at all times by holding the sample and reference pans separate with its own heating element (9).

In order to ensure trustworthy and reproducible results for the DSC methods, the instrument needs to be routinely calibrated for quality assurance (9). The temperature and caloric calibration is recommended in the guidelines given by the International Confederation for Thermal Analysis and Calorimetry (ICTAC) (11). Some of the common materials recommended for temperature calibration of DSCs are cyclopentane, water, gallium, indium, tin, lead, zinc, lithium sulfate, aluminum, silver and gold (12).

8.3 DSC thermograms

DSC curves (known as thermograms) are represented as heat flow vs temperature or time. A typical DSC curve is characterized by the "baseline" (part of the curve obtained during steady state conditions when no reaction or transition occurred). The "peak" caused from transitions or reactions; "interpolated baseline"; "initial peak temperature (Ti)"; 'extrapolated peak onset temperature (T_e); peak maximum temperature (T_p); extrapolated peak offset temperature (T_c); and final peak temperature (T_f) as depicted in Figure 8.2 (5). Various thermal transition of materials can be observed such as glass transition, melting, crystallization, oxidation, decomposition as seen in Figure 8.3.

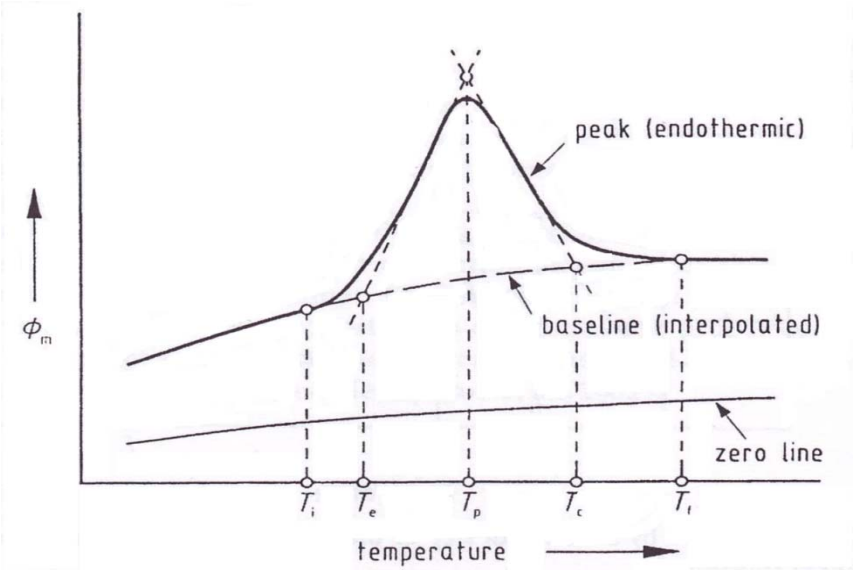

Figure 8.2: Characteristics of the DSC curve (9)

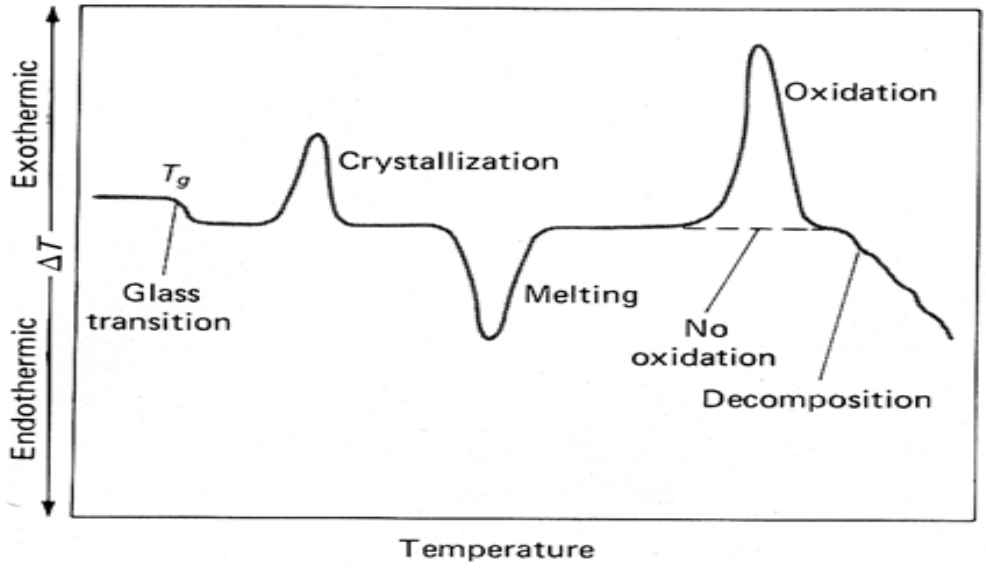

Figure 8.3: Typical DSC thermogram showing commonly observed transitions (13)

8.4 Application

DSC is routinely used in Industry for raw material inspection (QA/QC) (14), oxidative material stability (15), sub-ambient material classification (16); curing processes (17), liquid crystals (18) etc. Some of the common applications of DSC include:

- Measurement of Heat capacity (19)
- Heats of reaction (20)
- Kinetic investigation (21)
- Glass transition process (22)
- Thermal history/processing (23)
- Crystallization temperature (24)
- Degree of crystallinity (7)
- Degree of cure (25)
- Thermal safety/stability studies (11)
- Protein denaturation (26)
- Polymorphic transitions (16)
- Porosity measurements (18)

Chapter Nine

UV-Visible Spectroscopy

9.1 Introduction

UV-Visible spectroscopy is a type of absorption spectroscopy which is carried out in the UV region (approximately 200-400 nm) and visible region (approximately 400-800 nm) of the electromagnetic spectrum (1). UV-Visible spectroscopy is very useful as an analytical technique in chemical and biochemical research for two reasons: to identify some functional groups in the molecules and to determine concentration and strength (assay) of a substance (1).

9.2 Basic Principles

When light either UV or visible is absorbed by molecules, the valence electrons are promoted from their normal state to a higher energy state (Figure 8.1). The color of the sample affects the absorption of photons in the visible ranges, where molecules undergo electronic transitions. Only (π to π^*) and (n to π^*) transitions that occur in the UV-Vis region are observed. In UV/Visible Spectroscopy, the term chromophore is used to indicate a group of atoms that absorbs radiation in the UV or visible region. They cause electronic transitions within a molecule, promoting bonding and non-bonding electrons

into higher and less stable antibonding orbitals (2). Generally, chromophores are conjugated species, such as alkenes, aromatics, conjugated dienes, trienes etc. The absorption of UV-visible light typically leads not to single, sharp lines as sometimes observed in IR absorption, but to broad bands. Due to the contribution of vibrational and rotational energy levels of these electronic transitions, broad spectra are obtained.

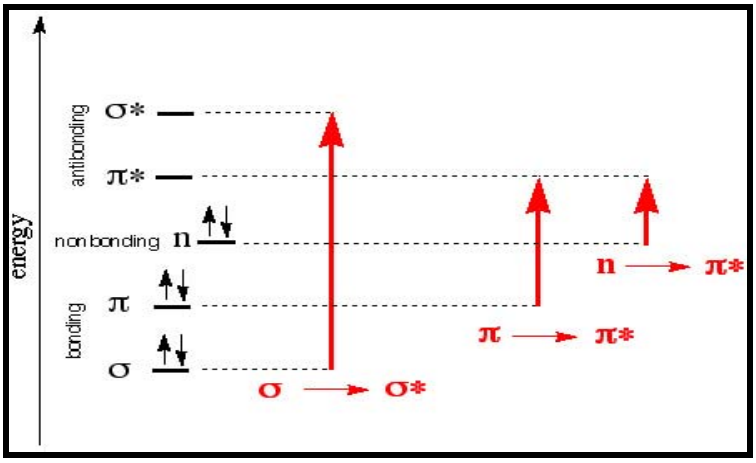

Figure 9.1: Hypothetical energy diagram showing possible electronic transitions (3)

Most of the UV-Visible spectra of compounds in solution obey the Beer-Lamber law (4). According to the Beer-Lambert law , the absorbance of a solution is directly proportional to the concentration of the absorbing species in the solution and the path length. Thus, for a fixed path length, UV/VIS spectroscopy can be used to determine the concentration of the absorber in a solution by using the equation given below.

$$A = -\log_{10}(I/I_0) = \epsilon \cdot c \cdot L \qquad \text{(Equation 9.1)}$$

where (*A)* is the measured absorbance, (I_0) is the intensity of the incident light at a given wavelength, (*I)* is the transmitted intensity, (*L)* the pathlength through the sample, and (*c)* the concentration of the absorbing species. For each species and wavelength, (ε) is a constant known as the molar absorptivity or extinction coefficient which is the fundamental molecular property in a given solvent, at a particular temperature and pressure.

There are a few terminologies used in UV-Visible spectroscopy which must be employed. A bathochromic shift is the change of absorption to a longer wavelength. A hypsochromic shift is the change of absorption to a lower wavelength. A hyperchromic shift is the increase in absorption intensity while a hypochromic shift refers to a decrease in absorption intensity.

9.3 Instrumentation

A UV-Visible Spectrophotometer consists of a light source (deuterium and tungsten-halogen lamps), dispersion element (prism, grating monochromator, interferometer), sample compartment and cells (cuvette, 96-well plate), detector (photomultiplier tubes, photodiode array, CCD cameras) and a data acquision system (computer) (2,5). The spectrophotometer may be of two types: single beam (Figure 9.2) or dual beam (Figure 9.3).

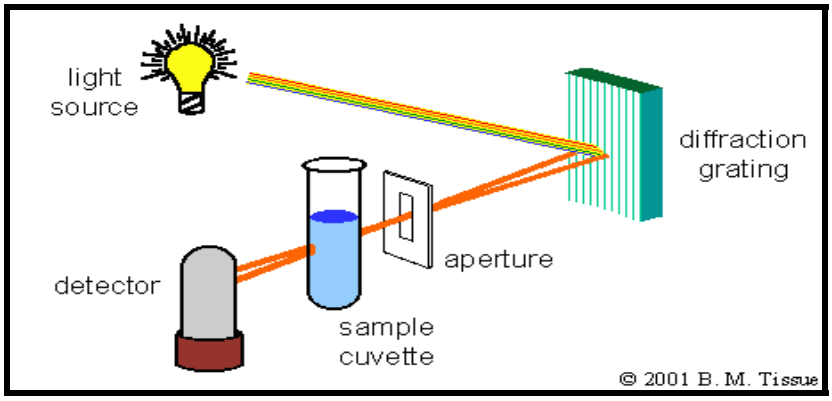

Figure 9.2: Schematic of a single-beam UV-Vis spectrophotometer (6)

In a single-beam instrument, the transmittance of the sample and solvent (reference) at each wavelength is measured manually, whereas the double-beam measures the transmittance of the sample and solvent simultaneously by splitting the single beam of light into two halves. Complete absorption spectra for a compound can be obtained by scanning the sample in the desired wavelength range.

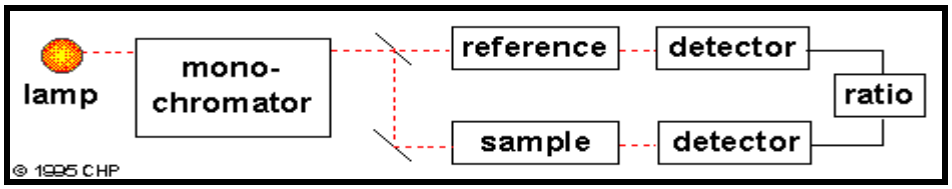

Figure 9.3: Schematic of a dual-beam UV-Vis spectrophotometer (7)

9.4 Sample preparation

Samples for UV-Visible spectroscopy are most often solutions. In special cases, gases and even solids can also be analyzed. Samples are typically placed in a transparent cell,

known as a cuvette made of high quality fused silica, quartz glass or plastic. These materials are transparent throughout the UV, visible and near infrared regions. The solvents used should have negligible absorbance in the UV region (2). Commonly used solvents are acetonitrile (190 nm), water (191 nm), cyclohexane (195 nm), methanol (201 nm), ethanol (204 nm), ether (215 nm), methylene chloride (220nm) etc.

9.5 Application

UV-Visible spectroscopy is routinely used to for quantitative determination of wide range of samples, solutions, such as inorganic anions, transition metals, inorganic complexes, organic complexes, highly conjugated organic compounds including drugs (8), biomolecules such as proteins (9-11) and nucleic acids (12,13). UV-Visible Derivative Spectroscopy is another analytical tool to study the resolution enhancement of overlapping peaks and elimination or reduction of background matrix absorption (14, 15). The Woodward Fischer Rule can be used to calculate the wavelength for maximum absorption (λ_{max}) for structural characterization of organic compounds containing conjugated systems (16).

Chapter Ten

In vitro Drug Release from Nanocarriers

10.1 Introduction

An in vitro drug release study is an integral part of characterization for any drug delivery system. It is considered an indicator of batch to batch variability associated with quality control (1). It can discriminate between various batches for the same formulation consisting of the same ingredients at various levels. Most interestingly, it can be used as an indicator for the in vivo performance of the formulation (2). There are several factors which can govern drug release from a polymeric nanoparticulate carrier such as: solubility; diffusion; desorption; matrix erosion; degradation; and particle size (3). No standardized methods are available to study the drug release from nanosized carries (4-5). The methods available for in vitro drug release from a nanosuspension can be classified into four categories: dialysis method; sample and separate method; flow-through cell; and in situ techniques (6).

10.2 Dialysis method

Dialysis is the separation process in which movement of molecules occurs by diffusion from high concentration to low concentration at unequal rates across a microporous membrane until equilibrium is reached (7). The artificial dialysis membrane consists of a spongy matrix of cross-linked cellulosic polymers. Each membrane has a certain porosity size rated as Molecular Weight Cut Off (MWCO). The value of the MWCO indicates that at least 90% of the molecules would be retained by the membrane. It is important to consider molecular shape, degree of hydration, ionic charge and polarity besides particle size while choosing an appropriate membrane. There are several factors which can affect the dialysis process such as: dialysis buffer volume; buffer composition; number of buffer changes; time; temperature; particle size; pore size; time; etc (8).

The dialysis method can be used to study drug release from nanosystems. Three techniques are used to investigate drug release: side-by-side diffusion cells with artificial or biological membranes; dialysis bag diffusion technique; and the reverse dialysis bag technique.

In the side-by-side diffusion cell, drug loaded nanocarrier dispersion is placed in a separate compartment (donor) while the receptor compartment is filled with buffer. Both compartments are separated by a semi-permeable dialysis membrane which allows only drug molecules to pass across the barrier. The in vitro release of various dosage forms including nanosuspensions (9-10), semisolids (11-12), and emulsions (13-14) are studied by this method. The most commonly used example is the Franz Diffusion Cell which is of two types: vertical and horizontal as shown in Figure 10.1 and 10.2, respectively. The

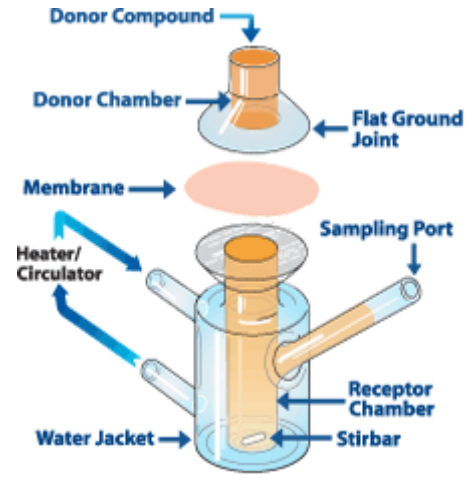

Figure 10.1: Vertical Franz Diffusion Cell (21)

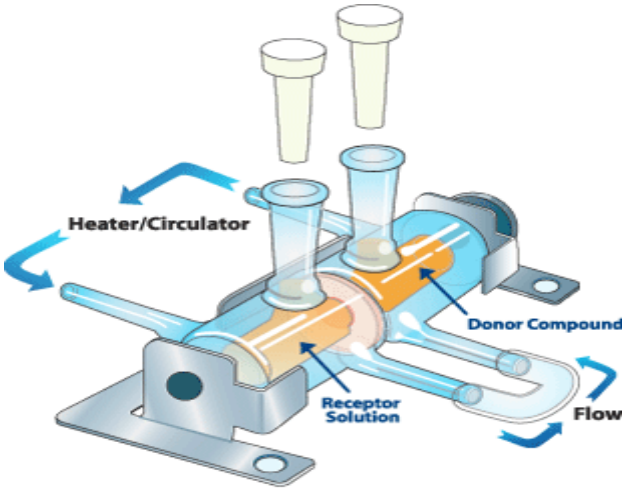

Figure 10.2: Horizontal Franz Diffusion Cell (21)

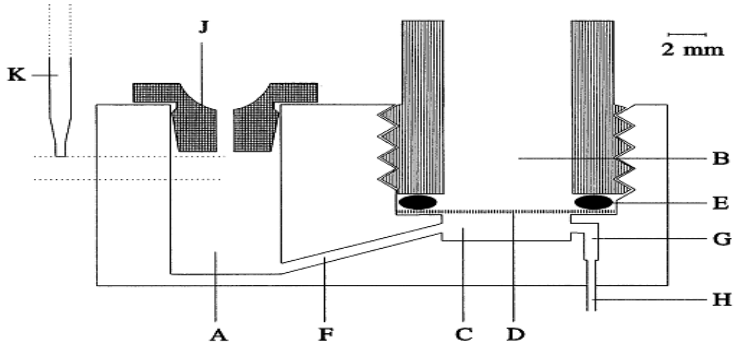

Figure 10.3: Schematic representation of the cross section of a Kelder-cell consists of inlet compartment (A), donor compartment (B), receptor compartment (C), membrane (D), o-ring (E), inlet channel (F), outlet channel (G), outlet tube (H), propylene cap (J), needle (K) (15)

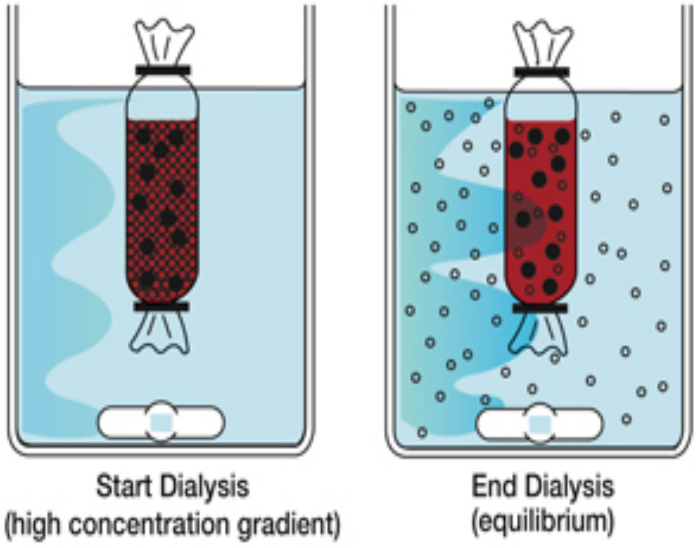

Figure 10.4: Dialysis bag diffusion (22)

cell consists of a donor compartment, receptor compartment, clamp, water jacket, and sampling port. Heated water is circulated to maintain the temperature in the cell. Another type of diffusion cell available is known as the dynamic diffusion cell, also known as Kelder-Cells shown in Figure 10.3 (15). It has an automatic sample preparation facility. The cell mimics the in vivo condition of the human skin. The volume and flow rate of the receptor solution can be controlled.

In the dialysis bag diffusion technique, drug loaded nanodispersion is placed into a dialysis bag or tube with both ends clamped. The bag is placed inside the agitated receptor compartment containing buffer medium (Figure 10.4). Several investigations have been performed to assess the in vitro release from nanosized carries. (16-19)

In reverse dialysis bag technique, the drug loaded nanodispersion is kept outside the dialysis bag. At prespecified time intervals, samples are collected from the dialysis bag containing receptor medium (20). The advantage of this method is that it leads to minimization of membrane clogging. Additionally the technique is more accurate in terms of mimicking the in vivo situation because of the infinite dilution following administration via intravenous or oral routes (14).

The disadvantage of the dialysis method is that the assessment of true drug release rate is often limited by the transportation of the drug across the membrane.

10.3 Sample and separate method

The Sample and separate method is another popular technique which provides direct and accurate measurement of in vitro drug release. In this method, the drug loaded nanodispersion is agitated in a dissolution vessel at a fixed temperature. At pre-

determined time intervals, samples are withdrawn from the release medium, separating the free drug from the bulk solution by centrifugation or filtration or centrifugal ultrafiltration and the concentration is assessed (23). Several factors commonly affect the release of drugs including container size, agitation, sampling technique, and replacement of buffer. Tube or vials are used for small volume of less than 10 mL, whereas bottles or Erlenmeyer flasks are used for large volumes (24-25). Agitation is provided by paddle, magnetic stirrer, wrist shaker, incubator shaker, shaking water bath, tumbling, etc (26). However the method suffers the drawbacks of high sampling frequency, time consuming, and difficulty in separating the released drug from the bulk mixture.

10.4 Flow through cell

The modified form of the USP Apparatus 3 (reciprocating cylinder) and 4 (flow through cell) was considered relevant for sustained release parenterals (27). In this technique, the release media is continuously circulated through a column containing the drug loaded system. Most of the apparatuses are designed in-house in order to employ a suitable modification of the system. In general, the drug loaded particles are dispersed in a small volume of the release media and kept inside a filtration cell. The constant flow of buffer is accomplished using a pump in order to maintain a constant volume in the cell. A sample is withdrawn, collected and analyzed. A schematic diagram of the apparatus used to study the release from microparticles is seen in Figure 10.5. The most important parameter affecting drug release by this method is the flow rate.

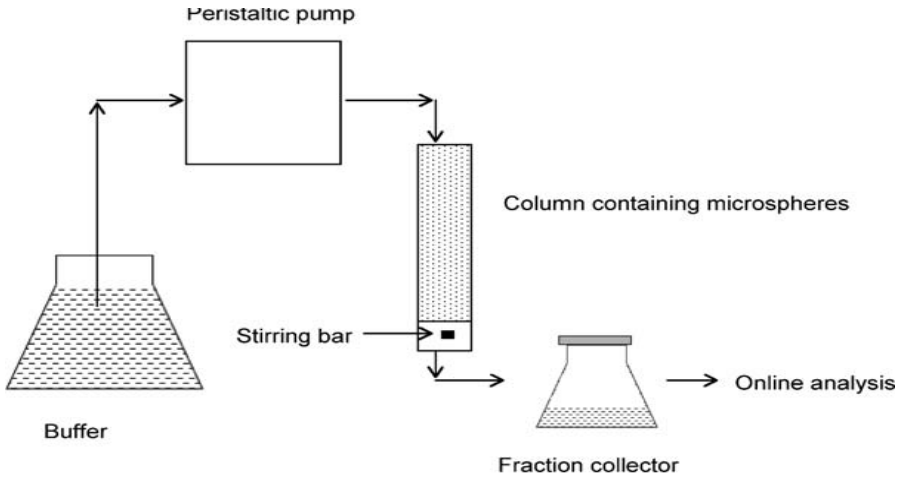

Figure 10.5: Schematic diagram of the flow through cell (28)

A lower flow rate causes incomplete hydration of the nanoparticles and results in a lower cumulative release. Higher flow rate can cause higher cumulative drug release. Additionally, replacement of the buffer to maintain sink condition is desired. The method has advantages such as: simulation of the in vivo condition; automated process; and continuous analysis of the samples. The limitations include: clogging of the filter; variation in flow rate; difficulty in rapid replacement of buffer; and low flow rate with ultafilters.

10.5 In situ methods

In the in situ method, the nanodispersion is incubated and agitated similar to the sample and separate technique. The only difference between the sample and separation method is that the released drug is analyzed in the release medium without sampling or separating the drug. The method is limited in one respect in that the free and entrapped drug should

have different spectral properties in order to differentiate them in the release media. Commonly used analytical techniques include fluorescence spectroscopy (5, 29), UV-spectroscopy (30), differential pulse polarography, etc (31).

All of the above mentioned techniques have some advantages and disadvantages. The selection of the in vitro release method depends on the nature of the drug delivery as well as the physicochemical properties of the drug. Due to the time consuming and tedious nature of the flow thorugh cells and sample and separate method, the dialysis method is the preferred method for assessment of drug release from drug loaded nanocarriers.

Chapter Eleven

Materials and Methods

11.1 Materials

11.1.1 Sulfacetamide

11.1.1.a Introduction

Source: Spectrum Chemical Mfg. Corp., Lot No. JI267, CAS # 144-80-9

Chemical Name: N-[(4-aminophenyl)sulonyl]acetamide

Molecular Formula: $C_8H_{10}N_2O_3S$

Molecular Weight: 214.243

Structural Formula:

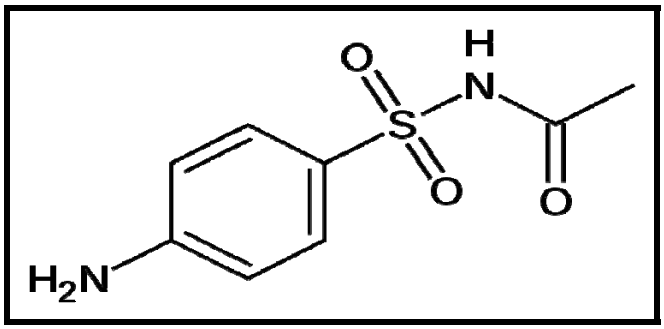

Figure 11.1: Chemical Structure of Sulfacetamide (1)

11.1.1.b Description

Sulfacetamide is a white, crystalline powder which is odorless and has characteristic sour taste. The drug is weakly acidic in nature (pKa 5.4), slightly soluble in its base form and melts between 182^0C to 184^0C. It has solubility of 1 gm in about 140 mL of water. It is also soluble in acetone, alcohol, slightly soluble in ether, very slightly soluble in chloroform, practically insoluble in benzene, freely soluble in dilute mineral acids, potassium and sodium hydroxides (2). Solution of sulfacetamide is sensitive to light and unstable in strongly acidic or alkaline media.

11.1.1.c Therapeutic use, mechanism of action, dose and toxicity

Sulfacetamide is a member of the sulfonamide class of drugs or "sulfa drugs". The drug is mainly used to treat pink eye or conjunctivitis(3-6), blepheritis(7-9), trachoma (10-11), keratitis (12-15), corneal ulcers (16-17) and other ocular diseased conditions (18, 19). Apart from ocular uses, sulfacetamide is used topically for skin diseases (20-22) and orally as an antibacterial agent in the therapy of urinary tract infections(23). It has plasma half life of 7 to 12.8 hrs (27).

Pharmacologically sulfacetamide is bacteriostatic in nature. The Woods-Fields theory is the most widely accepted mechanism of sulfa drugs including Sulfacetamide (24, 25). It concludes that sulfonamides inhibit bacterial synthesis of dihydrofolic acid by preventing condensation of pteridine with aminobenzoic acid through competitive inhibition of the enzyme dihydropteroate synthetase. It is also claimed to have antifungal property of the metal complexes of sulfacetamide derivatives by a CYP51A1-independent mechanism

(26). The usual adult dose for conjunctivitis is 1 to 2 drops into the conjunctival sac every 2 to 3 hrs for 7 to 10 days (27).

Sulfacetamide sodium USP is marketed as 10% ophthalmic solution under the brand names Bleph®, Ocu-sul®, AK-Sulf®, FML-S®, Blephamide® (27). The drug is available as a topical lotion for the treatment of acne and dermatitis under the brand names Ovace® and Plexion® (27). Adverse effects include headache, blurred vision, hypersensitivity reactions, exfoliative dermatitis (27).

11.1.2 Eudragit® RL100

11.2.2.a Introduction

Source: Röhm GmbH & Co. KG, Lot # 8370806103

Chemical Name: Ammonio Methacrylate Copolymer, Type A USP/NF

Molecular Weight: 150,000 (approx)

Structure Formula:

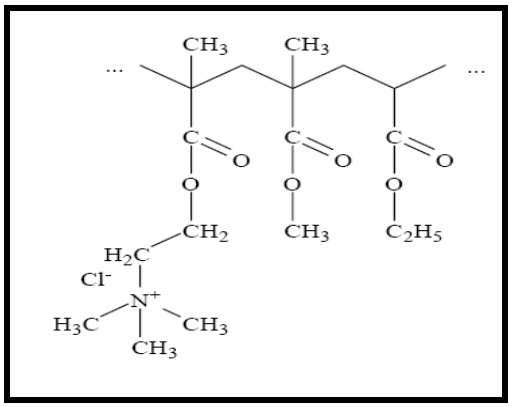

Figure 11.2: Chemical structure of Eudragit®RL 100 (28)

11.2.2.b Description and physical properties

Eudragit®RL 100 appears as a colourless, clear to cloudy granules with a faint amine-like odour. It has solubility of 1 g in 7 g aqueous methanol, ethanol and isopropyl alcohol, acetone, ethyl acetate, methylene chloride to give clear to cloudy solutions, practically insoluble in petroleum ether, 1 N sodium hydroxide and water (28).

Chemically, Eudragit®RL 100 is the copolymers of ethyl acetate, methyl methacrylate and a low content of a methacrylic acid ester with quaternary ammonium group (trimethylamminoethyl methacrylate chloride). The ammonium groups are present as salts and make the polymer permeable. The permeability of the polymers depends on the ratio of ethylacrylate (EA), methyl methacrylate (MMA) and trimethylammonioethyl methacrylate chloride (TAMCl) groups in the polymer. Those polymers having EA:MMA:TAMCl ratios of 1:2:0.2 (Eudragit RL) are more permeable than those with ratios of 1:2:0.1 (Eudragit RS). They are cationic in nature with 11.96% of the quarternary ammonium groups (USP/NF). They are inert polymer resins which are insoluble at physiological pH and have swelling property (28).

11.2.2.c Uses, Toxicity

They are widely used as film coating materials for solid oral dosage forms (29,30). Recently, Eudragit®RL 100 appeared to be a suitable inert nanocarrier for ophthalmic drug delivery system (31-36). They have the capability to form nanodispersions, positive surface charge (interacts with the negatively charged mucin layer of cornea), good stability, absence of any toxic or irritant effects on ocular tissues (37).

11.1.3 Pluronic® F108

11.1.3.a Introduction

Source: BASF Wyandotte Corp., Lot # WPWA-564B, CAS # 9003-11-6

Chemical Name: 2-methyloxirane; oxirane

Molecular Formula: $C_5H_{10}O_2$

Molecular Weight: 14600 (Average)

11.1.3.b Description

Pluronic®F108 is the trade name for Poloxamer 338. They are nonionic triblock copolymers consisting of a central hydrophobic chain of polyoxypropylene(poly(propylene oxide)) flanked by two hydrophilic chains of polyoxyethylene(ethylene oxide). The code "F" stands for flake solids, the first two digit multiplied by 300 indicates approximate molecular weight of the hydrophobic part while the last digit multiplied by 10 gives the percentage of polyoxyethylene content. It has melting point of 57^0C and an HLB value of > 24 and is soluble in cold water (38).

11.1.3.c Uses, Toxicity

Pluronics are useful for various industrial and research purposes. Due to their amphiphilic structure, they are used as surfactants in drug delivery systems including nanoparticles (39-41), transdermal gels (42). In bioprocess, they are added in culture media to provide less stressful conditions for cells (43, 44). They are slightly hazardous in case of skin contact (irritant), eye contact (irritant), ingestion or inhalation (45)

11.1.4. Acetone

11.1.4.a Introduction

Source: Fischer Scientific, Lot # 083349, CAS # 67-64-1

Chemical Name: Dimethyl ketone, 2-propanone

Molecular Formula: C_3H_60

Molecular Weight: 58.08

Structural Formula:

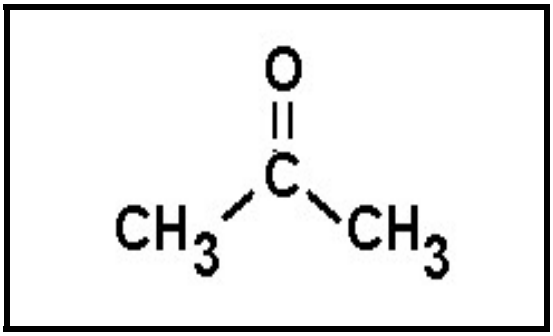

Figure 11.3: Chemical structure of acetone (46)

11.1.4.b Description

Acetone is a colorless, clear, volatile inflammable liquid with a characteristic odor. It has boiling point of 56.53^0C, specific gravity of about 0.785, congeals at about – 95^0C, viscosity of 0.3075 cp. Acetone is miscible with water, alcohol, ether, chloroform and with most volatile oils.

11.1.4.c Uses, Toxicity

Acetone is used as a a polar aprotic solvent in variety of organic reactions, by the pharmaceutical and chemical industry and as a denaturation agent in denatured alcohol

(47), cosmetic uses (48). Acetone exhibits moderate toxicity to CNS, eye and pulmonary system (49).

11.2 Methods

11.2.1 Preparation of Nanosuspension

The Eudragit® RL 100 nanoparticles were prepared by nanoprecipitaion method similar to that employed by Fessi et al (50) and other authors (51-56). Briefly, a 100 mg portion of Eudragit® RL100 and various proportions of drug were dissolved in 10 mL of acetone. This organic phase was poured dropwise into 20 mL of a 1% w/v of Pluronic® F-108 solution with moderate magnetic stirring at room temperature. Nanoparticles were spontaneously formed and turned the solution slightly turbid. Then, acetone was removed by continuing stirring for 20 hrs. The resulting particle suspension was filtered through 1.2 μm cellulose nitrate membrane filter in order to remove larger particle aggregates. The prepared suspension was centrifuged at 19,000 rpm at 15^0C f or 2 hours (Sorvel RC-5B refrigerated superspeed centrifuge, rotor SS-34, 33300g, K 446). The supernatant was removed and the sediment was freeze dried for 48 hrs for further analysis.

11.2.2 Particle size analysis and zeta potential measurement

The mean particle size for the formulations was determined by Photon Correlation Spectroscopy (PCS) with a Zetasizer Nano ZS-90 (Malvern Instruments Ltd., UK) equipped with the DTS softwear. The reading was carried out at a 90^0 angle with respect to the incident beam. The zeta potential was measured by a laser doppler anemometer coupled with the same instrument. A potential of ± 150 mV was set in the instrument. Disposable cuvettes of 0.75 mL capacity were used for all measurements. Statistical

analysis of the data were performed via one way analysis of variance (ANOVA) followed by Tucky test using Minitab softwear version 15.

11.2.3 Scanning Electron Microscopy

In order to examine the particle surface morphology and shape, Scanning Electron Microscopy (SEM) was used. A concentrated aqueous suspension was spread over a slab and dried under vacuum. The sample was shadowed in a cathodic evaporator with a gold layer 20 nm thick. Photographs were taken using a JSM-5200 Scanning Electron Microscope (Tokyo, Japan) operated at 10 kV.

11.2.4 Transmission Electron Microscopy

TEM helps to visualize the inherent matrix of individual particles and its shape. A drop of the suitably diluted sample was placed onto a holey carbon coated 400 mesh copper grid and dried in an oven at 40^0C for 20 minutes. The images were taken using a Hitachi Ultra-thin film evaluation system (HD-2300A) in Phase contrast, Z contrast, Secondary Electron (SE) modes.

11.2.5 Drug Entrapment Efficiency

A 20 mL portion of the freshly prepared nanosuspension was centrifuged at 19,000g for 2 hrs at 10-15^0C temperature using Sorvel RC-5B refrigerated superspeed centrifuge with rotor SS-34 at 33300 g and K 446. The amount of unincorporated drug was measured by taking the absorbance of appropriately diluted supernatant solution at 260 nm using single beam UV spectrophotometer (Genesis 10 UV, Thermoelectron Corporation, USA) against blank/control nanosuspension. By substraction from the initial amount of drug

taken, entrapment efficiency was calculated. The experiment was performed in triplicate for each batch and the average was calculated.

11.2.6 Differential Scanning Calorimetry (DSC)

DSC (model 822e, Mettler Toledo, OH, USA) with a Mettler MT50 analytical balance was used in order to analyze the thermal behaviour of different samples. Indium (3-5 mg, 99.999% pure, onset 156.6C, heat of fusion of 107.5 J/g) was used to calibrate the instrument. Samples (3-5 mg) were accurately weighed into 100 µl aluminium pans and then crimped. The thermograms were recorded over a temperature range of 10-200^{0}C at a rate of 10^{0}C/min under nitrogen purge gas at 50 mL/min. Mettler Toledo STARe softwear (version 8.10) was used to analyze data.

11.2.7 Powder X-Ray Diffractometry (PXRD)

The drug crystalline state in the polymer sample was evaluated by Powder X-Ray Diffraction (PXRD) analysis. X-ray spectra were recorded with X'Pert-PRO multipurpose X-Ray diffractometer (PANalytical, Tokyo, Japan) using Ni-filtered, CuKα radiation, a voltage of 45 kV, and a current of 40 mA with a scintillation counter. The instrument was operated in the continuous scanning speed of 4°/min over a 2θ range of 5° to 40°. The samples were grinded using a wedgwood mortar and pestle, placed into the cavity of an aluminum sample holder and packed smoothly using a glass slide. The results were evaluated using the X-Pert Data collector version 2.1 softwear.

11.2.8 Fourier Transform Infrared spectroscopy (FTIR)

The Fourier transform infrared analysis was conducted to verify the possibility of interaction of chemical bonds between drug and polymer. The FTIR spectrum was

performed by using a PerkinElmer 1600 spectrophotometer with a resolution of 2 cm^{-1}. The samples were scanned in the spectral region between 4000 and 400 cm^{-1} by taking an average of 8 scans per sample. Solid powder samples were oven dried at around 30^0C, finely crushed, mixed with potassium bromide (1:10 ratio by weight) and pressed at 15000 psig (using a Carver Laboratory Press, Model C, Fred S. carver Inc., WIS 53051) to make disc. The detector was purged carefully by clean dry nitrogen gas to increase the signal level and reduce moisture. For the analysis of the data, the spectrum GX series model softwear was used.

11.2.9 In vitro drug release study

The Static Franz diffusion cell was used for studying the *in vitro* release of the nanosuspension (Fig 4 shown). A cellulose acetate membrane (Dialysis membrane with molecular weight cut off value of 12,000-14,000, Spectra/por molecular porous membrane tubing, 25 mm diameter, Spectrum Medical Industries Inc., CA 90060) was adapted to the terminal portion of the cylindrical donor compartment. A 10 mL portion of the nanosuspension containing drug, sufficient for establishing sink conditions for the assay was placed into the donor compartment. The receptor compartment contained 90 mL of 0.2M Phosphate buffer solution of pH 7.4 maintained at 37°C under mild agitation using a magnetic stirrer. At specific time intervals, aliquots of 1mL were withdrawn and immediately restored with the same volume of fresh phosphate buffer. The amount of drug released was assessed by measuring the absorbance at 256 nm using a single beam UV spectrophotometer (Genesis 10 UV, Thermoelectron Corporation, USA).

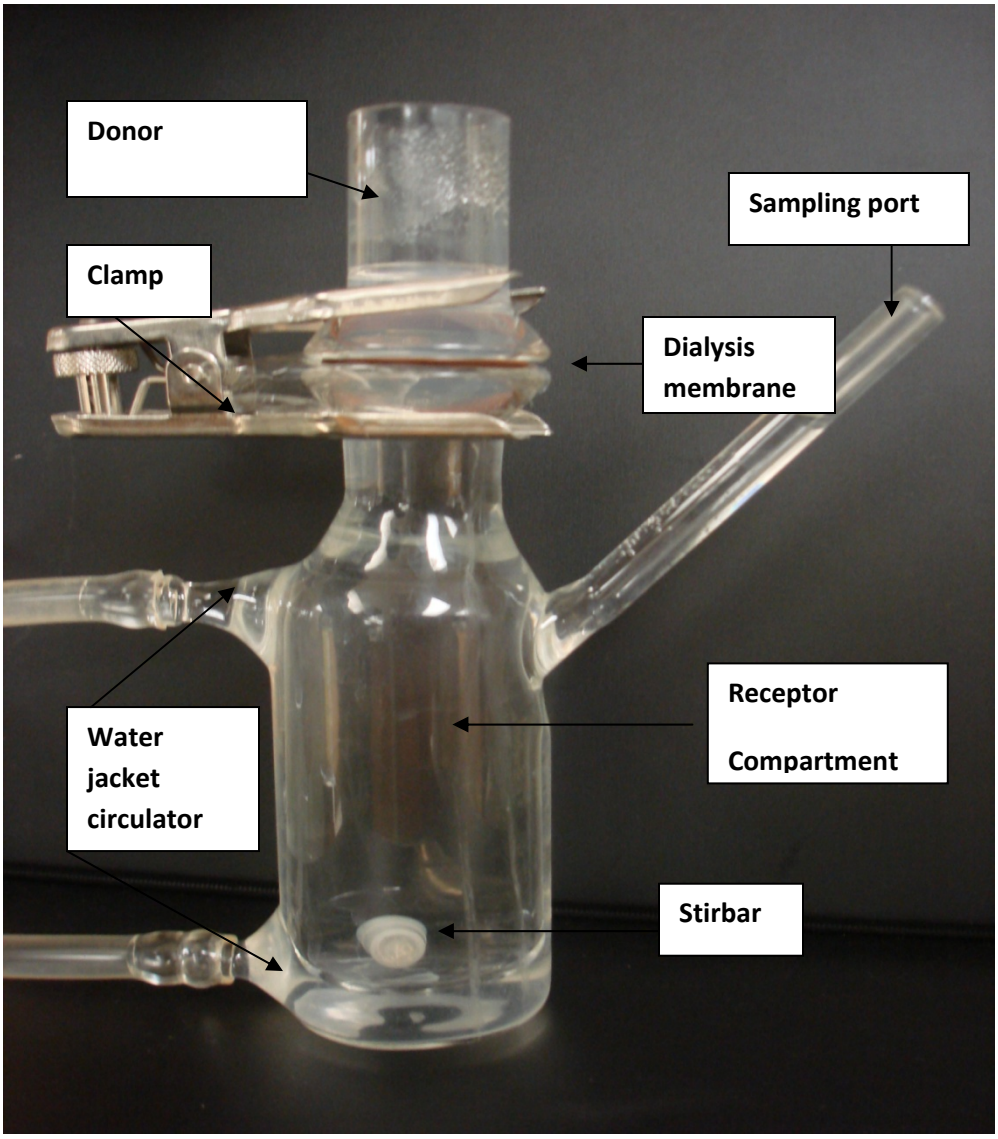

Figure 11.4: Photograph of the static Franz Diffusion cell (made in-house at Department of Chemistry, University of Toledo)

11.2.10 Kinetics of drug release

In order to analyze the drug release mechanism, in vitro release data were fitted into a zero-order (57), first order (58-60), Higuchi (61-63), Hixon-Crowell cube root law (64), Korsmeyer-peppas model (65-68).

The zero order rate Eq. (1) describes the systems where the drug release rate is independent of its concentration.

$$C = k_o t \qquad \text{(Equation 11.1)}$$

Where C is the concentration of the drug at time (t) and k_o is the zero-order release rate constant.

The first order Equation (Equation 11.2) describes the release from a system where the release rate is concentration dependent.

$$\log C = \log C_0 - kt / 2.303 \qquad \text{(Equation 11.2)}$$

Higuchi described the release of drugs from porous, insoluble matrix as a square root of time dependent process based on Fickian diffusion as shown in Equation 11.3.

$$Q = K_t^{1/2} \qquad \text{(Equation 11.3)}$$

The Hixson-Crowell cube root law Equation 11.4 describes the release from systems where there is a change in surface area and diameter of particles.

$$Q_0^{1/3} - Q_t^{1/3} = K_{HC}\, t \qquad \text{(Equation 11.4)}$$

To evaluate the mechanism of drug release, data for the first 60% of drug release were plotted into the Korsmeyer et al's equation (Equation 11.5) as log cumulative percentage of drug released vs log time, and the exponent (*n*) was calculated using the slope of the straight line.

$$Mt / M\infty = Kt^n \qquad \text{(Equation 11.5)}$$

where (M_t/M_∞) is the fractional solute release, (t) is the release time, (K) is a kinetic constant characteristic of the drug/polymer system, and (n) is an exponent that characterizes the mechanism of release of tracers (61). For cylindrical matrix tablets, if the exponent $n = 0.45$, then the drug release mechanism is Fickian diffusion, and if $0.45 < n < 0.89$, then it is non-Fickian or anomalous diffusion. An exponent value of 0.89 is indicative of Case-II Transport or typical zero-order release (62).

11.2.11 Freeze drying and redispersibility of nanosuspension

All the four batches (B1, B2, B3, B4) were freeze dried to obtain dry powder. Additionally, selected batch (B3) was taken to study effect of cryoprotectant on freeze drying and redispersibility of drug loaded nanosuspension. Two cryoprotectants were used: sucrose and mannitol both at 2.5% and 5% w/v concentration level. The nanosuspension sample was divided into four 2 mL parts and taken individually in small glass vial. Required amounts of cryoprotectants were added in each vial and shaken to dissolve. A 2 mL portion of the nanosuspension without the cryoprotectant was taken in vial as a control. The opening of the vial was covered with tissue paper wrapped by a cotton thread. The vials were placed inside a Dewar flask containing dry ice (i.e. solid

carbon dioxide) in order to supercool and freeze. The frozen samples were placed inside 600 mL Labconco® fast-freeze flask with attached adapter. Freeze-drying process was carried out in the Virtis Freezemobile model 12EL. Temperature was kept about - 70^0C and vacuum was kept at 162 mT. After 48 hours, lyophilized samples were collected and stored in dessicator for further analysis.

Redispersibility of lyophilized products was carried out by manual hand shaking in small glass vial with distilled water. Visual observation was done to investigate formation of any aggregates or precipitates after shaking. Particle size and size distribution after redispersion of the sample was performed using Zeta potential/Particle sizer (model Nicomp™ 380 ZLS, CA, USA).

11.2.12 Short term stability study of nanosuspension

Prepared nanosuspension (batch B3) was chosen to perform short term stability study of the nanosuspension. Samples were stored in glass vials for 1 month at room temperature (20^0C) and at 4^0C in freeze. After 1 month, samples were visually observed for any sedimentation. The particle size and size distribution was performed using Zeta potential/Particle sizer (model Nicomp™ 380 ZLS, CA, USA).

Chapter Twelve

Results and Discussions

12.1 Preparation of Nanosuspension

Eudragit® RL100 Nanosuspensions were successfully prepared by the solvent displacement or nanoprecipitation technique (11). The method is simple, reproducible, fast, economic and one of the easiest procedures for the preparation of nanospheres (2). Nanoparticles were spontaneously formed when the organic phase (acetone) containing Eudragit® RL 100 with/without Sulfacetamide was added dropwise into stirred aqueous surfactant solution (1% Pluronic® F 109), resulting in a transparent solution with a bluish opalescence. Instantaneous formation of a colloidal suspension occurred as a result of the polymer deposition on the interface between the organic phase and water when partially water miscible organic solvent (acetone) diffused out quickly into the aqueous phase from each transient particle intermediate. According to the "Marangoni effect", the transient particle intermediate causes a size reduction to the nano range (3). Formation of a colloidal nanodispersion can be visualized by the bluish opalescence (Figure 12.1 and

Figure 12.2). This phenomenon is known as the Tyndall effect. It is a phenomenon in which the scattering of light is caused by the dispersed colloidal particles (4).

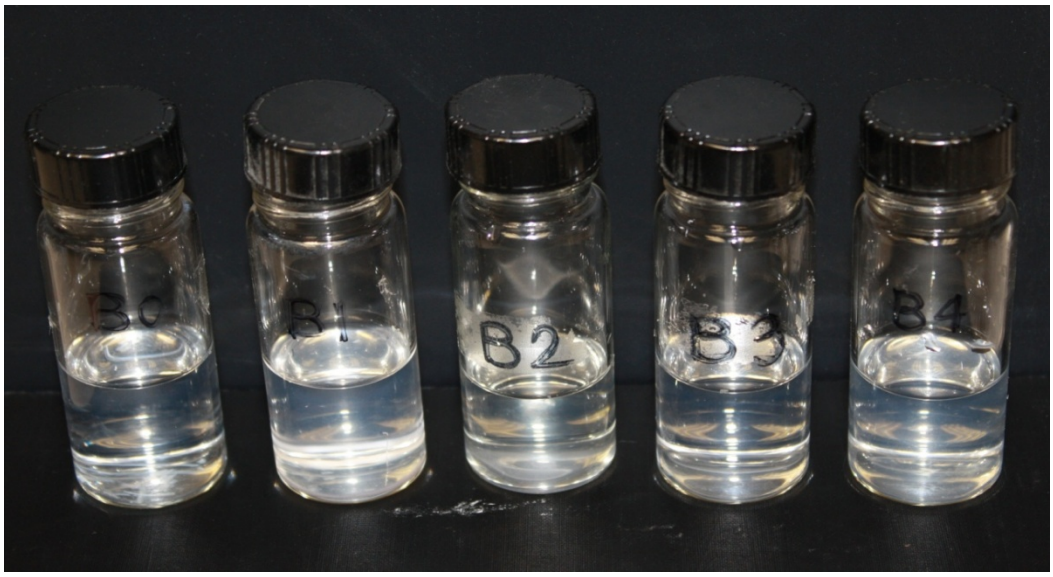

Figure 12.1: Photograph of the prepared nanosuspensions (from left to right: B0, B1, B2, B3, B4)

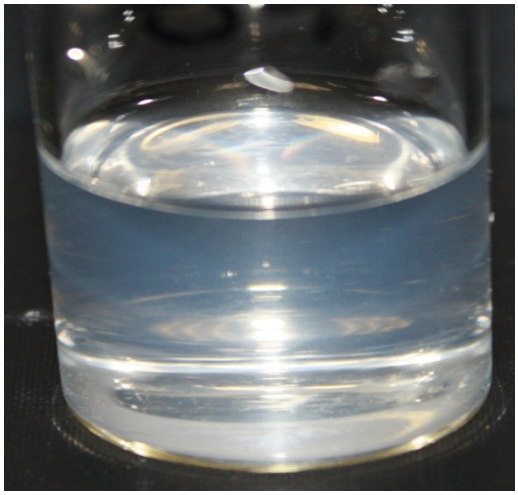

Figure 12.2: Photograph of the nanosuspension B4 showing bluish opalescence

12.2 Particle size and size distribution

The particle size and size distributions are critical parameters for ocular delivery purposes in order to avoid irritation to the ocular surface. Particle size for ophthalmic application should not exceed 10 µm (5). The United States Pharmacopoeia (USP) specifies that ophthalmic solutions should contain not more 50 particles with a diameter more than 10 µm, 5 particles with adiameter of not greater than 25 µm, and 2 particles with a diameter of not greater than 50 µm per mL of solution when using the microscopic particle count method (6). The experimental output of DLS experiments are seen in Figures 12.3 to 12.7.

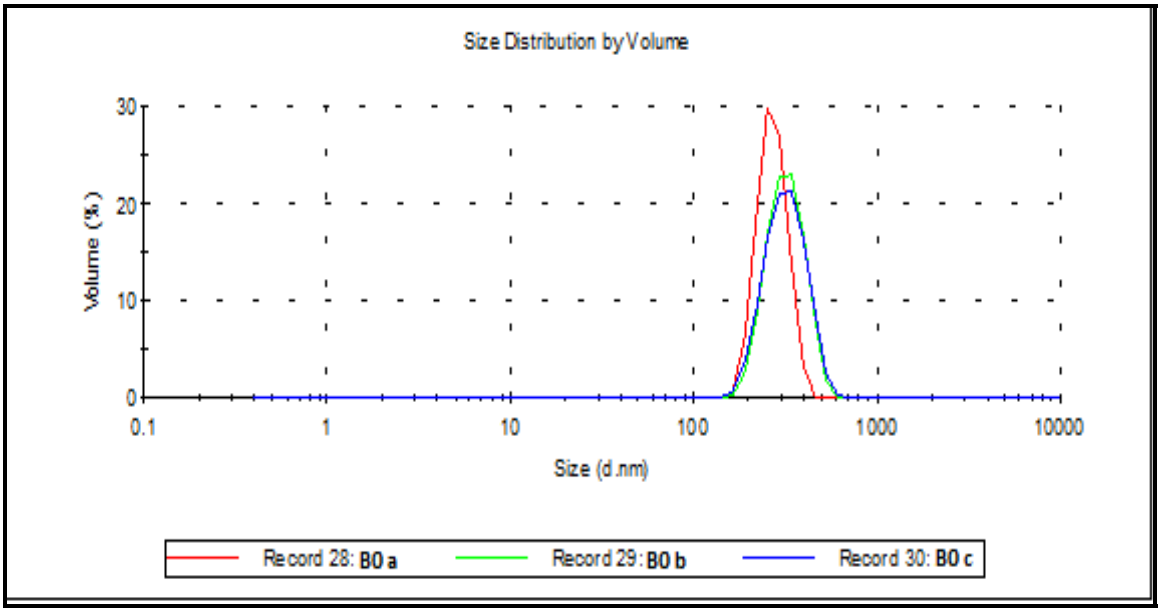

Figure 12.3: DLS plot for the size distribution vs number for batch B0 (n=3)

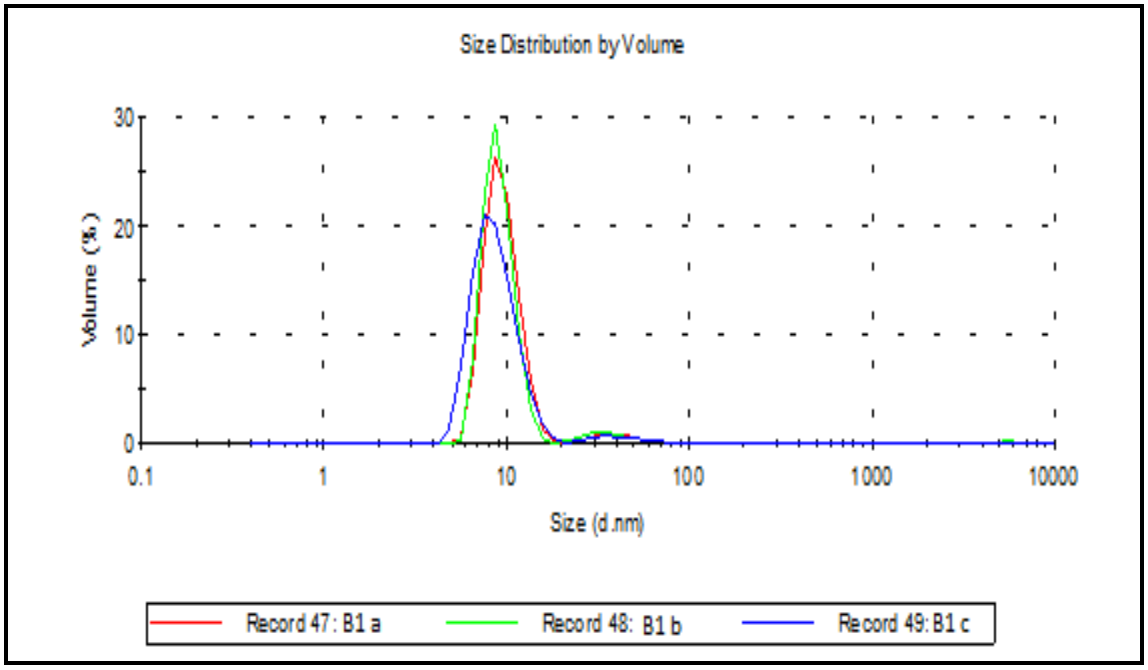

Figure 12.4: DLS plot for the size distribution vs number for batch B1 (n=3)

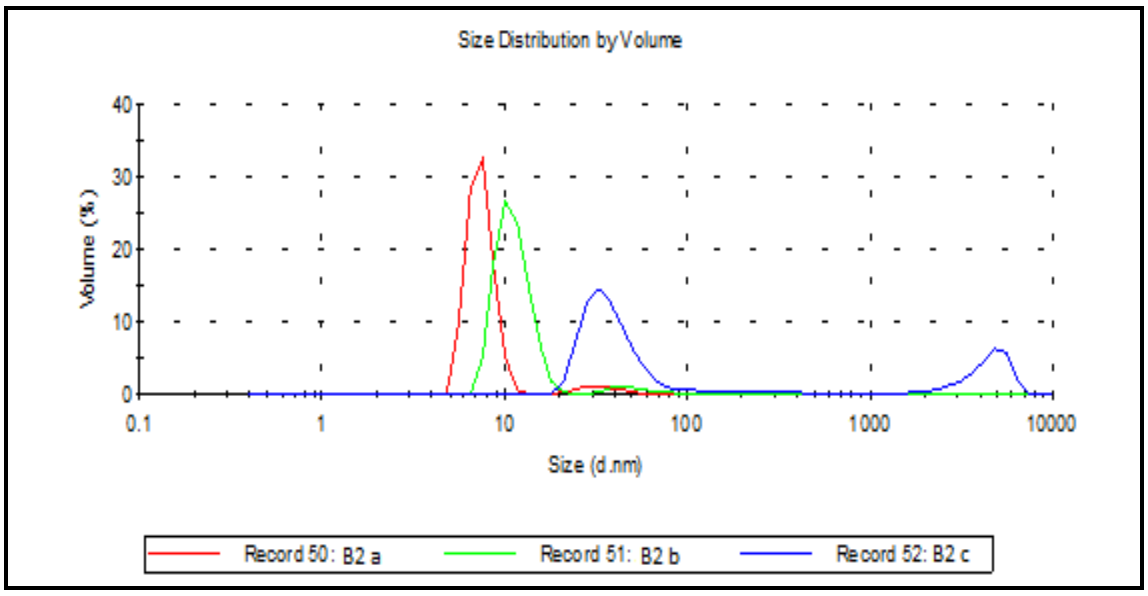

Figure 12.5: DLS plot for the size distribution vs number for batch B2 (n=3)

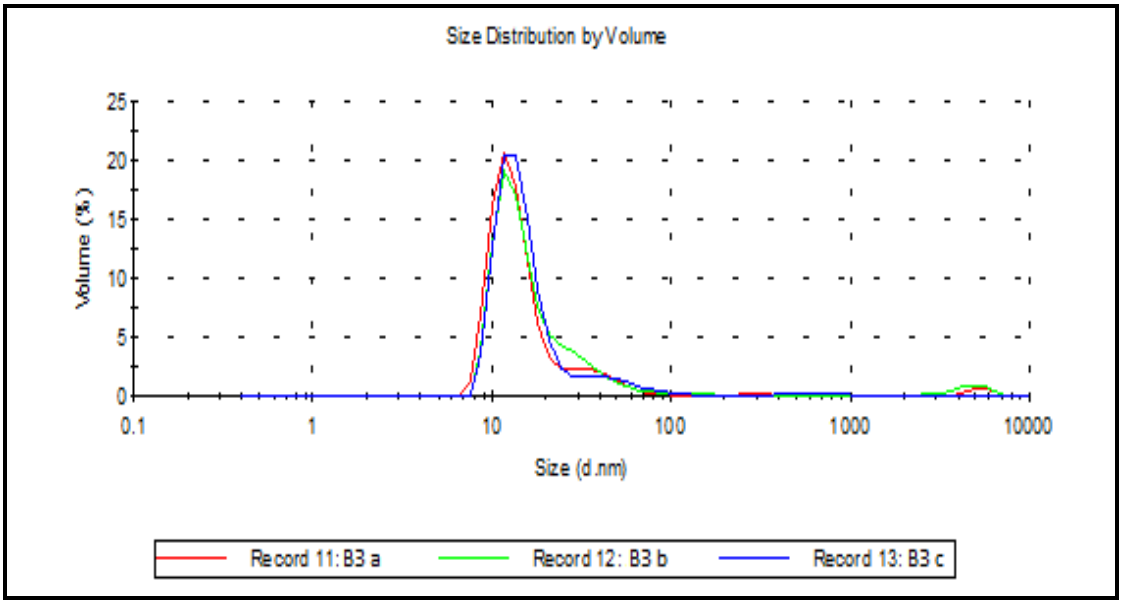

Figure 12.6: DLS plot for the size distribution vs number for batch B3 (n=3)

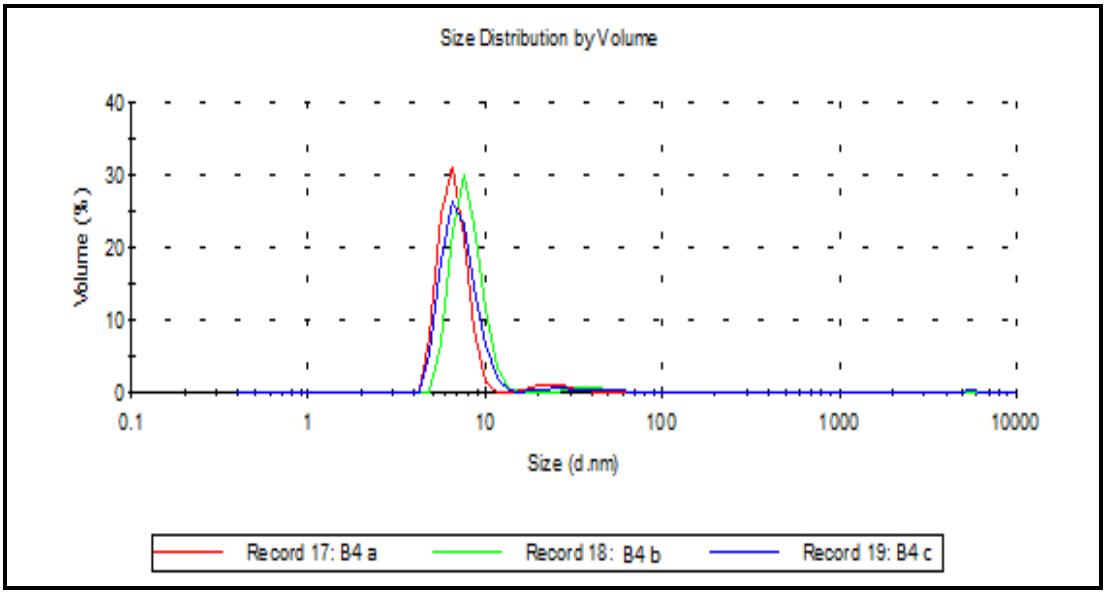

Figure 12.7: DLS plot for the size distribution vs number for batch B4 (n=3)

The effect of the drug to polymer ratio on size of the nanparticles were studied using four different weight ratios of drug and polymer, namely 10:100, 20:100, 30:100 and 40:100. Incorporation of the drug above 40% in the formulation resulted in aggregation and separation of particles to form white sediment immediately. Therefore, the study was carried out in the range of 10-40% drug incorporation in the formulation. Particle size data for nanosuspension matches was shown in Table 12.1. The batch B0 in which no drug was added showed a mean particle size of 398.1 nm and mean polydispersity index (PI) of 0.414. The mean particle size (Z-average diameter) for drug loaded batches (B1 to B4) varied in the narrow range from 112.4 nm to 140.6 nm.

Table 12.1: Particle size, Polydispersity index (PI), zeta potential of blank and Sulfacetamide-loaded Eudragit® RL100 Nanosuspensions (σ is Standard deviation, n=3)

Batch	Drug to Polymer ratio (by wt)	Z average diameter ± σ (nm)	Polydispersity Index (PI) ± σ	Zeta potential± σ (mV)
B0	0:100	398.1 ± 21.84	0.414±0.095	13.03±0.32
B1	10:100	140.6 ± 49.94	0.456±0.075	18.77±0.45
B2	20:100	127.9 ± 28.82	0.501±0.145	24.1±1.58
B3	30:100	118.9 ± 8.17	0.67±0.162	9.16±0.43
B4	40:100	112.4 ± 40.25	0.467±0.137	16.47±0.29

The mean PI values for the drug loaded formulation varied in the range of 0.456 to 0.67. It could be inferred from the results that there was no significant impact of the drug to

polymer ratio on the mean particle size of the drug loaded nanosuspension ($p < 0.05$). One way ANOVA followed by Tucky test showed that batch B0 showed significant difference in particle size compared to drug loaded batches ($p < 0.05$). Surprisingly, a trend of increasing drug content in the formulation with decreasing mean size of nanoparticles was observed. This observation is in conformity with the findings of Das et al for Amphotericin B loaded Eudragit® RL 100 nanoparticles (7). All batches of the nanoparticles showed mean sizes which were below 500 nm, therefore suitable for ocular application.

12.3 Zeta potential

The zeta potential values for nanosuspensions were shown in Table 12.1. The zeta potential remained in the range of positive values for all batches (+ 9.16 mV to + 24.1 mV) which is consistent with the findings of Pignatello et al (8). The positive surface charge of the nanoparticles was observed due to the presence of the quarternary ammonium groups of Eudragit® RL100. The positive surface charge for the nanoparticles could allow for a longer residence time for the particles by ionic interaction with the negatively charged sialic acid residues present in the mucous of the cornea and conjunctiva (9). Sulfacetamide belongs to a class of secondary sulfonamides in which the hydrogen on the nitrogen atom is acidic. Thus in basic medium, the nitrogen acquires negative charge on the conjugate base stabilized by resonance (10). The adsorbed surfactant (Pluronic® F108) present onto the nanoparticles surface may shield the particle surface, thus covering with the electrically neutral layers and causes a slight shift in

surface charge (11). The relative constancy of zeta potential with slight variation indicates that Sulfacetamide was encapsulated within the nanoparticles and a major part of the drug is not present on the nanoparticle surface.

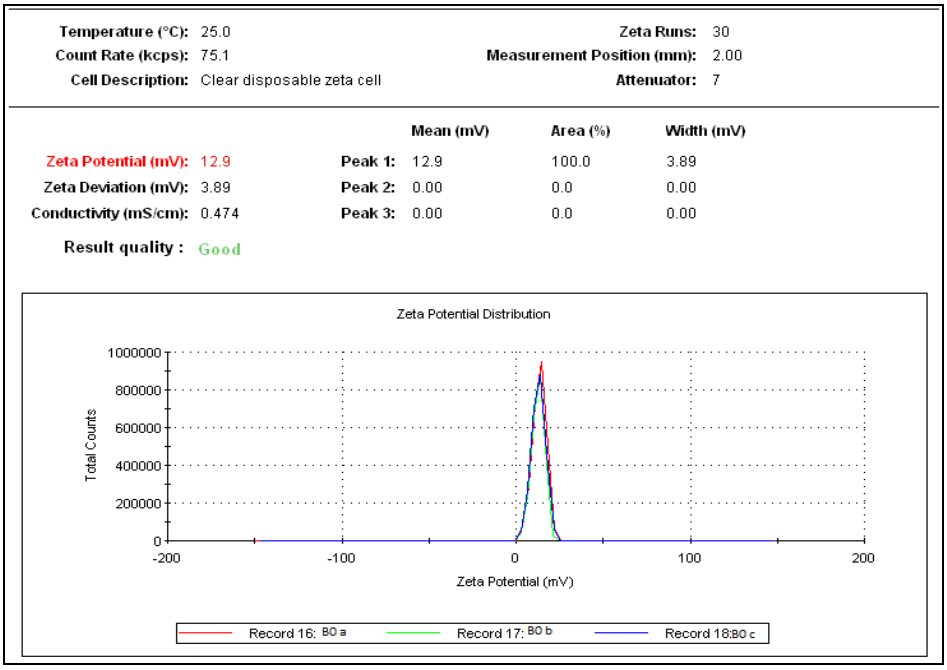

Figure 12.8: Plot of Zeta Potential distribution for the batch B0 (n=3)

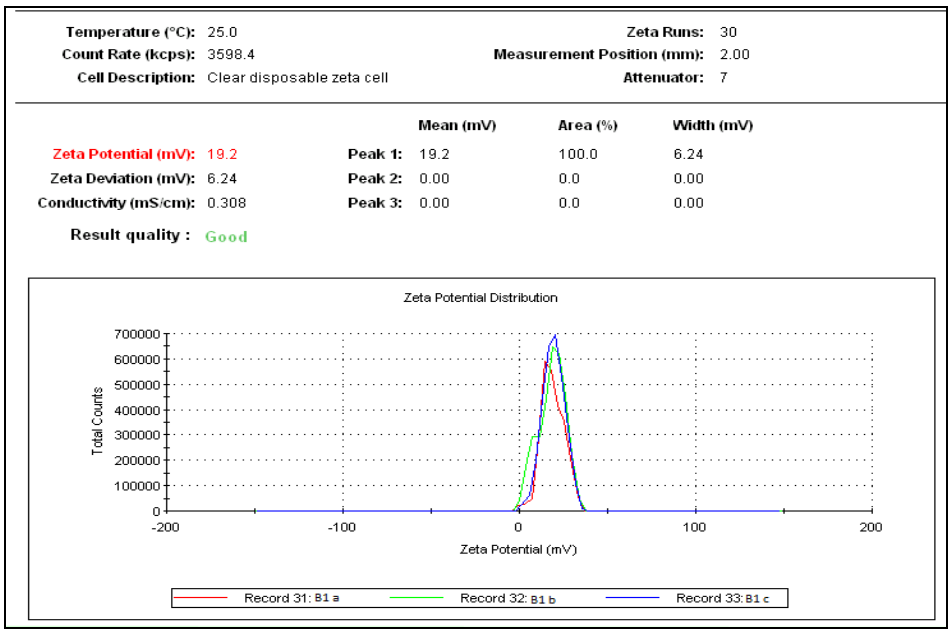

Figure 12.9: Plot of Zeta Potential distribution for the batch B1 (n=3)

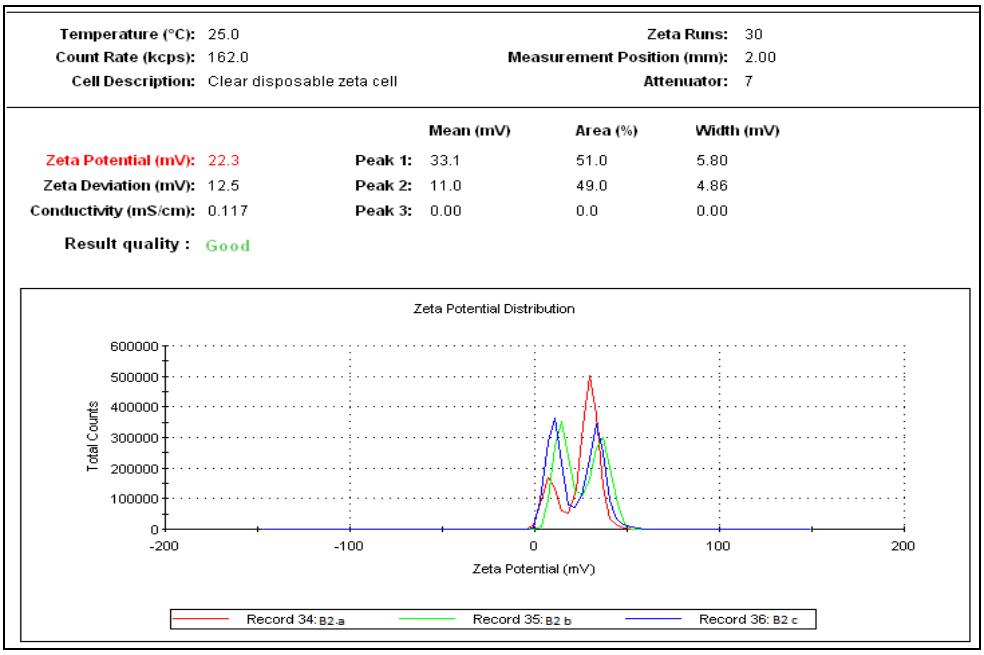

Figure 12.10: Plot of Zeta Potential distribution for the batch B2 (n=3)

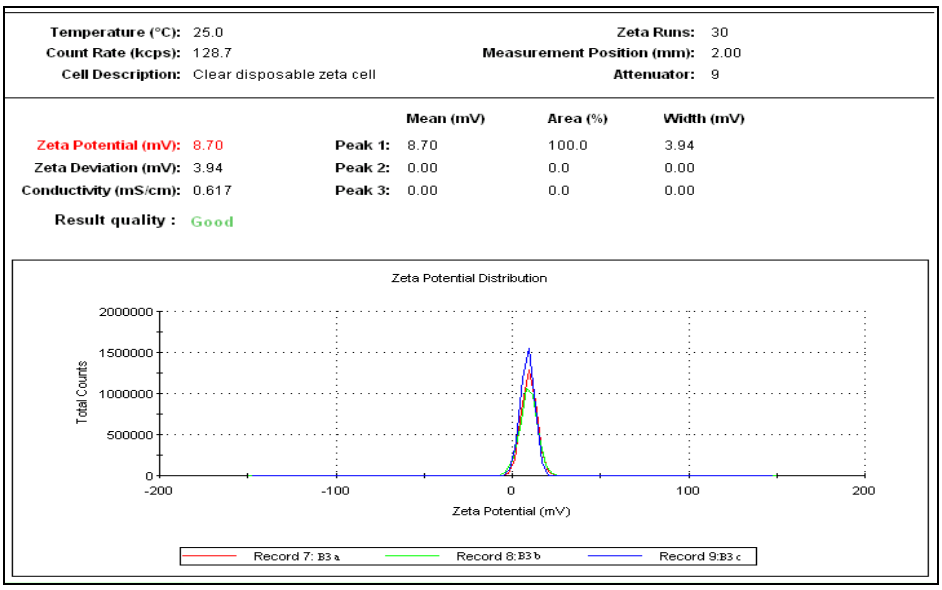

Figure 12.11: Plot of Zeta Potential distribution for the batch B3 (n=3)

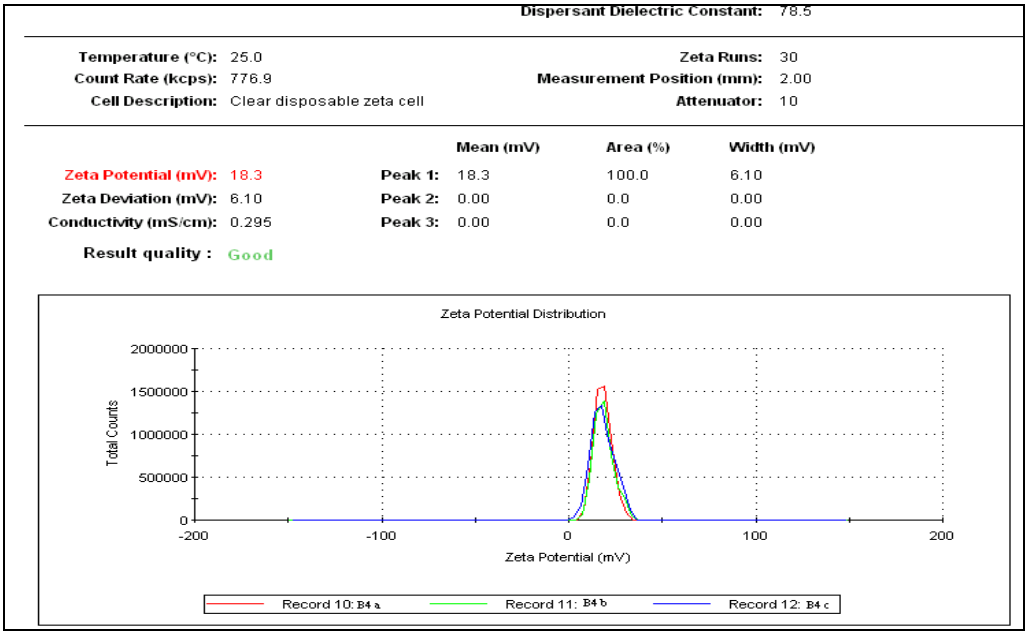

Figure 12.12: Plot of Zeta Potential distribution for the batch B4 (n=3)

12.4 SEM and TEM

Nanoparticle surface morphology and shape were visualized using SEM and TEM. SEM revealed that the blank nanoparticles were spherical to oval in shape with a larger size (Fig 12.13) whereas, the drug loaded nanoparticles were found to be distinct, spherical with a smooth surface (Fig 12.14). TEM images were also in conformity with the SEM and dynamic light scattering data for particle size. All particles were found to be spherical with a smooth surface for the various batches (Fig 12.15-17). Magnification of a single particle showed the internal cage like structure where the drug molecules are dispersed uniformly throughout the polymer matrix (Fig 12.18). The drug appears as white spots on the surface. It was observed that when a high energy electron beam were passed to scan the particles in TEM, the polymer burns out leaving the drug particles viewed as a cage like structure.

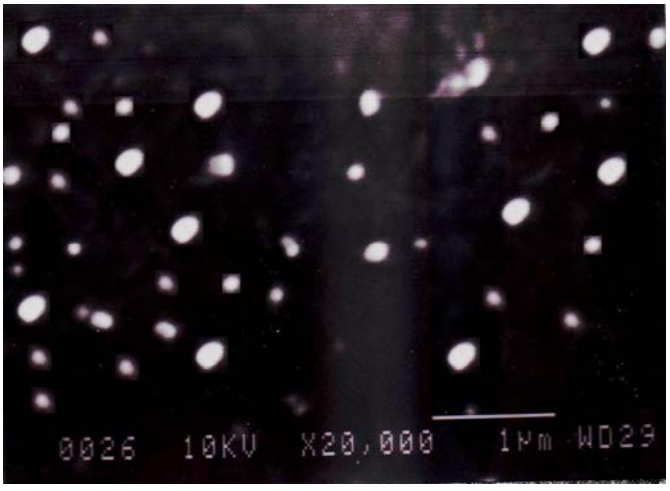

Figure 12.13: SEM image of Blank Eudragit RL 100 nanosuspension (batch B0) taken at 20,000 magnification and acceleration voltage of 10 kv.

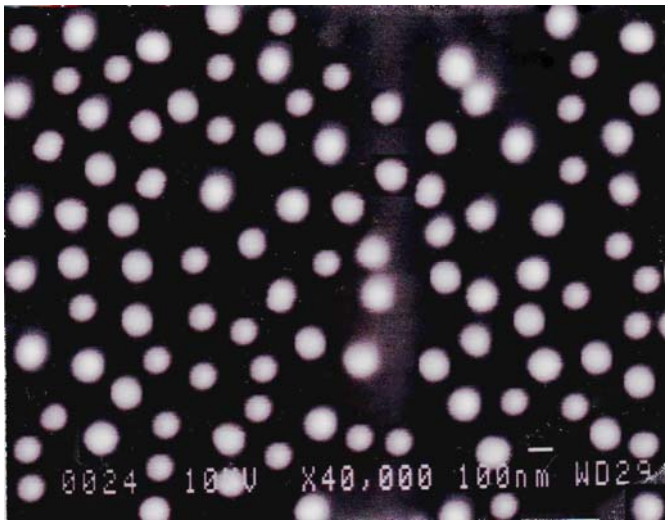

Figure 12.14: SEM image of drug loaded Eudragit® RL100 nanosuspension (batch B3) taken at 40,000 magnification and acceleration voltage of 10 kv

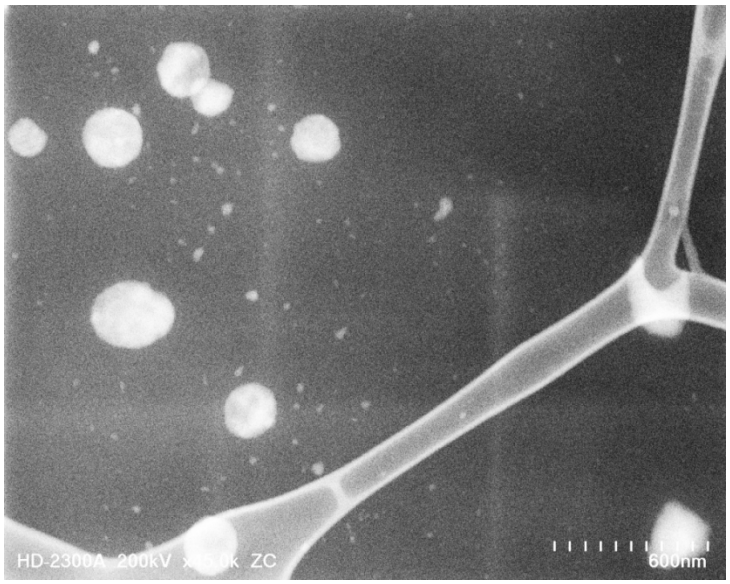

Figure 12.15: TEM image of a blank Eudragit® RL100 nanosuspension (batch B0) taken at Z contrast mode

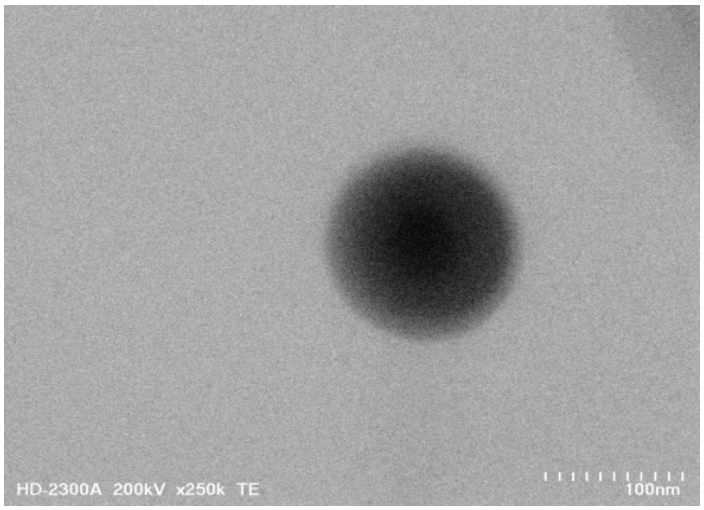

Figure 12.16: TEM image of drug loaded Eudragit® RL100 nanosuspension (batch B2)

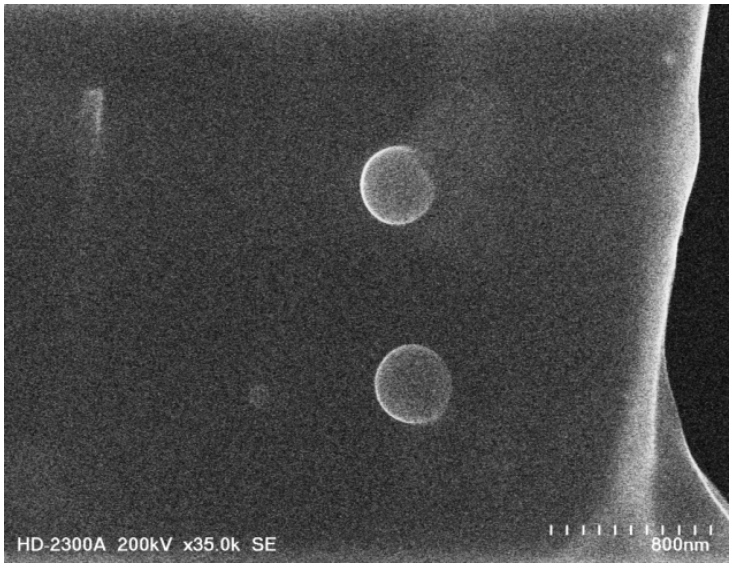

Figure 12.17: TEM image of drug loaded Eudragit® RL100 nanosuspension (batch B3) taken at the Scanning Electron mode

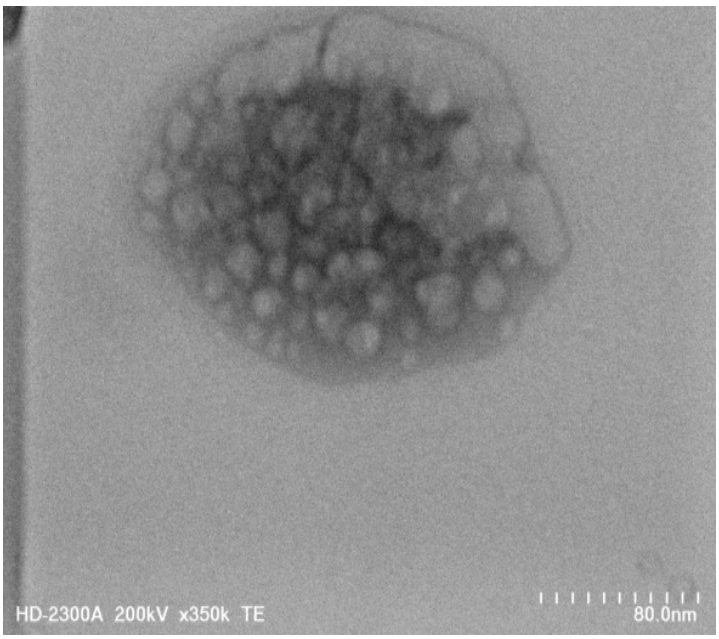

Figure 12.18: TEM image of a single nanoparticle (batch B3) showing internal structure and dispersed drug molecules in the polymer matrix

12.5 Drug Entrapment Efficiency

The indirect method was used to determine drug entrapment efficiency (DEE) (12). After preparing the fresh nanosuspension, it was centrifuged and the free drug present in the supernatant was analyzed by UV-Visible spectrophotomer using a calibration curve. The calibration curve was constructed by measuring the absorbance at 260 nm of solutions of five different concentrations of drug in water (Figure 12.19). By subtracting form initial amount of drug, DEE was calculated. The method is suitable for determining entrapment efficiency of nanosuspension when fairly high concentration of free drug is present in the supernatant after centrifugation (12). DEE of the Sulfacetamide loaded

nanosuspension was found to be in the range of 28.26 % to 35.74% for the four batches. The low DEE values indicate relatively low affinity of the drug with the polymer matrix. Another explanation for poor entrapment is probably solubility and ionization of the drug. Sulfacetamide is soluble in water and has an ionization constant of 5.4. The aqueous 1% Pluronic (surfactant) solution has a pH of about 6. Therefore, when the organic phase is added dropwise into the aqueous surfactant solution, part of the drug is ionized and escapes from the nanoparticles during diffusion of the acetone into the aqueous phase. Increasing the drug content in the formulation increased DEE inside the nanoparticles (Figure 12.20). However, when the drug content is 40% in the formulation (batch B4), saturation of the polymer particles occurs with such a high drug load. The excess drug escapes from the acetone phase into the water. Therefore, DEE dropped in

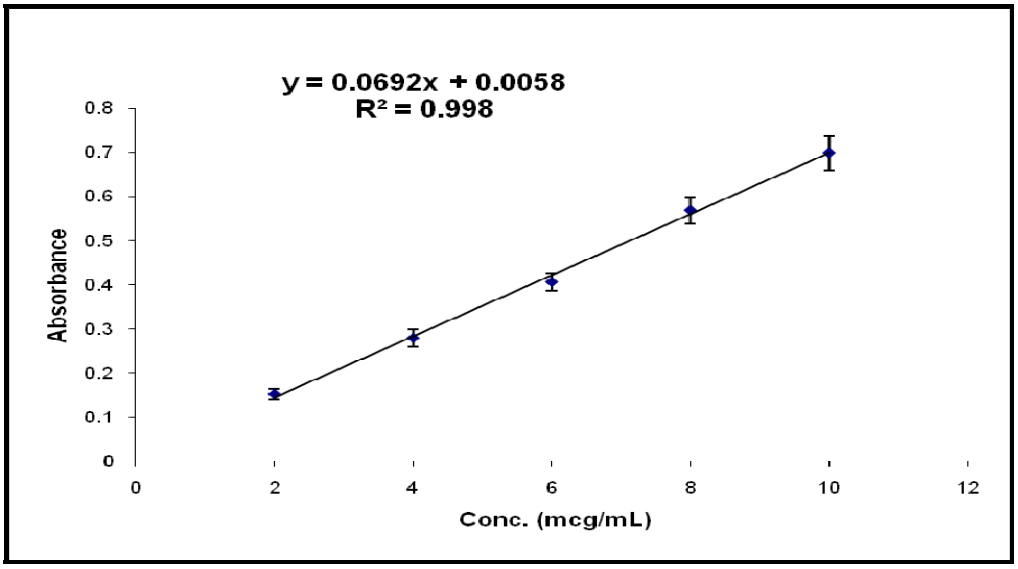

Figure 12.19: Calibration curve of Sulfacetamide in water (absorbance taken at wavelength of 260 nm) (n=3)

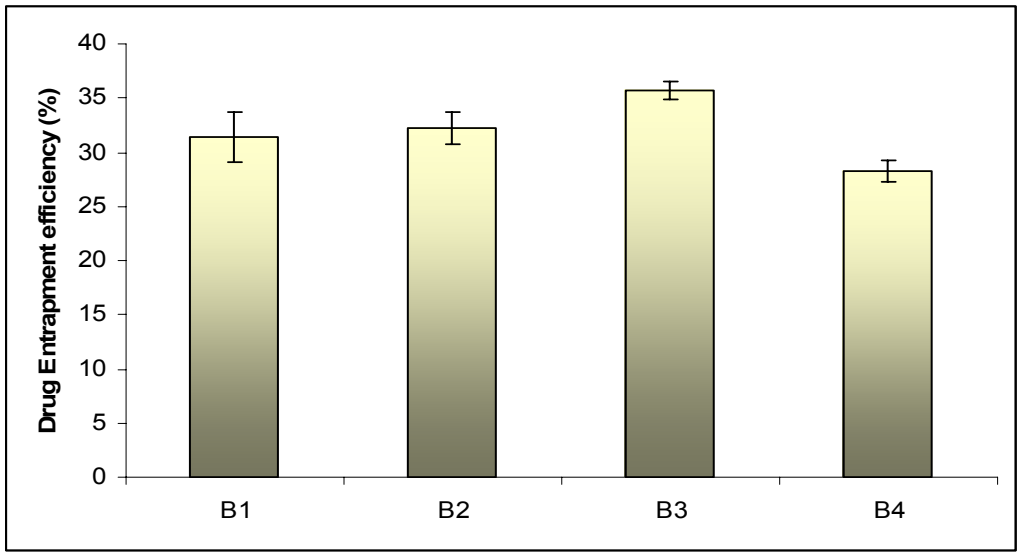

Figure 12.20: Drug entrapment efficiency of Sulfacetamide loaded Eudragit® RL100 nanosuspensions

batch B4. Another possibility for the decreased DEE at high drug content in the formulation can be explained by saturation of the cationic sites on the Eudragit® by anionic drug molecules. Therefore, excess drug is being lost from the particles during its formation process.

Three strategies were used to enhance DEE of the batch B3 such as effect of changing polymer content, changing external phase pH (13) and addition of Polymethyl methacrylate (PMMA) in the formulation (14). Changing the content of polymer in the formulation B3 did not improve the DEE of nanosuspension (data not shown). When the pH of the aqueous phase was adjusted to 3.4, significant improvement in DEE (~ 50%) was observed. This finding may be due to the suppression of ionization and decrease in

solubility of sulfacetamide during the formation of nanodroplets in solvent displacement method. Thus, drug molecules did not escape from the particles when the external aqueous surfactant solution phase was adjusted to acidic pH of 3.4, which is below the pKa (5.4) of the drug. When, 30 parts of PMMA was incorporated in B3, DEE increased to about 50%.

12.6 DSC

From the overaly of DSC thermograms, it has been observed that Sulfacetamide is crystalline in nature (Figure 12.21). It exhibited a sharp melting endotherm at an onset temperature of 180.1^0C, a peak temperature of 182.31^0C and a heat of fusion of 119.7 J/gm. The drug recrystallized at an onset temperature of 241.76, a peak temperature of 245.09 and had an energy of activation of about 80.16 J/gm. Eudragit® RL 100 polymer exists as a completely amorphous form with a glass transition temperature (Tg) of about 60^0C (15). The amorphous polymer did not show any fusion peak or phase transition, apart from a broad signal around 55–60^0C due to a partial loss of residual humidity (16).

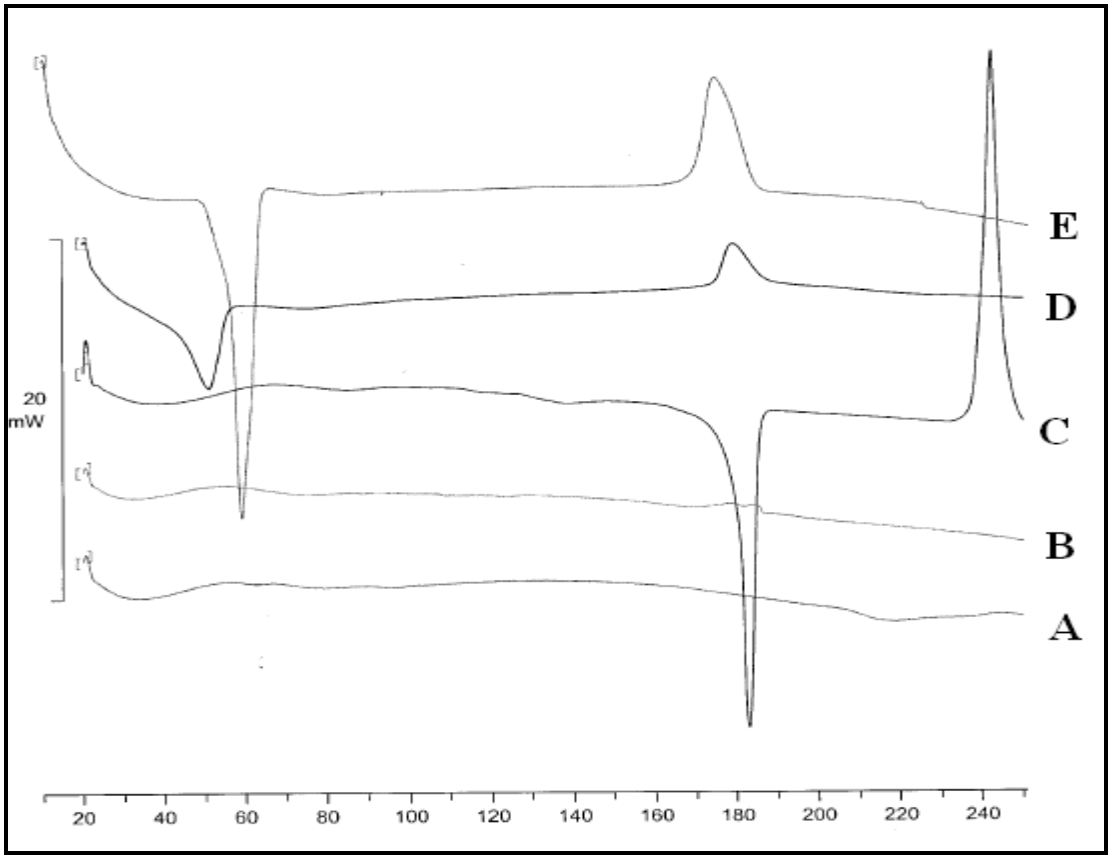

Figure 12.21: DSC thermograms of Eudragit®RL100 (A), Physical mixture of Sulfacetamide and Eudragit® RL100 (B), Sulfacetamide (C), Freeze dried nanosuspension of Sulfacetamide and Eudragit® RL100 batch B3 (D), Pluronic® F108 (E)

The thermal behavior of the freeze dried nanoparticles suggested that the polymer inhibited the melting of the drug crystals. The possible occurrence of ionic interaction may have existed in the physical mixture as observed for the furosemide and Eudragit® RL 100 system (17). However, the physical mixture of drug and polymer did not show any drug melting peak or crystallization peak. Freeze dried drug loaded nanosupension (batch B3) showed an broad endothermic transition at an onset of 21.57, a peak at

50.89^0C. Similar observation was noted for other three batches. This observation can be explained from the effect of adsorbed poloxamer as surfactant onto the drug loaded nanoparticles. Pluronic® F108 exhibited a melting onset of 55.52^0C, a peak of 58.51^0C consistent with the finding of Passerini et al (18). The exothermic crystallization peak of Pluronic® F108 was observed at an onset of 169.86^0C and a peak of 175.05^0C. The most probable reason for the appearance of slightly shifted broad endothermic peak and exothermic peak is due to melting and crystallization of the adsorbed poloxamer present on the nanoparticle surface.

12.7 PXRD

In order to investigate the physical nature of the encapsulated drug, the Powder X-ray Diffraction technique was used. Solid state analysis of the nanosuspension system after freeze drying showed that the drug is dispersed in the polymeric matrices in a semicrystalline to microcrystalline form. While the polymer is completely amorphous in nature, entrapment of crystalline sulfacetamide (sharp intense peaks as seen in Figure 12.22) into the polymeric nanoparticles reduced its crystallinity to a greater extent. Similar observation was noted for the other three batches. This is evident from the disappearance of most peaks in the nanoparticles compared to the drug or the physical mixture of drug/polymer. There may also be the possibility of overlapping of drug peaks by the background diffraction pattern of the amorphous structure (19). Thus, it can be inferred that the drug is present inside the nanoparticles in a semicrystalline to microcrystalline form. This finding was also in agreement with the flurbiprofen loaded acrylate polymer nanosuspension prepared by Pignatello et al (8).

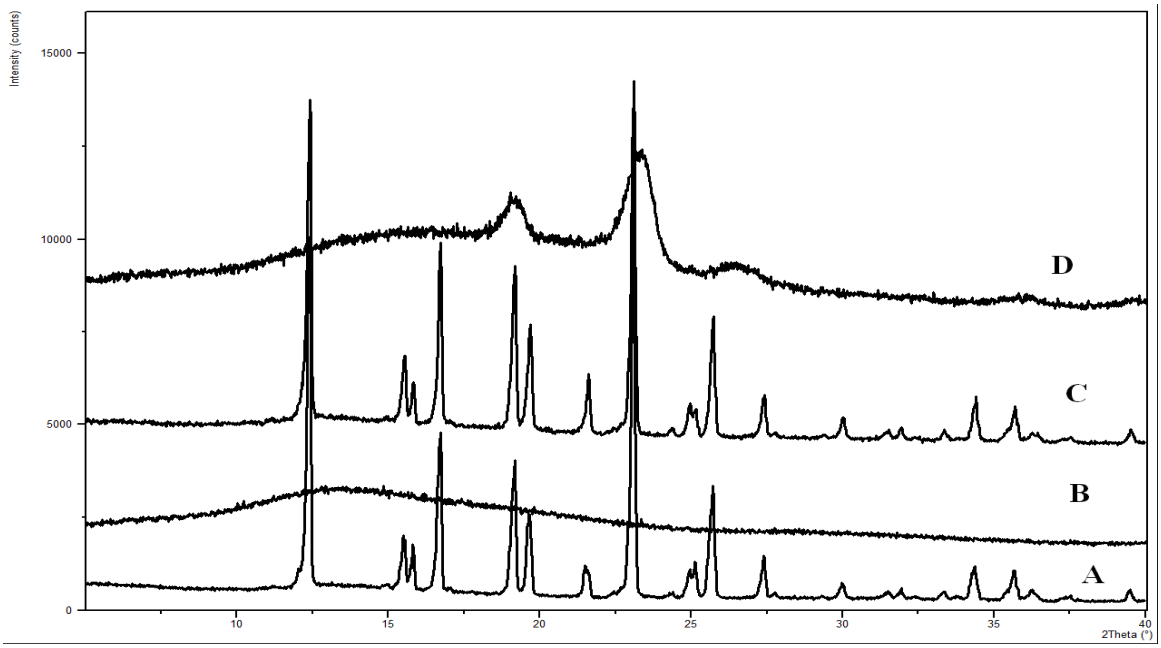

Figure 12.22: PXRD of Sulfacetamide (A), Eudragit® RL100 (B), Physical mixture of Sulfacetamide and Eudragit® RL100 (C), Freeze dried nanosuspension of Sulfacetamide and Eudragit® RL100 batch B3 (D)

12.8 FTIR

Pure sulfacetamide has characteristic IR peaks at 3471.93 cm^{-1} (NH stretch), 1686.3 cm^{-1} (CO), 1642 cm^{-1}, 1596.18 cm^{-1}, 1505.61 cm^{-1}, 1440.51 cm^{-1}, 1375.01 cm^{-1}, 1322.8 cm^{-1} (sym SO2), 1233 cm^{-1}, 1155 cm^{-1} (asym SO2). This finding is in agreement with the findings of Nagendrappa G (20). Figure 12.23 showed that the characteristic bands of the ester groups at 1,150 - 1,190 cm^{-1} and 1,240- 1,270 cm^{-1}, as well as the C = O ester vibration at 1,730 cm^{-1}. In addition, CHX vibrations can be discerned at 1385 cm^{-1}, 1450

cm^{-1}, 1475 cm^{-1} and 2,950 - 3,000 cm^{-1}. Eudragit has characteristics IR absorption frequency at 3437.91 (OH stretch), 2952.37 (*sp*3 CH stretch), 1733.89 (CO stretch).

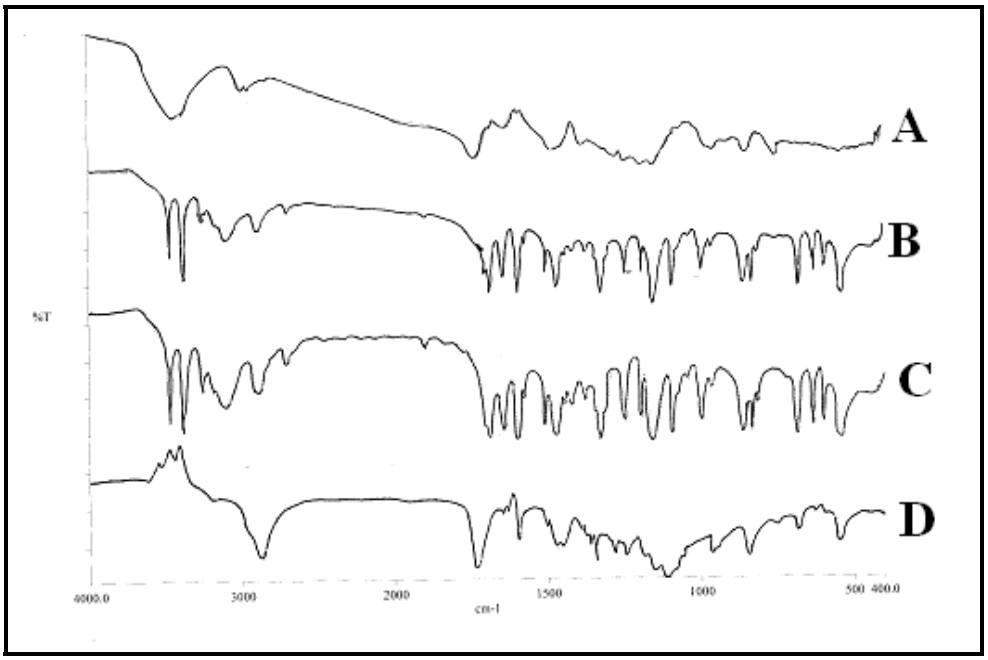

Figure 12.23: FTIR spectra of Eudragit®RL100 (A), Sulfacetamide (B), Physical mixture of Sulfacetamide and Eudragit® RL100 (C), Freeze dried nanosuspension batch B3 (D)

Freeze dried solid sample of sulfacetamide loaded nanosuspension (batch B3) exhibited mainly the Eudragit® absorption peaks with few overlapping peaks from the sulfacetamide. It can be concluded that no strong drug polymer interaction occurred inside the nanoparticles. Similar observation was noted for other three batches of drug loaded nanosuspension.

12.9 In vitro drug release

In vitro drug release from the nanosuspension in phosphate buffer pH 7.4 was performed by the dialysis experiment using the static Franz diffusion cell. The calibration curve of the drug was constructed to determine concentration from the absorbance at 256 nm with phosphate buffer 7.4 as blank (Figure 12.24). The in vitro drug release profiles obtained

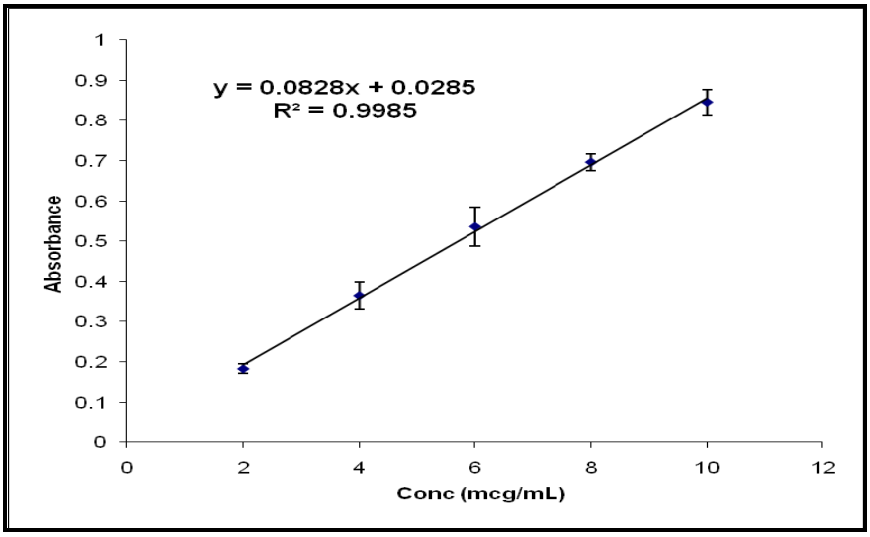

Figure 12.24: Calibration curve of Sulfacetamide in Phosphate Buffer pH 7.4 with absorbance taken at 256 nm

from the dialysis experiment was shown in Figure 12.25. The amount of drug incorporation in the formulation and drug entrapment efficiency have a direct effect on the drug release profile from the four formulations. As the content of the drug in the formulation increased, the release rate also increased. Batch B4 had the lowest drug entrapment efficiency (DEE) of 28.26% with a smaller average particle size (112.4 nm)

gave 100% drug release within 2 hours. The progressive saturation of the quaternary group in the polymer by drug molecules, occurred a at high drug content which increased drug release from the formulation (7). Batch B1 had a DEE of 31.35 % with a larger

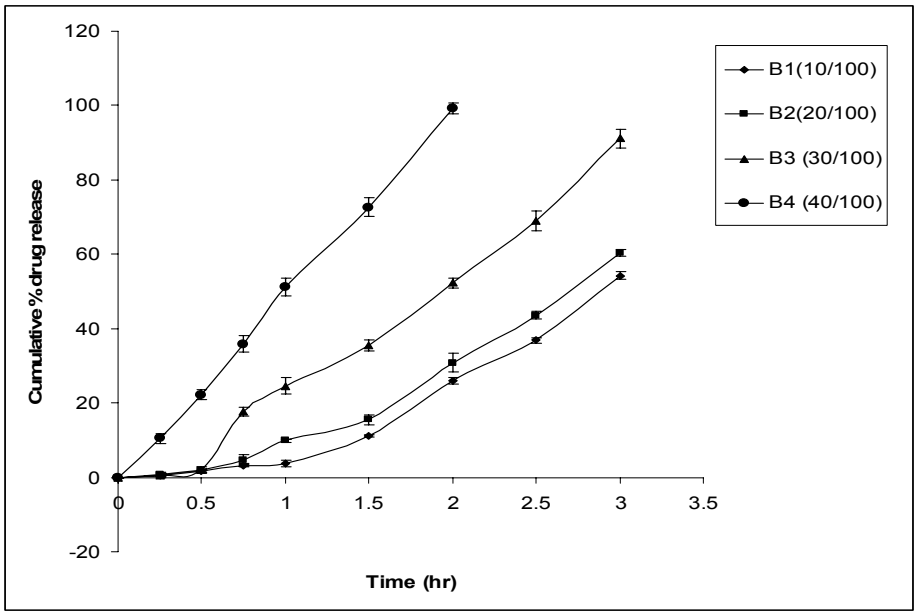

Figure 12.25: In vitro release of sulfacetamide loaded nanosuspensions in phosphate buffer pH 7.4 at 37^0C

average particle size (140.6 nm), gave a prolonged drug release profile with only about 54.22% drug release after 3 hours. A similar tendency was observed for Batch B2 (DEE 32.24% and particle size 127.9 nm) which released about 60.46% of the drug after 3 hours. Batch B3 with a particle size of 118.9 nm and DEE of 35.74% showed 91.17% drug release after 3 hrs. Thus, a correlation between drug release from the nanosuspensions with mean particle size was observed. Thus, it can be inferred that

larger particles have a small initial burst release and a longer sustained release than smaller particles (21).

12.10 Kinetics of drug release

The release data were fitted to various kinetic models in order to calculate the release constant and regression coefficients (R^2) as seen in Table 12.2. Among the models tested, the drug release profiles for the batch B1 and B2 were best fitted with Hixon crowell cube root model based on the regression coefficients (R^2 of 0.97 and 0.95 respectively). Batches B3 and B4 followed zero order model (R^2 of 0.98 and 0.99 respectively). With Korsemeyer-Peppas equation which plots the logarithm of cumulative percentage of drug release up to 60% versus the logarithm of time showed an excellent fit for the model (R^2~ 0.97). The diffusion exponent (n) values for all batches were within 0.4 which indicated that drug release mechanism followed pure Fickian diffusion. Pignatello et al, showed that the drug release from Eudragit® RL 100 particles was complex in nature which involves the occurrence of dissolutive and diffusive phenomena (22). Overall the drug release rate was faster which is probably due to the high water permeability and swellability of Eudragit®. The presence of a high content of quaternary ammonium groups makes the polymer permeable to water.

Table 12.2: Kinetic release rate constants, correlation coefficient and diffusion exponent of various models (n=3)

Batch	Zero order		First order		Higuchi model		Hixon-crowell		Korsemeyer peppas		
	K_0	R^2	K_1	R^2	K_h	R^2	K_H	R^2	K	n	R^2
B1	17.876	0.915	0.784	0.868	70.587	0.892	0.630	0.975	0.057	1.953	0.986
B2	20.228	0.948	0.747	0.894	54.035	0.845	0.645	0.953	0.080	1.856	0.995
B3	30.942	0.982	0.498	0.836	34.213	0.765	0.745	0.879	0.159	2.28	0.921
B4	50.036	0.998	0.122	0.750	29.745	0.715	1.036	0.792	0.502	1.14	0.999

12.11 Freeze drying and redispersibility of nanosuspension

The batch B3 (drug to polymer ratio of 30/100) was selected for freeze drying since it had the highest drug entrapment efficiency with a small particle size and sustained release behavior. The effect of using cryoprotectants on redispersibility in distilled water was investigated visually to observe the formation of any aggregates upon manual hand shaking. Freeze dried nanoparticles without cryoprotectants appeared as off-white fluffy and sheet-like materials. Using sucrose as the cryoprotectant resulted in the formation of a white, brittle, crystalline material with perforated structure. Mannitol formed a white spongy, cotton-like material upon lyophilization. Freeze dried nanoparticles without cryoprotectants can be seen in Figure 12.26. The freeze dried sample without cryoprotect-

Figure 12.26: Photograph of the freeze dried nanosuspension (Left to Right: B1, B2, B3, B4) without cryoprotectant

-tants did not redisperse in water after manual hand shaking. Large aggregates were observed. Mannitol containing samples showed good redispersibility upon manual shaking. No difference was observed for 2.5% and 5% mannitol containing samples. Sucrose containing samples showed excellent redispersibility within a few minutes of shaking for samples with 5% sucrose. Sample containing 2.5% sucrose formed slight turbidity and foaming upon shaking.

Particle size of the 5% sucrose containing batch was 304.7 ± 30.4 nm whereas 5% mannitol containing batch contained 156.2 ± 18.1 nm average particle size. Therefore, 5% Mannitol containing batch appeared to be the most suitable cryoprotectant for the batch B3.

11.2.12 Short term stability study of nanosuspension

Physical appearance of the B3 nanosuspension did not change when samples were stored at 4^0C for 1 month. A loose, thin layer of sediment was observed when nanosuspension was stored at room temperature for 1 month. However, the sediment disappeared with slight hand shaking. The average particle diameters were 125.2 ± 25.1 nm and 98.2 ± 21.3 nm when samples were stored at room temperature and 4^0C respectively. The particle size for the batch B3 was 118.9 ±8.17 nm before performing stability study. It can be inferred from the observed data that the prepared nanosuspension B3 was stable after 1 month of storage at room temperature and 4^0C.

Chapter Thirteen

Conclusion

In this study, the potential of Eudragit® RL 100 nanosuspension with potential for ocular delivery of Sulfacetamide was investigated. Nanosuspension was prepared by solvent displacement technique which is the easiest and reproducible method to prepare nanoparticles without need of any sophisticated instruments. Size range of all the batches was within 500 nm with polydispersity index of 0.4 to 0.6 suitable for ocular administration. Additionally, SEM and TEM images showed almost spherical particles with smooth surface. The positive surface charge on the particle would provide ionic interaction with the mucous membrane of cornea, resulting in sustained drug release and improved ocular penetration. No major drug polymer interaction was detected using FTIR, DSC, PXRD studies done for solid state characterization. Batch B1 and B2 showed sustained drug release profile whereas release from batch B3 and B4 were comparatively faster. Drug entrapment efficiency was found to be in the range of 28.28% to 35.74% which is low due to the ionization and solubility of sulfacetamide. In terms of entrapment efficiency, batch B3 containing 30 parts sulfacetamide to 100 parts Eudragit® RL 100 showed relatively higher drug entrapment efficiency. This batch was selected to study the effect of three approaches to increase drug entrapment efficiency. There are three strategies employed to

increase drug entrapment such as: changing polymer content in formulation, changing external phase pH and addition of another polymer in the formulation. Changing pH to about 3.4 suppressed ionization and increased drug entrapment efficiency. Similarly, addition of 30 parts of PMMA in the formulation B3 increased drug entrapment efficiency to about 50%. Overall the study objectives are fulfilled based on the experimental results. Freeze dried nanosuspension using sucrose and mannitol as cryoprotectant exhibited good redispersibility upon manual hand shaking. Short term stability study revealed stable nanosuspension with no significant change in particle size distribution. Several strategies are currently under investigation in order to increase entrapment efficiency of the nanoparticles. Sterilization, long term stability and in vivo studies could further be performed in order to characterterize the delivery system for clinical use.

References

Chapter One

1. **Ding S,** "Recent developments in ophthalmic drug delivery". *Pharmaceutical Science and Technology Today*, November 1998, vol. 1, no. 8, 328-335.
2. **Desai SD and Blanchard J,** *Encyclopedia of Pharmaceutical Technology*, Swarbrick, J and Boylan, JC, (eds), 1995, Marcel Dekker, New York, 43–75.
3. **Mishima S, Gasset A, Klyce SDJ and Baum JL,** "Determination of tear volume and tear flow". *Investigative Ophthalmology and Visual Science*. 1966, vol. 5, no. 3, 264-276.
4. **Peyman GA, Ganiban GJ,** "Delivery systems for intraocular routes". *Advanced Drug Delivery Reviews*, August 1995, vol.16, no. 1, 107-123.
5. **Hull DS, Green K, Boyd M and Wynn HR, "**Corneal endothelium bicarbonate transport and the effect of carbonic anhydrase inhibitors on endothelial permeability and fluxes and corneal thickness". *Investigative Ophthalmology and Visual Science* , October 1977, vol. 16, no. 10, 883-892.
6. **Mezei M and Meisner D,** *Biopharmaceutics of Ocular Drug Delivery,* 2003, Edman, P.(ed.), CRC Press, Boca Raton, FL, USA, 91–104.
7. **Vander ZJA, Valuck RJ, Bunch CL, Perlman JI, Anderson C and Wortman GI,** "Systemic adverse effects of ophthalmic beta-blockers". *The Annals of Pharmacotherapy.* December 2001, vol. 35, no. 12, 1633-1637.

8. **Jennifer JKD and William FM, "**Thermoresponsive hydrogels as a new ocular drug delivery platform to the poterior segment of eye". *Transactions of the American Ophthalmological Society*, 2008, vol. 106, 206-214
9. **Joshi A,** "Microparticulates for Ophthalmic Drug Delivery". *Journal of Ocular Pharmacology and Therapeutics*. Spring 1994, vol. 10, no. 1, 29-45.
10. **Nagarwal RC, Kant S, Singh PN, Maiti P and Pandit JK,** "Polymeric nanoparticulate system: A potential approach for ocular drug delivery". May 2009, vol. 136, no. 1, 2-13.
11. **Nagarsenker MS, Londhe VY and Nadkarni GD,** "Preparation and evaluation of liposomal formulations of tropicamide for ocular delivery". *International Journal of Pharmaceutics,* November 1999, vol. 190, no. 1, 63-71.
12. **Yoel G., Guy K.** "Use of collagen shields for ocular-surface drug delivery*". Expert Review of Ophthalmology*, December 2008, vol. 3, no. 6, 627-633(7)
13. **Bloomfield S.E., Miyata T., Dunn M.W., Bueser N., Stenzel K.H., Rubin A.L.** "Soluble Gentamicin Ophthalmic Inserts as a Drug Delivery System". *Archives of Ophthalmology.* May 1978, vol. 96, no. 5, 885-887.
14. **Vandamme TF., Brobeck L.** "Poly(amidoamine) dendrimers as ophthalmic vehicles for ocular delivery of pilocarpine nitrate and tropicamide". *Journal of Controlled Release*, 2005, vol. 102, no. 1, 23-38.
15. **Monti D., Saccomani L., Chetoni P., Burgalassi S., Saettone M.F.** "Effect of iontophoresis on transcorneal permeation 'in vitro' of two β-blocking agents, and on corneal hydration". *International Journal of Pharmaceutics*, 2003, vol. 250, no. 2, 423-429.

16. **Antoine B.R., Francine B.C., David B., Robert G., Florence D.** "Polymeric nanoparticles for drug delivery to the posterior segment of the eye". *Chimia*, 2005, vol. 59, no. 6, 344-347
17. **Kreuter J.** "Nanoparticles. In Colloidal drug delivery systems", J. K. Ed. Marcel Dekker: New York, 1994, 219-342
18. **Roth H.W., Leimbeck R., Sonnenschein B., Anger C.B., Weber S.,** "The effective antibacterial spectrum of sulfacetamide", *Klin Monbl Augenheilkd* , March 1992, vol. 200, no. 3, 182-186.
19. **Abboud I., Massoud W.H.,** "Effect of blephamide in blepharitis", *Bulletin of the Ophthalmological Society of Egypt,* 1972, vol. 65, no.69, 539-543.
20. **Chhibber P R,** "Treatment of trachoma", *Indian Journal of Medical R esearch*. 1964, vol. 58, 3-8.
21. **Colomina J, Esparza L, Buesa J, Marí J,** "Corneal ulcer caused by Nocardia asteroides after penetrating keratoplasty", *Medicina clínica*, March 1997, vol. 108, no. 11, 424-425.
22. **Sridhar M.S., Sharma S., Reddy M.K., Mruthyunjay P., Rao G.N.,** "Clinicomicrobiological review of Nocardia keratitis", *Cornea: The Journal of Cornea and External Disease*, January 1998, vol. 17, no.1, 17-22.
23. **Brown G.M.**, "Inhibition by sulfonamides of the biosynthesis of folic acid". *International Journal of L eprosy and Ot her Mycobacterial Diseases* , October – December 1967, vol. 35, no. 4, 580-589.
24. **Lacy C.F., Armstrong L.L., Goldman M.P., Lance L.L.** Drug information handbook. 12th edition, Laxi-Comp inc, Hudson, Ohio, page 1354.

25. **Bucolo C., Maltese A., Puglisi G., Pignatello R. "**Enhanced ocular anti-inflammatory activity of ibuprofen carried by an Eudragit RS100 nanoparticle suspension**".** *Ophthalmic Research*, September – October 2002, vol. 34, no.5, 319-323.
26. **Pignatello R., Bucolo C., Ferrara P., Maltese A., Puleo A., Puglisi G.** "Eudragit RS100 nanosuspensions for the ophthalmic controlled delivery of ibuprofen". *European Journal of Pharmaceutics*. July 2002, vol. 16, no. 1-2, 53-61.
27. **Castelli F., Messina C., Sarpietro M.G., Pignatello R., Puglisi G.** "Flurbiprofen Release from Eudragit RS and RL Aqueous Nanosuspensions: a Kinetic Study by DSC and Dialysis Experiments". *AAPS PharmSciTech*. 2002, vol. 3, no. 2, article 9.
28. **Pignatello R. ; Bucolo C. ; Spedalieri G. ; Maltese A. ; Puglisi G. "** flurbiprofen-loaded acrylate polymer nanosuspensions for ophthalmic application". *Biomaterials,* August 2002, vol. 23, no. 15, 3247-3255.
29. **Pignatello R., Ricupero N., Bucolo C., Maugeri F., Maltese A., Puglisi G.** "Preparation and Characterization of Eudragit Retard Nanosuspensions for the Ocular Delivery of Cloricromene". *AAPS PharmSciTech*, 2006, vol. 7, no. 1, Article 27.

30. **Adibkia K., Siahi Shadbad M.R., Nokhodchi A., Javadzedeh A., Barzegar-Jalali M., Barar J., Mohammadi G., Omidi Y.** "Piroxicam nanoparticles for ocular delivery: physicochemical characterization and implementation in endotoxin-induced uveitis". *Journal of Drug Targeting,* July 2007, vol. 15, no. 6, 407-416.
31. **Adibkia K., Omidi Y., Siahi M.R., Javadzadeh A.R., Jalali M.B., Jaleh Barar, Maleki N., Mohammadi G., Nokhodchi A.** "Inhibition of Endotoxin-Induced Uveitis by

Methylprednisolone Acetate Nanosuspension in Rabbits". *Journal of O cular Pharmacology and Therapeutics*. October 2007, vol. 23, no. 5, 421-432.

32. **Das S., Sureshb P.K., Desmukhc R.** "Design of Eudragit® RL 100 nanoparticles by nanoprecipitation method for ocular drug delivery". *Nanomedicine: Nanotechnology, Biology and Medicine ,* October 2009. (in press)

33. **Fessi H., Puisieux F., Devissaguet J.P., Ammoury N., Benita S.** "Nanocapsule formation by interfacial polymer deposition following solvent displacement". *International Journal of Pharmaceutics*, 1989, vol. 55, no. 1, r1-r4

34. **Hornig S, Heinze T., Becer C.R., Schubert U.S. "**Synthetic polymeric nanoparticles by nanoprecipitation"**.** *Journal of Material Chemistry*, 2009, vol.**19**, 3838 – 3840

35. **Peltonen L., Aitta J., Hyvönen S., Karjalainen M., Hirvonen J.** "Improved Entrapment Efficiency of Hydrophilic Drug Substance During Nanoprecipitation of Poly(l)lactide Nanoparticles". *AAPS PharmSciTech*. 2004, vol. 5, no. 1, article 16.

36. **Govender T., Stolnik S., Garnett M.C., Illum L., Davis S.S.** "PLGA nanoparticles prepared by nanoprecipitation: drug loading and release studies of a water soluble drug" *Journal of Controlled Release*. February 1999, vol. 57, no. 2, 171-185

37. **Sensoy D., Cevher E., Sarıcı A., Yılmaz M., Özdamar A., Bergişadi N. "**Bioadhesive sulfacetamide sodium microspheres: Evaluation of their effectiveness in the treatment of bacterial keratitis caused by *Staphylococcus aureus* and *Pseudomonas aeruginosa* in a rabbit model". *European Journal of Phar maceutics and Biopharmaceutics* , August 2009, vol. 72, no. 3, 487-495

38. **Qaddoumi M.G., Ueda H., Yang J., Davda J., Labhasetwar V., Lee V.H.** "The characteristics and mechanisms of uptake of PLGA nanoparticles in rabbit conjunctival epithelial cell layers". *Pharmaceutical Research*, April 2004, vol. 21, no. 4, 641-648.

Chapter Two

1. **Desai M.P., Labhasetwar V., Walter E., Levy R.J., Amidon G.L**. "The mechanism of uptake of biodegradable microparticles in Caco-2 cells is size dependent", *Pharmaceutical Research,* November 1997, vol. 14, no. 11, 1568-1573.
2. **Kreuter J.** "Nanoparticles. In Colloidal drug delivery systems", J. K. Ed. Marcel Dekker: New York, 1994, 219-342
3. **Bae Y., Diezi T.A., Zhao A., Kwon G.S**. "Mixed polymeric micelles for combination cancer chemotherapy through the concurrent delivery of multiple chemotherapeutic agents", *Journal of Controlled Release*, October 2007, vol. 122, no. 3, 324-330.
4. **Ljubimova J.Y., Fujita M., Khazenzon N.M., Lee B.-S., Wachsmann-Hogiu S., Farkas D.L., Black K.L., Holler E.** "Nanoconjugate based on polymalic acid for tumor targeting", *Chemico-Biological Interactions*, January 2008, vol. 171, no. 2, 195-203.
5. **Kreuter, J.** "Evaluation of nanoparticles as drug-delivery systems. I. Preparation methods". *Pharmaceutica Acta Helvetiae,* 1983, vol. 58, 196-209.
6. **Kreuter J**. "Nanoparticles as drug delivery system. In: Nalwa HS, editor. "Encyclopedia of nanoscience and nanotechnology", 2004, vol. 7. New York: American Scientific Publishers. 161–180.

7. **Wissing S.A., Kayser O., Muller R.H**. "Solid lipid nanoparticles for parenteral drug delivery", *Advanced Drug Delivery Reviews,* May 2004, vol. 56, no. 9, 1257-1272.
8. **Bhattacharya R., Mukherjee P**. "Biological properties of "naked" metal nanoparticles". *Advanced Drug Delivery Reviews*, August 2008, vol. 60, no. 11, 1289-1306.
9. **Manchester M., Singh P**. "Virus-based nanoparticles (VNPs): Platform technologies for diagnostic imaging", *Advanced Drug Delivery Reviews,* December 2006, vol. 58, no. 14, 1505-1522.
10. **Vauthier C., Bouchemal K**. "Methods for the Preparation and Manufacture of Polymeric Nanoparticles", *Pharmaceutical Research,* May 2009, vol. 26, no. 5, 1025- 1058.
11. **Desai M.P., Labhasetwar V., Amidon G.L., Levy R.J**. "Gastrointestinal uptake of biodegradable microparticles: effect of particle size", *Pharmaceutical Research,* December 1996, vol. 13, no. 12, 1838—1845
12. **Soppimath K.S., Aminabhavi T.M., Kulkarni A.R., Rudzinski W.E**. "Biodegradable polymeric nanoparticles as drug delivery devices", *Journal of Controlled Release,* January 2001, vol. 70, no. 1-2, 1-20.
13. **Gurny R., Peppas N. A., Harrington D. D., and Banker G. S**. "Development of biodegradable and injectable lattices for controlled release potent drugs", *Drug Deelopment and Inustrial Pharmacy,* 1981, vol. 7, 1–25.
14. **Tice TR, Gilley RM.** "Preparation of injectable controlled-release microcapsules by solvent-evaporation process", *Journal of Control Release,* 1985, vol. 2, 343 - 352.

15. **Soppimath KS, Aminabhavi TM, Kulkarni AR, Rudzinski WE**. "Biodegradable polymeric nanoparticles as drug delivery devices", *Journal of Control Release,* January 2001, vol. 70, no. 1-2, 1 - 20.

16. **Avgoustakis. K**. "Pegylated poly(lactide) and poly(lactide-coglycolide) nanoparticles: preparation, properties and possible applications in drug delivery", *Current Drug Delivary* , October 2004, vol. 1, no. 4, 321–333.

17. **Gref R, Minamitake Y, Peracchia M. T. Trubetskoy V., Torchilin V., and Langer R.** "Biodegradable long-circulating polymeric nanospheres", *Science,* March 1994, vol. 263, no. 5153, 1600–1603.

18. **Brigger I., Chaminade P., Desmaële D., Peracchia M. T. J. d'Angelo, Gurny R., Renoir M., and Couvreur P.** "Near infrared with principal component analysis as a novel analytical approach for nanoparticle technology", *Pharmaceutical Research,* September 2000, vol. 17, no. 9, 1124–1132.

19. **Bodmeier R., Chen H.** "Indomethacin polymeric nanosuspensions prepared by microfluidization". *Journal of Controlled Release*, May 1990, vol. 12, no. 3, 223- 233.

20. **Sa´nchez A., Vila Jato J.L., Alonso M.J.** "Development of biodegradable microspheres and nanospheres for the controlled release of cyclosporine". *International Journal of Pharmaceutics* October 1993, vol. 99, no. 2-3, 263- 273.

21. **Ueda H., Kreuter J.** "Optimization of the preparation of loperamideloaded poly (l-lactide) nanoparticles by high pressure emulsification solvent evaporation". *Journal of Microencapsulation*, September- October 1997, vol. 14, no. 5, 593- 605.

22. **Mainardes R.M, Evangelista R.C.** "PLGA nanoparticles containing praziquantel: effect of formulation variables on size distribution". *International Journal of Pharmaceutics,* February 2005, vol. 290, no. 1-2, 137- 144.

23. **Ya-Ping L. , Yuan-Ying P., Xian-Ying Z., Zhou-Hui Gu., Zhao-Hui Z., Wei-Fang Y., Jian-Jun Z., Jian-Hua Z., Xiu-Jian G.** "PEGylated PLGA nanoparticles as protein carriers: synthesis, preparation and biodistribution in rats". *Journal of Controlled Release* , April 2001,vol. 71, no. 2, 203-211

24. **Gurny R., Peppas N.A., Harrington D.D., Banker G.S.** "Development of biodegradable and injectable lattices for controlled release of potent drugs". *Drug Development and Industrial Pharmacy* , 1981, vol. 7, 1 – 25.

25. **Pinto Reis C., Neufeld R.J., Ribeiro A.J., Veiga F**. "Nanoencapsulation I. Methods for preparation of drug-loaded polymeric nanoparticles", *Nanomedicine: Nanotechnology, Biology, and Medicine*, March 2006, vol. 2, no. 1, 8-21.

26. **Fessi H., Puisieux F., Devissaguet J.P., Ammoury N. , Benita S.** "Nanocapsule formation by interfacial polymer deposition following solvent displacement", *International Journal of Pharmaceutics*, October 1989, vol. 55, no. 1, R1–R4.

27. **Molpeceres J., Guzman M., Aberturas M.R., Chacon M., Berges L.** "Application of central composite designs to the preparation of polycaprolactone nanoparticles by solvent displacement ", *Journal of Pharmaceutical Science*, February 1996, vol. 85, no. 2, 206–213.

28. **Guterres S.S., Fessi H., Barrat G., Devissaguet J.P., Puisiex F**. "Poly (DL-Lactide) nanocapsules containing diclofenac:1. Formulation and stability study", *International Journal of Pharmaceutics*, January 1995, vol. 113, no. 1, 57–63.

29. **Chacon M., Berges L., Molpeceres J., Aberturas M.R**. "Optimised preparation of poly DL-(lactic-glycolic) microspheres and nanoparticles for oral administration", *International Journal of Pharmaceutics*, September 1996, vol. 141, no. 1, 81–91.
30. **Legrand P., Lesieur S., Bochot A., Gref R., Raatjes W., Barratt G., and Vauthier C.** "Influence of polymer behaviour in organic solution on the production of polylactide nanoparticles by nanoprecipitation", *International Journal of Pharmaceutics,* November 2007, vol. 344, no. 1-2, 33–43.
31. **Quintanar-Guerrero D, Alle´mann E, Fessi H, Doelker E**. "Preparation techniques and mechanism of formation of biodegradable nanoparticles from preformed polymers", *Drug Devlopment and Industrial Pharmacy,* December 1998, vol. 24, no. 12, 1113-1128.
32. **Ammoury N, Fessi H, Devissaguet J-P, Dubrasquet M, Benita S**. "Jejunal absorption, pharmacological activity, and pharmacokinetic evaluation of indomethacin-loaded poly(d,l-lactide) and poly(isobutylcyanoacrylate) nanocapsules in rats", *Pharmaceutical Res earch,* January 1991, vol. 8, no. 1, 101- 105.
33. **Seijo B, Fattal E, Roblot-Treupel L, Couvreur P**. "Design of nanoparticles of less than 50 nm diameter: preparation, characterization and drug loading", *International Journal of Pharmaceutics*, July 1990, vol. 62, no. 1, 1 - 7.
34. **Bilati U., Allémann E., and Doelker E**. "Nanoprecipitation Versus Emulsion-based techniques for the encapsulation of proteins into biodegradable nanoparticles and process-related stability issues", *AAPS ParmSciTech,* December 2005, vol. 6, no. 4, E594–E604.

35. **Barichello J. M., Morishita M., Takayama K., and Nagai T.** "Encapsulation of hydrophilic and lipophilic drugs in PLGA nanoparticles by the nanoprecipitation method*",* *Drug Development and Industrial Pharmacy*, January 1999, vol. 25, no. 4, 471–476.

36. **Molpeceres J., Guzman M., Aberturas M. R., Chacon M., and Berges L.** "Application of central composite design to the preparation of polycaprolactone nanoparticles by solvent displacement", *Journal of Pharmaceutical Science,* February 1996, vol. 85, no. 2, 206– 213.

37. **Duclairoir C., Nakache E. , Marchais H. and Orecchioni A. M.** "Formation of gliadin nanoparticles: influence of the solubility parameter of the protein solvent", *Colloidal Polymer. Science*, May 1998, vol. 276, no. 4, 321–327.

38. **Skiba M., Wouessidjewe D, Puisieux F., Duchène D., and Gulik A**. "Characterization of amphiphilic fl-cyclodextrin nanospheres", *International Journal of Pharmaceutics* , September 1996, vol. 142, no. 1, 121–124.

39. **Skiba M., Morvan C., Duchene D., Puisieux F. and Wouessidjewe D**. "Evaluation of gastrointestinal behaviour in the rat of amphiphilic β-cyclodextrin nanocapsules, loaded with indomethacin", *International Journal of Pharmaceutics* , December 1995, vol. 126, no. 1-2, 275–279.

40. **Némati F., Dubernet C., Fessi H., Verdière A. C., Poupon M. F., Puisieux F. and Couvreur P.** "Reversion of multidrug resistance using nanoparticles in vitro: influence of the nature of the polymer", *International Journal of Pharmaceutics,* July 1996, vol. 138, no. 2, 237–246.

41. **Moinard-Chécot D., Chevalier Y., Briançon S., Fessi H. , and Guinebretière S**. "Nanoparticles for drug delivery: review of theformulation and process difficulties illustrated by the emulsiondiffusion process", *Journal of Nanoscience and Nanotechnology*, September-October 2006, vol. 6, no. 9–10, 2664–2681**.**

42. **Battaglia L., Trotta M., Gallarate M., Carlotti M. E., Zara G. P. and Bargoni A**. "Solid lipid nanoparticles formed by solvent-inwater emulsion–diffusion technique: Development and influence on insulin stability", *Journal of Microencapsulation,* November 2007, vol. 24, no. 7, 660–672.

43. **Quintanar-Guerrero D., Tamayo-Esquivel D., Ganem- Quintanar A., Allémann E. and Doelker E**. "Adaptation and optimization of the emulsification–diffusion technique to prepare lipidic nanospheres", *Europian Journal of Pharmaceutics and Biopharmaceutics,* October 2005, vol. 26, no. 2, 211–218.

44. **Quintanar-Guerrero D., Allémann É., Fessi H., and Doelker E.** "Influence of stabilizing agents and preparative variables on the formation of poly(-lactic acid) nanoparticles by an emulsification– diffusion technique", *International Journal of Pharmaceutics* , November 1996, vol. 143, no. 2, 133–141.

45. **Quintanar-Guerrero D., Ganem-Quintanar A., Allemann E. , Fessi H. and Doelker E**. "Influence of the stabilizer coating layer on the purification and freeze-drying of poly(D,L-lactic acid) nanoparticles prepared by an emulsion–diffusion technique", *Journal of Microencapsulation,* January- February 1998, vol. 15, no. 1, 107–119.

46. **Quintanar-Guerrero D., Allémann É., Doelker É. and Fessi H.** "Preparation and characterization of nanocapsules from preformed polymers by a new process based on emulsification– diffusion technique", *Pharmceutical Research,* July 1998, vol. 15, no. 7, 1056–1062.

47. **Bindschaedler, C., Gurny, R., Doelker, E. "**Process for preparing a powder of water-insoluble polymer which can be redispersed in a liquid phase, the resulting powder and utilization thereof", 1988, Patent WO 88/08011.

48. **Quintanar-Guerrero D., Alle´mann E., Fessi H., Doelker E**. "Preparation techniques and mechanism of formation of biodegradable nanoparticles from preformed polymers", *Drug Devlopment and Industrial Pharmacy,* December 1998, vol. 24, no. 12, 1113- 1128.

49. **Jung T., Kamm W., Breitenbach A., Kaiserling E., Xiao J.X., Kissel T.** "Biodegradable nanoparticles for oral delivery of peptides: is there a role for polymers to affect mucosal uptake?", *Europian Journal of Pharmaceutics and Biopharmaceutics,* July 2000, vol. 50, no. 1, 147- 160.

50. **Lambert G., Fattal E., Couvreur P.** "Nanoparticulate system for the delivery of antisense oligonucleotides", *Advanced Drug Delivery Reviews,* March 2001, vol. 47, no. 1, 99 - 112.

51. **Couvreur P., Dubernet C., Puisieux F.** "Controlled drug delivery with nanoparticles: current possibilities and future trends", *Europian Journal of Pharmaceutics and Biopharmaceutics,* 1995, vol. 41, no. 1, 2 - 13.

52. **Kreuter J.** "Large-scale production problems and manufacturing of nanoparticles", In: Tyle P, editor. Specialized drug delivery system. New York7 Marcel Dekker; 1990. 257- 66.

53. .**Vauthier C., Dubernet C., Fattal E., Pinto-Alphandary H., Couvreur P.** "Poly (alkylcyanoacrylates) as biodegradable materials for biomedical applications", *Advanced Drug Delivery Reviews,* April 2003, vol. 55, no. 4, 519- 548.

54. **Ekman B., Sjfholm I.** "Improved stability of proteins immobilized in microparticles prepared by modified emulsion polymerization technique", *Journal of Pharmaceutical Science,* May 1978, vol. 67, no. 5, 693 - 696.

55. **Rolland A., Gibassier D., Sado P., Le Verge R.** "Purification et proprie´te´s physico-chimiques des suspensions de nanoparticules de polyme`re", *Journal de Pharmacie de Belgique,* 1986, vol. 41, 94 - 105.

56. **Li V.H.K., Wood R.W., Kreuter J., Harmia T., Robinson J.R.** "Ocular drug delivery of progesterone using nanoparticles", *Journal of Microencapsulation,* July- September1986, vol. 3, no. 3, 213 - 218.

57. **Maincent P., Le Verge R, Sado P., Couvreur P., Devissaguet J.P.** "Disposition kinetics and oral bioavailability of vincamine-loaded polyalkyl cyanoacrylate nanoparticles", *Journal of Pharmaceutical Science,* October 1986, vol. 75, no. 10, 955 - 958.

58. **Mbela T.K.M., Poupaert J.H., Dumont P.** "Poly (diethylmethyldene malonate) nanoparticles as primaquine delivery system to liver", *International Jour nal of Pharmacy,* 1992, vol. 79, 29 - 38.

59. **Alle´mann E., Leroux J.C., Gurny R.** "Polymeric nano-microparticles for the oral delivery of peptides and peptidomimetics", *Advanced Drug Delivery Reviews,* December 1998, vol. 34, no. 2-3, 171- 89.

60. **Couvreur P., Barrat G., Fattal E., Legrand P., Vauthier C.** "Nanocapsule technology", *Critical Reviews in Therapeutic Drug Carrier Systems,* 2002, vol. 19, no. 2, 99- 134.

61. **Watnasirichaikul S., Davies N.M., Rades T., Tucker I.G.** "Preparation of biodegradable insulin nanocapsules from biocompatible microemulsions", *Pharmaceutical Reseaerc,* June 2000, vol. 17, no. 6, 684- 9.

62. **Lambert G., Fattal E., Pinto-Alphandary H., Gulik A., Couvreur P.** "Polyisobutylcyanoacrylate nanocapsules containing an aqueous core as a novel colloidal carrier for the delivery of oligonucleotides", *Pharmaceutical Reseaerch,* June 2000, vol. 17, no. 6, 707- 714.

63. **Lenaerts V., Labib A., Chouinard F., Rousseau J., Ali H., Lier J.** "Nanocapsules with a reduced liver uptake: targeting of phthalocyanines to EMT-6 mouse mammary tumour in vivo", *Europian Journal of Pharmaceutics and Biopharmaceutics.* 1995, vol. 41, 38 - 43.

64. **Montasser I., Fessi H., Coleman A.W.** "Atomic force microscopy imaging of novel type of polymeric colloidal nanostructures", *Europian Journal of Pharmaceutics and Biopharmaceutic,* November 2002, vol. 54, no. 3, 281- 284.

65. **Bouchemal K., Briançon S. , Fessi H., Chevalier Y. , Bonnet I., and Perrier E.** "Simultaneous emulsification and interfacial polycondensation for the preparation of colloidal suspension of nanocapsules", *Material Science and Engineering: C,* March2006, vol. 26, no. 2-3, 472–480.

66. **Bouchemal K, Briancon S, Perrier E, Fessi H, Bonnet I, Zydowicz N**. "Synthesis and characterization of polyurethane and poly(ether urethane) nanocapsules using a new technique of interfacial polycondensation combined to spontaneous emulsification", *International Journal of Pharmaceutics,* January 2004, vol. 269, no. 1, 89- 100.

67. **Mansouri S, Lavigne P, Corsi K, Benderdour M, Beaumont E, Fernandes JC**. "Chitosan-DNA nanoparticles as non-viral vectors in gene therapy: strategies to improve transfection efficacy", *Europian Journal of Pharmaceutics and Biopharmaceutics* , January 2004, vol. 57, no. 1, 1 - 8.

68. **Mao H-Q, Roy K, Troung-Le VL, Janes KA, Lin KY, Wang Y**. "Chitosan-DNA nanoparticles as gene carriers: synthesis, characterization and transfection efficiency", *Journal of Control Release,* February 2001, vol. 70, no. 3, 399- 421.

69. **Illum L, Farraj NF, Davis SS**. "Chitosan as novel nasal delivery system for peptide drugs", *Pharmaceutical Reseaerch,* August 1994, vol. 11, no. 8, 1186- 1189.

70. **Kreuter J., Hekmatara T., Dreis S., Vogel T., Gelperina S., Langer K**. "Covalent attachment of apolipoprotein A-I and apolipoprotein B-100 to albumin nanoparticles enables drug transport into the brain", *Journal of Controlled Release* , March 2007, vol. 118, no. 1, 54-58.

71. **Yoshioka T., Hashida M., Muranishi S., Sezaki H.** "Specific delivery of mitomycin C to the liver, spleen, and lung: nano- and microspherical carriers of gelatin", *International Journal of Pharmaceutics*, April 1981, vol. 8, no. 2, 131 - 141.

72. **Aslani P., Kennedy R.A.** "Studies on diffusion in alginate gels. I. Effect of cross-linking with calcium or zinc ions on diffusion of acetaminophen", *Journal of Control Release,* October 1996, vol. 42, no. 1, 75- 82.

73. **Wang N., Wu X.S., Mesiha M.** "A new method for preparation of protein-loaded agarose nanoparticles", *Pharmaceutical Reseaerch*, 1995, vol. 12, S257.

74. **Duclairoir C., Orecchioni A.M., Depraetere P., Nakache E**. "a-Tocopherol encapsulation and in vitro release from wheat gliadin nanoparticles", *Journal of Microencapsulation,* January 2002, vol. 19, no. 1, 53 - 60.

75. **Mohantya B., Aswalb V.K., Kohlbrecherc J., Bohidar H.B. "**Synthesis of Gelatin Nanoparticles via Simple Coacervation*", Journal of Surface Science and Technology,* November 2005, vol. 21, no. 3-4, 1-12.

76. **Calvo P., Remunan-Lopez C., Vila-Jato J.L., Alonso M.J.** "Novel hydrophilic chitosan-polyethylene oxide nanoprticles as protein carriers", *Journal of Applied Polymer Science,* December 1998, vol. 63, no. 1, 125-132.

77. **Wang Y., Dave R.N., Pfeffer R.**"Polymer coating/encapsulation of nanoparticles using a supercritical anti-solvent process", *Journal of Supercritical Fluids,* 2004, vol. 28, 85- 99.

78. **Thote A.J., Gupta R.B.** "Formation of nanoparticles of a hydrophilic drug using supercritical carbon dioxide and microencapsulation for sustained release", *Nanomedicine: Nanotech. Biology Medicine,* 2005, vol. 1, no. 1, 85-90.

79. **Sun Y., Mezian M., Pathak P., Qu L.** "Polymeric nanoparticles from rapid expansion of supercritical fluid solution". *Chemistry.* September 2004, vol. 11, no. 5, 1366-1373.

80. **Elvassore N., Bertucco A., Caliceti P.** "Production of insulin-loaded poly (ethylene glycol)/poly (l-Lactide) (PEG/PLA) nanoparticles by gas antisolvent techniques", *Journal of Pharmaceutical Sciences,* September 2001, vol. 90, no. 10, 1628- 1636.

81. **Limayem I. Charcosset C., Fessi H**. "Purification of nanoparticle suspensions by a concentration/diafiltration process", *Separation and Purification Technology,* July 2004, vol. 38, no. 1, 1-9.

82. **Krause H.J., Schwartz A. , Rohdewald P**. "Interfacial polymerization, a useful method for the preparation of polymethylcyanoacrylate nanoparticles", *Drug Devlopment and Industrial Pharmacy,* March 1986 , vol. 12 , no. 4, 527-552.

83. **Allémann E., Doelker E., Gurny R**. "Drug loaded poly (lactic acid) nanoparticles produced by a reversible salting-outprocess: purification of an injectable dosage form", *Europian Journal of Pharmaceutics and Biopharmaceutics,* 1993, vol. 39, 13.

84. **Beck P., Scherer D., Kreuter J**. "Separation of drug-loadednanoparticles from free drug by gel filtration", *Journal of Microencapsulation*, 1990, vol. 7, no. 4, 491-496.

85. **Rolland A.** "Clinical pharmacokinetics of doxorubicin inhepatoma patients after a single intravenous injection of free or nanoparticle-bound anthracycline", *International Journal of Pharmaceutics*, 1989, vol. 54, 113.

86. **Tishchenko G., Luetzow K., Schauer J., Albrecht W., Bleha M**. "Purification of polymer nanoparticle by diafiltration with polysulfone/hydrophilic polymer blend membranes", *Separation and Purification Technology*, March 2001, vol. 22-23, 403-415.

87. **Attwood D. Disperse systems, in: M.E. Aulton (Ed.)**, "Pharmaceutics, the Science of Dosage Form Design", Churchill Livingstone, London, 2002, pp. 70–100.

88. **Magneheim B., Benita S**. "Nanoparticles characterization: a comprehensive physicochemical approach", *STP Pharmaceutical Science*, 1991, vol. 1, 221–241.

89. **Jiang J., Oberdörster G.and Biswas P**. "Characterization of size, surface charge, and agglomeration state of nanoparticle dispersions for toxicological studies", *Journal of Nanoparticle Research,* January 2009, vol. 11, no. 1, 177-189

90. **Coffin M.D., McGinity J.W. "**Biodegradable pseudolatexes: the chemical stability of poly (D, L-lactide) and poly (ε-caprolactone) nanoparticles in aqueous media". *Pharmaceutical Research,* 1992, vol. 9, 200–205.

91. **Belbella A, Vauthier C, Fessi H, Devissaguet JP, Puisieux F**, "In vitro degradation of nanospheres from poly(D,Llactides) of different molecular weights and polydispersities", *International Journal of Pharmaceutics,* March 1996, vol. 129, no. 1-2, 95–102.

92. **Williams N.A., Polli G.P**., "The lyophilization of pharmaceuticals: a literature review". *Journal of Parenter. Science and Technology*, March- April 1984, vol. 38, no. 2, 48–59.

93. **Pikal M.J., Shah S., Roy M.L., Putman R**. "The secondary drying stage of freeze-drying: drying kinetics as a function of temperature and chamber pressure", *International Journal of Pharmaceutics,* 1990, vol. 60, 203–217.

94. **Abdelwahed W., Degobert G., Stainmesse S., and Fessi H. "**Freeze-drying of nanoparticles: Formulation, process and storage considerations", *Advanced Drug Delivery Reviews,*December 2006, vol. 58, no. 15, 1688-1713.

95. **Chacon M. , Molpeceres J., Berges L. , Guzman M.**, **Aberturas M.R.** "Stability and freeze-drying of cyclosporine loaded poly (D, L lactide-glycolide) carriers", *Europian Journal of Pharmaceutical Science*, May 1999, vol. 8, no. 1, 99–107.

96. **Auvillain M., Cavé G., Fessi H., Devissaguet J.P. "**Lyophilisation de vecteurs colloïdaux submicroniques", *STP Pharmaceutical Science*, 1989, vol. 5, 738–744.

97. **Quintanar-Guerrero D., Ganem-Quintanar A., Allémann E., Fessi H., Doelker E**., "Influence of the stabilizer coating layer on the purification and freeze-drying of poly (D,L-lactic acid) nanoparticles prepared by an emulsion–diffusion technique", *Journal of Microencapsulation*, 1998, vol. 15, no. 1, 107–119.

98. **Zimmermann E., Müller R.H., Mäder K**. "Influence of different parameters on reconstitution of lyophilized SLN", *International Journal of Pharmmaceutics* , March 2000, vol. 196, no. 2, 211–213.

99. **Tang X., Pikal M.J.**, "Design of freeze-drying processes for pharmaceuticals: practical advice", *Pharmaceutical Research,* February 2004, vol. 21, no. 2, 191–200.

100. **Desai M.P., Labhasetwar V., Walter E., Levy R.J., Amidon G.L**. "The mechanism of uptake of biodegradable microparticles in Caco-2 cells is size dependent", *Pharmaceutical Research,* November 1997, vol. 14, no. 11, 1568-1573.

101. **Desai M.P., Labhasetwar V., Amidon G.L., Levy R.J**. "Gastrointestinal uptake of biodegradable microparticles: effect of particle size", *Pharmaceutical Research,* December 1996, vol. 13, no. 12, 1838—1845

102. **Kroll R.A., Pagel M.A., Muldoon L.L., Roman-Goldstein S., Fiamengo S.A., Neuwelt E.A**. "Improving drug delivery to intracerebral tumor and surrounding brain in a rodent model: a comparison of osmotic versus bradykinin modification of the blood-brain and/or blood-tumor barriers", *Neurosurgery,* 1998, vol. 43: 879-889.

103. **Kreuter J., Ramge P., Petrov V., Hamm S., Gelperina S.E., Engelhardt B., Alyautdin R., von Briesen H., Begley D.J.** "Direct evidence that polysorbate-80-coated poly (butylcyanoacrylate) nanoparticles deliver drugs to the CNS via specific mechanisms requiring prior binding of drug to the nanoparticles", *Pharmaceutical Research,* March 2003, vol. 20, no. 3,409-416.

104. **Redhead H.M., Davis S.S., Illum L.** "Drug delivery in poly (lactide-co-glycolide) nanoparticles surface modified with poloxamer 407 and poloxamine 908: in vitro characterisation and in vivo evaluation". *Journal of Controlled Release*, February 2001, vol. 70, no. 3, 353-363.

105. **Dunne M., Corrigan O.I., Ramtoola Z.** "Influence of particle size and dissolution conditions on the degradation properties of polylactide-co-glycolide particles", *Biomaterials*, August 2000, vol. 21, no. 16, 1659-1668.

106. **Muller R.H., Jacobs C., Kayser O**. "Nanosuspensions as particulate drug formulations in therapy: Rationale for development and what we can expect for the future", *Advanced Drug Delivery Reviews*, March 2001, vol. 47, no. 1, 3-19.

107. **Vila A., Sanchez A., Tobio M., Calvo P. and Alonso M.J.** "Design of biodegradable particles for protein delivery", *Journal of Controlled Release* , January 2002, vol. 78, no. 1-3, 15-24.

108. **Grislain L., Couvreur P., Lenaerts V., Roland M., Deprez- Decampeneere D., Speiser P.** "Pharmacokinetics and distribution of a biodegradable drug-carrier", *International Journal of Pharmaceutics*, July 1983, vol. 15, no. 3, 335-345.

109. **Janes K.A., Calvo P., Alonso M.J.** "Polysaccharide colloidal particles as delivery systems for macromolecules", *Advanced Drug Delivery Reviews*, March 2001, vol. 47, no. 1, 83-97.

110. **Cheng Y.-H., Illum L., Davis S.S.** "A poly (D,L-lactide-co-glycolide) microsphere depot system for delivery of haloperidol" *Journal of Controlled Release* , November 1998, vol. 55, no. 2-3, 203-212.

111. **Avgoustakis K., Beletsi A., Panagi Z., Klepetsanis P., Karydas A.G, Ithakissios D.S ,** **"**PLGA-mPEG nanoparticles of cisplatin: In vitro nanoparticle degradation, in vitro drug release and in vivo drug residence in blood properties", *Journal of Controlled Release*, February 2002, vol. 79, no.1-3, 123-135.

112. **Peracchia M.T., Fattal E., Desmaele D., Besnard M., Noel J.P., Gomis J.M., Appel M., Couvreur P.** "Stealth (®) PEGylated polycyanoacrylate nanoparticles for intravenous administration and splenic targeting" *Journal of Controlled Release* , June 1999, vol. 60, no. 1, 121-128.

113. **Chen Y., McCulloch R.K., Gray B.N.** "Synthesis of albumin-dextran sulfate microspheres possessing favourable loading and release characteristics for the anti-cancer drug doxorubicin", *Journal of Controlled Release*, August 1994, vol. 31, no. 1, 49-54.

114. **Govender T., Stolnik S., Garnett M.C., Illum L., Davis S.S.** "PLGA nanoparticles prepared by nanoprecipitation: drug loading and release studies of a water soluble drug", *Journal of Controlled Release*, February 1999, vol. 57, no.2, 171-185.

115. **Govender T., Riley T., Ehtezazi T., Garnett M.C., Stolnik S.Illum L., Davis S.S.** "Defining the drug incorporation properties of PLA-PEG nanoparticles", *International Journal of Pharmaceutics*, 2000, vol. 199, no.1, 95-110.

116. **Magenheim B., Levy M.Y., Benita S.** A. "new in vitro technique for the evaluation of drug release profile from colloidal carriers - ultrafiltration technique at low pressure". *International Journal of Pharmaceutics*, June 1993, vol. 94, no. 1-3, 115-123.

117. **Matsumoto J., Nakada Y., Sakurai K., Nakamura T., Takahashi Y.** "Preparation of nanoparticles consisted of poly(L-lactide) – poly(ethylene glycol) – poly(L-lactide) and their evaluation in vitro", *International Journal of Pharmaceutics* , August 1999, vol. 185, no. 1, 93– 101.

118. **Fukumori Y., Ichikawa H.** "Nanoparticles for cancer therapy and diagnosis", *Advanced Powder Technology*, 2006, vol. 17, no. 1, 1-28.

119. **Maeda H.** "The enhanced permeability and retention (EPR) The use of nanoparticles in imaging is also effect in tumor vasculature: the key role of tumor-selective macromolecular drug targeting", *Advances in Enzyme Regulation*, May 2001, vol. 41, no. 1, 189–207.

120. **Storm G., Belliot S.O., Daemen T. , Lasic D.D.** "The enhanced permeability and retention (EPR) The use of nanoparticles in imaging is also effect in tumor vasculature: the key role of tumor-selective macromolecular drug targeting", *Advanced Drug Delivery Reviews*, 1995, vol. 17, 31–48.

121. **Chavanpatil M.D., Patil Y., Panyam J.** "Susceptibility of nanoparticle-encapsulated paclitaxel to P-glycoprotein-mediated drug efflux", *International Journal of Pharmaceutics,* August 2006, vol. 320, no. 1-2, 150-156

122. **Kreuter J. "**Influence of the surface properties on nanoparticle- mediated transport of drugs to the brain", *Journal of Nanoscience and Nanotechnology,* May 2004, vol. 4, no. 5, 484–488.

123. **Ringe K., Walz C.M., Sabel B.A.** "Nanoparticle drug delivery to the brain". *Encyclopedia of Nanoscience and Nanotechnology*, 2004, vol. 7, 91–104.

124. **Alyautdin R.N., Tezikov E.B., Ramge P., Kharkevich D.A., Begley D.J.** "Significant entry of tubocurarine into the brain of rats by adsorption to polysorbate 80-coated polybutylcyanoacrylate nanoparticles: an in situ brain perfusion study", *Journal of Microencapsulation,* January- February 1998**,** vol. 15, no. 1, 67–74.

125. **Michaelis K., Hoffmann M.M., Dreis S.** "Covalent linkage of Apolipoprotein E to albumin nanoparticles strongly enhances drug transport into the brain", *Journal of Pharmacology and Experimantal Therapeutics*, June 2006, vol. 317, no. 3, 1246–1253.

126. **Kreuter J.** "Nanoparticulate systems for brain delivery of Drugs", *Advanced Drug Delivery Reviews*, 2001, vol. 47, 65–81.

127. **Kawashima Y.** "Pulmonary delivery of insulin with nebulized -lactide/glycolide copolymer (PLGA) nanospheres to prolong hypoglycemic effect", *Journal of Controlled Release*, vol. 62, 279–287

128. **Zahoor A., Sharma S., Khuller G.K.** "Inhalable alginate nanoparticles asantitubercular drug carriers against experimental tuberculosis" *International Journal of Antimicrobial Agents,* October 2005, vol. 26, no. 4, 298–303

129. **Vaughn, J.M.** "Single dose and multiple dose studies of itraconazole nanoparticles", *Europian Journal of Pharmaceutics and Biopharmaceutics,* June 2006, vol. 63, no. 2, 95–102

130. **Nagarwal R.C., Kant S., Singh P.N., Maiti P., Pandit J.K**. "Polymeric nanoparticulate system: A potential approach for ocular drug delivery" *Journal of Controlled Release* , May 2009, vol. 136, no. 1, 2-13.

131. **Le Bourlais C., Acar L., Zia H., Sado P.A., Needham T., Leverge R.** "Ophthalmic drug delivery systems - Recent advances", *Progress in Retinal and Eye Research* , January 1998, vol. 17, no. 1, 33-58.

132. **Zimmer A., Kreuter J.** "Microspheres and nanoparticles used in ocular delivery systems" *Advanced Drug Delivery Research,* August 1995, vol. 16, no. 1, 61-73.

133. **Desai M., Hilfinger J., Amidon G., Levy R.J., Labhaset- Niwa V., Futaki S., Kiwadar H.** "Immune response with biodegradable nanospheres and alum: Studies in rabbits using staphylococcal entertoxin localization signal: Qualitative and quantitative evaluation of B-toxoid", *Journal of Microencapsulation*, 1999, vol. 17, 215–225.

134. **Raghuvanshi R.J., Mistra A., Talwar G.P., Levy R.J.** "Enhanced immune response with a combination of alum and biodegradable nanoparticles containing tetanus toxoid", *Journal of Microencapsulation*, 2001, vol. 18, no. 6, 723–732.

135. **Bonadio J., Smiley E., Patil P., Goldstein S**. "Localized, direct plasmid gene delivery in vivo: prolonged therapy results in reproducible tissue regeneration", *Nature Medicine,* 1999, vol. 5, 753–759.

136. **Labhasetwar V., Bonadio J., Goldstein S.A., Levy R.J., Berkland C., King M., Cox A., Kim K., Pack D.W.** "Precise transfection using biodegradable nanospheres: results in control of PLG microsphere size provides enhanced control tissue culture and a rat osteotomy model, Colloids Surfaces of drug release rate", *Journal of Controlled Release* , 2002, vol. 82, 137–147.

Chapter Three

1. **Merkus HG,** "Laser Diffraction" in *Particle Size Measuremen ts: Fundamentals, Practice, Quality*, 2009, chapter 10, Springer, Netherlands, 259-285.
2. **Hallett FR,** "Size distributions from static light scattering" in *Monographs on the Physics and Chemistry of Materials,* 1996, Clarendon Press, Oxford, 477-493.
3. **Schnablegger H and Glatter O,** "Simultaneous determination of size distribution and refractive index of colloidal particles from static light-scattering experiments", *Journal of colloid and interface science*, 1993, vol. 158, no.1, 228-242.
4. **Ma Z, Merkus HG and Scarlett B,** "Particle-size analysis by laser diffraction with a complementary metal-oxide semiconductor pixel array*", Applied Op tics,* 2000, vol. 39, 4547–4556.
5. **Barabanenkov YN,** "The Fraunhofer approximation in the theory of multiple wave scattering*", Radiophysics and Quantum Electronics,* February, 1971, vol. 14, no, 2, 188-194.
6. **Mie G**, "Contributions to the optics of turbid media, especially colloidal metal Solutions", *Annalen der Physik*, 1908, vol. 25, 377–445.
7. **Merkus HG,** "Dynamic light scattering" in *Particle Size Measurements: Fundamentals, Practice, Quality,* 2009, Springer, Netherlands, 301-302.
8. **Bruce JB**, "Chemical and biological applications of laser light scattering", *Accunts of Chemical Research*, 1973, vol. 6, no. 9, 318–322.
9. http://www.malvern.com/LabEng/technology/dynamic_light_scattering/classical_90_degree_scattering.htm

10. **Bruce JB and Robert Pecora,** *Dynamic light scatter ing: with applic ations to ch emistry, biology, and physics*, 2000, Ed 2, Courier Dover Publications.
11. Metzler R and Klafter J, "Accelerating Brownian motion: A fractional dynamics approach to fast diffusion". *Europhysics Letter,* 2000, vol. 51, no. 5, 492.
12. **Wolfgang S,** "Sample preparation" in *Light Scattering from Polymer Solutions and Nanoparticle Dispersions*, 2007, Springer Berlin Heidelberg, 43-44.
13. **Christoph H,** "Particle measurement by dynamic scattered light"*, LaborPraxis*, 1995, vol. 19, no. 6, 34-5.

Chapter Four

1. **Schwarz J.A., Contescu C.I.** *Surfaces of nanoparticles and porous materials* , vol. 78, CRC Press, 1999.
2. **Goto Y., Matsuno R., Konno T., Takai M., Ishihara K.** "Polymer Nanoparticles Covered with Phosphorylcholine Groups and Immobilized with Antibody for High-Affinity Separation of Proteins". *Biomacromolecules*, March 2008, vol. 9, no. 3, 828–833.
3. **Miller D., Yalamanchili M.R., Kellar J.J.** "Surface charge of alkali halide particles as determined by laser-Doppler electrophoresis". *Langmuir*, May 1992, vol. 8, no. 5, 1464–1469.
4. **Uzgiris E.E.** "Laser Doppler methods in electrophoresis". *Progress in Surface Science*, 1981, vol. 10, no. 1, 53-164.

5. **Stoltz J.F., Janot C., Saur F., Weber M., Malher E., Duvivier C.** "Use of a laser-Doppler electrophoresis method in bacteriology (preliminary results)". *Biorheology Suppliment,* 1984, vol.1, 303-307.
6. **Uzgiris E.E.** "Electrophoresis of particles and biological cells measured by the doppler shift of scattered laser light". *Optics Communications*, September 1972, vol. 6, no. 1, 55-57.
7. **Lyklema J.** *"Fundamentals of Interface and Colloid Science",* vol.2*,* page.3.208*,* 1995
8. **Dukhin S.S., Derjaguin B.V.** *"*Electrokinetic Phenomena*", Surface and Colloid Science,* Ed. E. Matijevic, John Willey *&* Sons, NY, *(*1974*)* 23.
9. **Reuss F.F.,** *Mém. Soc. Impériale Naturalistes de Moscow 2 (*1809*), p.* 327.
10. **Martin A.** *Physical Pharmacy* . 4th ed. Lippincott Williams & Wilkins, Philadelphia, PA, 1993, pp. 386–388.
11. www.symphotic.com/images/ZetaPotentialDiagram.gif
12. **Smoluchowski M.,** Bull. Int. Acad. Sci. Cracovie, 184 (1903)
13. **Lyklema J.** "*Fundamentals of Interface and Colloid Science*", vol.2, page.3.208, 1995
14. *Zeta Potential of Colloid s in Water and Waste Water* , ASTM Standard D 4187-82, American Society for Testing and Materials, 1985
15. **Vidal S.D., Simonin J.P, Turq P., Bernard O.** "Acoustophoresis Revisited. 1. Electrolyte Solutions". *Journal of Physical Chemistry*, April 1995, vol. 99 no. 17, 6733–6738
16. www.tut.fi/units/me/ener/laitteistot/EFD/LDA.html

17. **Yeh Y., Cummins H.** "Localised fluid flow measurements with a He-Ne laser spectrometer". *Applied Physics Letters,* 1964, vol. 4, 176-178.
18. http://www.malvern.com/LabEng/technology/zeta_potential/zeta_potential_LDE.htm

Chapter Five

1. **Zhou W., Apkarian R.P.,Wang Z.L., Joy D.** "Fundamentals of Scanning Electron Microscopy (SEM) in Zhou, Weilie", editor; Wang, Zhong Lin, editor, Scanning Microscopy for Nanotechnology: Techniques and Applications, Springer, New York,2007
2. **Li Q., Ono Y., Homma Y., Nakai I., Fukuda K., Sasaki T., Tanaka K., Nakayama S.** "Morphology and chemical composition analysis of inorganic nanosheets by the field-emission scanning electron microscope system". *Journal of Electron Microscopy* (Tokyo). January 2009, vol. 58, no. 1, 1-6.
3. **Dillaman R.M., Hart H.V.** "X-ray evaluation of SEM technique for determining the crystallography of echinoid skeletons". Scanning Electron Microscopy, 1981, (Pt 3):313-20.
4. **Gallo P.J., Kulik A. J., Burnham N.A., Oulevey F., Gremaud G.** "Electrical-conductivity SFM study of an ultrafiltration membrane". *Nanotechnology*, March 1997, vol. 8, no. 1, 10-13
5. http://serc.carleton.edu/research_education/geochemsheets/electroninteractions.html
6. **Haine M.E., Cosslett V.E.** "The Electron Microscope", Spon, London (1961).
7. www4.nau.edu/.../Images/SEM_schematic.jpg

8. **Seligman A.M., Wasserkrug H.L., Hanker J.S.** "A new staining method for enhancing contrast of lipid-containing membranes and droplets in osmium tetroxide-fixed tissue with osmiophilic thiocarbohydrazide (TCH)". *Journal of Cell Biology* , August 1966, vol. 30, no. 2, 424–432.
9. **Stokes D,** "Principles and practice of variable pressure/environmental scanning electron microscopy (VP-ESEM)". John Wiley and Sons, 2008
10. **Wright E, Conticello V, Apkarian R,** "Cryo Cryoetch and Tandem Cryo HRSEM Correlated with Cryo STEM of Elastin Mimetic Block Copolymers". *Microscopy and Microanalysis*, 2003, vol. 9(Suppl 2), 254-255
11. **Hayak MA,** *Principles and Techniques of Scanning Electron Microscopy* , Van Nostrand Reinhold Co., 1978
12. **Broglie L.de.** "The wave nature of the electron Nobel Lecture", 12, 1929
13. **Williams D.B., Carter C.B., Williams D.B., Carter C.B.** "Transmission Electron Microscopy: A Textbook for Materials Science". Springer US, 2009
14. **Kienle L., Duppel V., Mattausch H., Schaloske M.C., Simon A.** "Application of TEM for Real Structure Determination of Rare Earth Metal Compounds". EMC 2008 14th European Microscopy Congress 1–5 September 2008, Aachen, Germany.
15. http://www.udel.edu/biology/Wags/histopage/illuspage/lec1/iintro9.gif
16. **Michler, G.H.** "Electron Microscopy of Polymers". Springer Berlin Heidelberg, 2008.
17. **Sawyer L.C., Grubb, David.T., Meyers G.F.** "Polymer Microscopy". Springer New York, 2008.
18. **Egerton, R.** Physical principles of electron microscopy. Springer, 2005.

19. **Ourmazd A., Taylor D.W., Cunningham J., Tu C.W.** Phys. Rev. Lett. **62**, 933 (1989)

20. **MauriceJ.L., Schwander P., Baumann F.H., Ourmazd A.** Ultramicroscopy 68, 149 (1997)

21. **Grogger W., Hofer F., Warbichler P., Kothleitner G.** "Quantitative Energy-filtering Transmission Electron Microscopy in Materials Science". *Microscopy and Microanalysis* , 2000, vol. 6, 161-172.

22. **Browning N.D., Chisholm M.F., Pennycook S.J.** "Atomic-resolution chemical analysis using a scanning transmission electron microscope". *Nature*, 1993, vol. 366, 143–146.

Chapter Six

1. **Smith BC,** "Fundamentals of Fourier transform infrared spectroscopy". CRC Press, Boca Raton, 1996

2. **Bracewell RN,** "The Fourier Transform and Its Applications", 2000, 3rd ed, Boston: McGraw-Hill.

3. www.atmos.washington.edu/~hakim/301/handouts.html

4. **Kludt JR, Kwong GYW and McDonald RL,** "Far-infrared spectra of tertiary ammonium salts". *Journal of Physical Chemistry*, February 1972, vol. 76, no. 3, 339–342

5. **Yoo BH, Park CM, Oh TJ, Han SH, Kang HH and Chang IS, "**Investigation of jewelry powders radiating far-infrared rays and the biological effects on human skin". *Journal of Cosmetic Science,* May- June 2002, vol. 53, no. 3, 175-184.

6. **Udagawa Y and Nagasawa H,** "Effects of far-infrared ray on reproduction, growth, behavior and some physiological parameters in mice". *In Vivo*, March- April 2000, vol. 14, no. 2, 321-326.

7. http://mmrc.caltech.edu/FTIR/FTIRintro.pdf
8. **Hans K, "**Solid-State Spectroscopy: An Introduction". Springer, Berlin, Heidelberg, 2009.
9. http://felix.physics.sunysb.edu/~allen/252/PHY251_Michelson.html
10. http://www.cem.msu.edu/~reusch/VirtualText/Spectrpy/InfraRed/infrared.htm
11. **Tilstone WJ,** "Forensic Science: An Encyclopedia of History, Methods, and Techniques". ABC-CLIO, Inc 2006
12. **Coleman PB,** "Practical sampling techniques for infrared analysis". CRC Press, 1993.
13. **Ishida H,** "Symposium on "Fourier Transform Infrared Characterization of Polymers", Div. of Polymer Chemistry, Plenum Publ. Corp., October 1987.
14. **Neubert R, Collin B and Wartewig S,** "Quantitative analysis of drug content in semisolid formulations using step-scan FT-IR photoacoustic spectroscopy". *Vibrational Spectroscopy*, January 1997, vol. 13, no. 2, 241-244.
15. **Gerwert K,** "Molecular reaction mechanisms of proteins as monitored by time-resolved FTIR spectroscopy". *Current Opinion in Structural Biology* , October 1993, vol. 3, no. 5, 769-773.
16. http://www.fdmspectra.com/fdm_acd_structure_searching.htm
17. **Chan KLA, Kazarian SG, Vassou D, Gionis V and Chryssikos GD,** "In situ high-throughput study of drug polymorphism under controlled temperature and humidity using FT-IR spectroscopic imaging". *Vibrational Spectroscopy*, January 2007, vol. 43, no. 1, 221-226.

18. **Chan KLA and Kazarian SG,** "FTIR Spectroscopic Imaging of Dissolution of a Solid Dispersion of Nifedipine in Poly (ethylene glycol)". *Molecular Pharmaceutics*, July- August 2004, vol. 1, no. 4, 331–335.
19. **Takka S,** "Propranolol hydrochloride-anionic polymer binding interaction" *Farmaco*, October 2003, vol. 58, no. 10, 1051-1056.
20. **Lira AAM, Nanclares DMA, Federman NA and Marchett JM,** "Drug–polymer interaction in the all- trans retinoic acid release from chitosan microparticles". *Journal of Thermal Analysis and calorimetry*. March 2007, vol. 87, no. 3, 899-903.
21. **Chen JF, Zhang JY, Shen ZG, Zhong J and Yun J,** "Preparation and Characterization of Amorphous Cefuroxime Axetil Drug Nanoparticles with Novel Technology: High-Gravity Antisolvent Precipitation". *Industrial & Engineering Chemistry Research* , November 2006, vol. 45, no. 25, 8723–8727

Chapter Seven

1. **Smart L, Moore E.A.** "Solid state chemistry: an introduction", 3rd Edition, 2005, CRC Press, Florida.
2. **Faqir H., Chiba H., Kikuchi M., Syono Y., Mansori M., Satre P., Sebaoun A**. "High-Temperature XRD and DTA Studies of BiMnO3Perovskite", *Journal of Solid State Chemistry*, January 1999, vol. 142, no. 1, 113-119.
3. **Collet E, Buron M, Cailleau H, Lorenc M, Servol M, Rabiller P, Toudic B**. "X-ray diffraction for material science". *UVX 2008*, July 2009, 21-27.

4. **Bisognin G., Vangelista S., Bruno E**." High-resolution X-ray diffraction by end of range defects in self-amorphized Ge", *Materials Science and Engineering B: Solid-State Materials for Advanced Technology*, December 2008, vol. 154-155, no. 1-3, 64-67.
5. **Alexander, L. E.** "X-ray diffraction methods in polymer science". 1969, New York, Wiley Interscience.
6. **Chu, B. and B. S. Hsiao.** "Small-Angle X-ray Scattering of Polymers", *Chemical Reviews*, May 2001, vol. 101, no. 6, 1727-1762.
7. **Jenkins R, Snyder RL**. "Introduction to X-Ray Powder Diffractometry", 1996, Wiley, NY.
8. http://epswww.unm.edu/xrd/xrdclass/01-XRD-Intro.pdf
9. **James R. W**. "The Optical Principles of the Diffraction of X-Rays". Volume 2, 1954,
10. http://imr.chem.binghamton.edu/labs/xray/xray.html
11. **Cullity B. D**. "Elements of x-ray diffraction". Addison-Wesley series in metallurgy and materials, 2nd edition, 1978, MA.
12. **Klug H. P., Alexander L. E**. "X-ray diffraction procedures for polycrystalline and amorphous materials", 1974, Wiley Interscience , NY.
13. **Glatter O., Kratky O**. "Small-Angle X-Ray Scattering", 1982, Academic Press, MA.
14. **Pecharsky VK, Zavalij PY**, Fundamentals of Powder Diffraction and Structural Characterization of Materials, 2009, Chapter 11, Springer US, 292-296.
15. **Cullity B.D**. "Elements of X-ray diffraction", 2nd Edition, 1978, Addison- Wesley, New York, ch. 8, 233.
16. **Will G. "***Powder diffraction: the Rietveld method and the two-stage method to determine and refine crystal structures from powder diffraction data*". Birkhäuser, 2006

17. Suryanarayanan R, Rastogi S, "X-Ray Powder Diffractometry" in *Enclycopedia of Pharmaceutical Technology*, Informa healthcare, 2006.

Chapter Eight

1. **Wunderlich B,** "Development towards a single-run DSC for heat capacity measurements", *Journal of Thermal Analysis and Calorimetry*, November 1987, vol. *32, no. 6*, 1949-1955.

2. **Schick C**, "Differential scanning calorimetry (DSC) of semicrystalline polymers", Analytical and Bioanalytical Chemistry, November 2009, vol. 395, no. 6, 1589-1611.

3. **Watson EL and O'Neil MJ,** "Differential Microcalorimeter". US Patent 3263484, April 1962.

4. www.materials.npl.co.uk/matsol/dpscdtsc.jpg

5. **Hemminger W,** "Calorimetric methods", Calorimetry and thermal Analysis of Polymers, 1994, Mathot VBF (ed.), Hanser Publisher, Munich.

6. **Reading M and Hourston DJ,** *Modulated temperature differential scanning calorimetry: theoretical and practical applications in polymer characterization*, 2006, Springer, New York.

7. **Fakirov S, Banerjee S and Richard JTL,** "On the Degree of Crystallinity from DSC in the Case of Multiple Melting of Synthetic Polymers". *Journal of Macromolecular Science, Part B*, March 2007, vol. *46*, no. 2, 317 – 320.

8. **Abu-Sehly AA, Alamri SN and Joraid AA,** "Measurements of DSC isothermal crystallization kinetics in amorphous selenium bulk samples", *Journal of Alloys and Compounds*, May 2009, vol. 476, no. 1-2, 348-351.

9. **Pandini S, Pegoretti A, Riccò T,** "DSC analysis of post-yield deformed pbt. Effects of thermal history", *Journal of Thermal Analysis and Calorim etry*, December 2008, vol. 94, no. 3, 825-833.

10. **Ruiz CSB, Machado LDB, Vanin JA and Volponi JE,** "Cure Degree Estimation of Photocurable Coatings by DSC and Differential Photocalorimetry". *Journal of Thermal Analysis and Calorimetry*, February 2002, vol. 67, no. 2, 335-341.

11. **Pielichowski K, Slotwinska D and Pielichowski J,** "Application of DSC Method for Thermal Stability and Flammability Assessment of Modified Polyurethanes". *Journal of Thermal Analysis and Calorimetry*, January 2001, vol. 63, no. 1, 317-321.

12. **Hutchinson JM,** "Studying the Glass Transition by DSC and TMDSC", *Journal of Thermal Analysis and Calorimetry*, May 2003, vol. 72, no. 2, 619-629.

13. **Skoog DA, Holler FJ and Nieman TA,** "Principle of Instrumental Analysis", 1998, 5th Ed, Saunder's College Publishing, USA, pp 806.

14. **Bansal NP and Doremus RH,** "Determination of reaction kinetic parameters from variable temperature DSC or DTA", *Journal of Therm al Analysis and Calorimetry* , January 1984, vol. 29, no. 1, 115-119.

15. **Lepock JR,** "Measurement of protein stability and protein denaturation in cells using differential scanning Calorimetry", *Methods*, February 2005, vol. 35, no. 2, 117-125.

16. **Marthi K, Ács M, Pokol G, Tomor K and Eröss-Kiss K,** "DSC studies on the polymorphism and pseudopolymorphism of pharmaceutical substances". *Journal of Thermal Analysis and Calorimetry*, April 1992, vol. 38, no. 4, 1017- 1025.

17. **Zeng JL, Cao Z, Yang DW, Xu F, Sun LX, Zhang L and Zhang XF,** "Phase diagram of palmitic acid-tetradecanol mixtures obtained by DSC experiments". *Journal of T hermal Analysis and Calorimetry*, February 2009, vol. 95, no. 2, 501- 505.

18. **Faroongsarng D and Peck GE,** "Thermal Porosity Analysis of Croscarmellose Sodium and Sodium Starch Glycolate by Differential Scanning Calorimetry", *AAPS PharmSciTech.* 2003, vol. 4, no.4, article 67.

19. **Koski L and Saarela K,** "Oxidation stability of polymeric materials dynamic DSC/DTA method", *Journal of Thermal Analysis and Calorimetry* , October 1982, vol. 25, no. 1, 167-173.

20. **Navard P and Haudin JM,** "The height of DSC phase transition peaks application to liquid crystals", *Journal of Thermal Analysis and Calorimetry*, January 1985, vol. 30, no. 1, 61- 64.

21. **Macedo RO and Nascimento TG,** "Quality control of thiabendazole pre-formulation and tablets by TG and DSC coupled to the photovisual system", *Thermochimica Acta,* September 2002, vol. 392-393, 85-92.

22. **Hutchinson JM,** "Studying the Glass Transition by DSC and TMDSC", *Journal of Thermal Analysis and Calorimetry*, May 2003, vol. 72, no. 2, 619-629.

23. **Pandini S, Pegoretti A and Riccò T,** "DSC analysis of post-yield deformed pbt. Effects of thermal history", *Journal of Thermal Analysis and Calorim etry*, December 2008, vol. 94, no. 3, 825-833.

24. **Abu-Sehly AA, Alamri SN and Joraid AA,** "Measurements of DSC isothermal crystallization kinetics in amorphous selenium bulk samples", *Journal of Alloys and Compounds* , May 2009, vol. 476, no. 1-2, 348-351.
25. **Ruiz CSB, Machado LDB, Vanin JA and Volponi JE,** "Cure Degree Estimation of Photocurable Coatings by DSC and Differential Photocalorimetry". *Journal of Thermal Analysis and Calorimetry*, February 2002, vol. 67, no. 2, 335-341.
26. **Lepock JR,** "Measurement of protein stability and protein denaturation in cells using differential scanning Calorimetry", *Methods*, February 2005, vol. 35, no. 2, 117-125.

Chapter Nine

1. **Jaffé HH and Orchin M,** *Theory and applications of ultraviolet spectroscopy* , 1970, Wiley, New York.
2. **Perkampus HH, Grinter HC and Threfall TL,** *UV-VIS spectroscopy and its applications* , 1992, Berlin, Heidelberg.
3. http://www.chem.ucla.edu/~bacher/UV-vis/uv_vis_tetracyclone.html.html
4. **Ingle JDJ and Crouch SR,** *Spectrochemical Analysis*, 1988, Prentice Hall, New Jersey.
5. **Clark BJ, Frost T and Russell MA,** *UV spectroscopy: techniqu es, instrumentation, data handling*, 1993, Springer, New York.
6. www.files.chem.vt.edu/.../uv-vis/singlebeam.html
7. http://spotlite.nih.gov/assay/index.php/Section17:Spectrophotometry

8. **Kitamura K and Ryo M, "**Determination of salicylic acid in aspirin powder by second derivative ultraviolet spectrometry". *Analytical Chemistry*, January 1983, vol. 55, no. 1, 54-56.
9. **Holden AJ, Littlejohn D and Fell GS,** "Determination of citrate in plasma protein solutions by UV-visible spectrophotometry and ion chromatography". *Journal of Pharmaceutical and Biomedical Analysis*, April 1996, vol. 14, no. 6, 713-719.
10. **Deka J, Paul A and Chattopadhyay A, "**Sensitive Protein Assay with Distinction of Conformations Based on Visible Absorption Changes of Citrate-Stabilized Gold Nanoparticles". *Journal of Physical Chemistry C*, April 2009, vol. 113, no. 17, 6936–6947.
11. **Gill SC and Hippel PHV,** "Calculation of protein extinction coefficients from amino acid sequence data". *Analalytical Biochemistry,* November 1989, vol. 182, no. 2, 319-326.
12. *Kielbassa C, Roza L and Epe B, "Wavelength dependence of oxidative DNA damage induced by UV and visible light"*. Carcinogenesis, *April 1997, vol. 18, no. 4, 811-816*
13. **Storhoff JJ, Lucas AD, Garimella V, Bao YP and Müll UR,** "Homogeneous detection of unamplified genomic DNA sequences based on colorimetric scatter of gold nanoparticle probes". *Nature Biotechnol*ogy, July 2004, vol. 22, no. 7, 883–887.
14. **Martin AE,** "Difference and derivative spectra"**.** *Nature,* 1957, vol.180, 231-233.
15. **Morrison JD,** "Ionization efficiency. III. The detection and interpretation of fine structure*"*. *Journal of Chemical Physics,* 1953, vol. 21, 1767-1772.
16. **Tan B and Soderstrom DN,** "Qualitative aspects of UV-vis spectrophotometry of beta-carotene and lycopene". *Journal of Chemical Education* , March 1989, vol. 66, no. 3, 258-260.

Chapter Ten

1. **Lachman L., Lieberman H., Kanig J.** (eds.), "*The Theory and Practice of Industrial Pharmacy*", Lea & Febiger, PA, 1987.
2. **Emami J.** 'In vitro - In vivo Correlation: From Theory to Applications". *Journal of pharmacy & pharmaceutical sciences*, 2006, vol. 9, no.2, 169-189.
3. **Mohanraj V.J., Chen Y. "Nanoparticles – A Review".** *Tropical Journal of Pharmaceutical Research*, June 2006, vol. 5, no. 1, 561-573
4. **Kostanski J.W., DeLuca P.P.** "A Novel In Vitro Release Technique for Peptide Containing Biodegradable Microspheres". *AAPS PharmSciTech*, 2000, vol. 1, no.1, article 4.
5. **Chorny M., Fishbein I., Danenberg H.D., Golomb G. "**Study of the drug release mechanism from tyrphostin AG-1295-loaded nanospheres by in situ and external sink methods". *Journal of Controlled Release*, October 2002, vol. 83, no. 3, 401-414.
6. **Villiers M.M., Aramwit P., Kwon G.S. "***Nanotechnology in Drug Delivery* **", Springer 2008.**
7. **Martin A.** "*Physical Pharmacy*". 4th ed. Lippincott Williams & Wilkins, Philadelphia, PA, 1993, 324.
8. www.piercenet.com/files/TR0020-Dialysis-overview.pdf
9. **Wissing S.A., Muller R.H.** "Solid lipid nanoparticles as carrier for sunscreens: In vitro release and in vivo skin penetration" *Journal of Controlled Release* , June 2002, vol. 81, no. 3, 225-233.

10. **Jenning V., Schafer-Korting M., Gohla S.** "Vitamin A-loaded solid lipid nanoparticles for topical use: Drug release properties". *Journal of Cont rolled Releas e*, May 2000, vol. 66, no. 2-3, 115-126.
11. **Chattaraj S.C., Swarbrick J., Kanfer I.** "A simple diffusion cell to monitor drug release from semi-solid dosage forms" *International Journal of Pharmaceutics*, June 1995, vol. 120, no. 1, 119-124.
12. **Bonferoni M. C., Rossi S., Ferrari F., Caramella C.** "A Modified Franz Diffusion Cell for Simultaneous Assessment of Drug Release and Washability of Mucoadhesive Gels". *Pharmaceutical Development and Technology*, 1999, vol. 4, no. 1, 45 – 53.
13. **Oza K.P., Frank S.G.** "Drug Release From Emulsions Stabilized by Colloidal Macrocrystalline Cellulose". *Journal of Dispersion Science and Technology,* 1989, vol. 10, no.2, 187 - 210
14. **Chidambaram N., Burgess D.J.** "A Novel in Vitro Release Method for Submicron Sized Dispersed" Systems. *AAPS PharmSci*., 1999, vol. 1, no. 3, article 11.
15. **Bosman I.J., Avegaart S.R., Lawant A.L., Ensing K., De Zeeuw R.A. "**Evaluation of a novel diffusion cell for in vitro transdermal permeation: Effects of injection height, volume and temperature". *Journal of Pharmaceutical and Biomedical,* July 1998, vol. 17, no. 3, 493-499.
16. **Leo E., Cameroni R., Forni F.** "Dynamic dialysis for the drug release evaluation from doxorubicin-gelatin nanoparticle conjugates". *International Journal of Pharmaceutics* , March 1999, vol. 180, no. 1, 23-30.

17. **Saarinen-Savolainen P., Jarvinen T., Taipale H., Urtti A.** "Method for evaluating drug release from liposomes in sink conditions" *International Journa l of Pharmaceutics* , December 1997, vol. 159, no. 1, 27-33.

18. **Lu D., Wen X., Liang J., Gu Z., Zhang X., Fan Y.** "A pH-sensitive nano drug delivery system derived from pullulan/doxorubicin conjugate*". Journal of Biomedical Materials Research*, September 2008, vol. 89B, no. 1**, 177 – 183.**

19. **Mukherjee B., Patra B., Layek B., Mukherjee A.** "Sustained release of acyclovir from nano-liposomes and nano-niosomes: An in vitro study". *International Journal of Nanomedicine*, June 2007, vol. 2, no. 2, 213–225.

20. **Muthu M. S., Singh S.** "Poly (D, L-Lactide) Nanosuspensions of Risperidone for Parenteral Delivery: Formulation and In-Vitro Evaluation'. *Current Drug Delivery,* January 2009, vol. 6, no. 1, 62-68.

21. www.permegear.com/sbs.htm

22. http://www.spectrapor.com/dialysis/Fund.html

23. **Hickey T., Kreutzer D., Burgess D. J., Moussy F.** "Dexamethasone/PLGA microspheres for continuous delivery of an anti-inflammatory drug for implantable medical devices". *Biomaterials*, April 2002, vol. 23, no. 7, 1649-1656.

24. **Jeong Y.I., Song J.G., Kang S.S., Ryu H.H., Lee Y.H., Choi C., Shin B.A., Kim K.K., Ahn K.Y., Jung S.** "Preparation of poly(-lactide-co-glycolide) microspheres encapsulating all-trans retinoic acid". *International Journal of Pharmaceutics,* June 2003, vol. 259, no. 1-2, 79-91.

25. **Volland C., Wolff M., Kissel T.** "The influence of terminal gamma-sterilization on captopril containing poly(-lactide-coglycolide) microspheres". *Journal of Controlled Release* , 1994, vol. 31, no.293-305.
26. **D'Souza S.S., DeLuca P.P.** "Methods to Assess *in Vitr o* Drug Release from Injectable Polymeric Particulate Systems". *Pharmaceutical Research,* March 2006, vol. 23, no. 3, 460-474
27. **D'Souza S.S., DeLuca P.P.** "Development of a Dialysis In Vitro Release Method for Biodegradable Microspheres". *AAPS PharmSciTech*, 2005, vol. 6, no. 2, E323-E328.
28. **Cortesi R., Esposito E., Menegatto E., Gambari R., Nastruzzi C.** "Gelatin microspheres as a new approach for the controlled delivery of synthetic oligonucleotides and PCR-generated DNA fragments". *International Journal of Pharmaceutics,* May 1994, vol. 105, no. 2, 181-186.
29. **Landry F.B., Bazile D.V., Spenlehauer G., Veillard M., Kreuter J.** "Release of the fluorescent marker Prodan® from poly(D,L-lactic acid) nanoparticles coated with albumin or polyvinyl alcohol in model digestive fluids (USP XXII)". *Journal of Controlled Release*, February 1997, vol. 44, no. 2-3, 227-236.
30. **Qiu X., Leporatti S., Donath E., Möhwald H.** "Studies on the Drug Release Properties of Polysaccharide Multilayers Encapsulated Ibuprofen Microparticles*". Langmuir,* July 2001, vol. 17, no. 17, 5375–5380.
31. **Charalampopoulos N., Avgoustakis K., Kontoyannis C.G.** "Differential pulse polarography: A suitable technique for monitoring drug release from polymeric nanoparticle dispersions". *Analytica Chimica Acta*, September 2003, vol. 491, no. 1, 57-62.

Chapter Eleven

1. http://www.drugbank.ca/drugs/DB00634
2. **Mann RL,** "Antimicrobial Drugs". *Remington: The Science and Practice of Pharmacy* ; Ed. Hanson GR, Gennaro AR. Lippincot Williams and Wilkins, USA; 20th Edition, 2005, Chapter 74, 1257-1257.
3. **Chawla R, Kellner JD and Astle WF**, "Acute infectious conjunctivitis in childhood", *Paediatric Child Health*, July-August 2001, vol. 6, no. 6, 329-335.
4. **Roth HW, Leimbeck R, Sonnenschein B, Anger CB and Weber S,** "The effective antibacterial spectrum of sulfacetamide", *Klin Monbl Augenheilkd* , March 1992, vol. 200, no. 3, 182-186.
5. **Lohr JA, Austin RD, Grossman M, Hayden GF, Knowlton GM and Dudley SM,** "Comparison of three topical antimicrobials for acute bacterial conjunctivitis", *The Pediatric Infectious Disease Journal*, September 1988, vol. 7, no. 9, 626-629.
6. **Goscienski PJ, Sexton RR,** "Follow-up studies in neonatal inclusion conjunctivitis", *American Journal of Diseases of Children*, August 1972, vol. 124, no. 2, 180-182.
7. **Czepita D, Kuźna-Grygiel W, Czepita M, Grobelny A,** "Demodex folliculorum and Demodex brevis as a cause of chronic marginal blepharitis", *Ann Acad Med Stetin* , 2007, vol.53, no. 1, 63-67
8. **Morgan RJ and Coston TO,** "Demodex blepharitis", *Southern Medical Journal***,** June 1964 ; 57: 694-699.
9. **Abboud I and Massoud WH,** "Effect of blephamide in blepharitis", *Bulletin of the Ophthalmological Society of Egypt,* 1972, vol. 65, no.69, 539-543.

10. **Mitsui Y, Hanabusa J, Fukushima S, Sakanashi M, Nishiyama S,** "Treatment of trachoma with erythromycin- sulfacetamide ointment (CT-877)", *Antibiotic me dicine & clinical therapy*, October 1958, vol. 5, no.10, 586-592.

11. **Chhibber P R,** "Treatment of trachoma", *Indian Journal of Medical Research* . 1964, vol. 58, 3-8.

12. **Chaidaroon W, Tantayakom T,** "Nocardia keratitis in a human immunodeficiency virus patient", *Japanese journal of ophthalmology*, May-June 2004, vol. 48, no. 3, 272-275.

13. **Sridhar MS, Sharma S, Reddy MK, Mruthyunjay P, Rao GN,** "Clinicomicrobiological review of Nocardia keratitis", *Cornea: The Journal of Cornea and External Disease*, January 1998, vol. 17, no.1, 17-22.

14. **Webber JJ, Edwards LD and McLeod IK,** "Topical treatment of ovine keratoconjunctivitis", *The Australian Veterinary Journal*, March 1988, vol. 65, no. 3, 95-97.

15. **Ostler HB,** "Corneal perforation in nontuberculous (staphylococcal) phlyctenular Keratoconjunctivitis", *American Journal of Ophthalmology,* March 1975, vol. 79, no. 3, 446-448.

16. **Colomina J, Esparza L, Buesa J, Marí J,** "Corneal ulcer caused by Nocardia asteroides after penetrating keratoplasty", *Medicina clínica*, March 1997, vol. 108, no. 11, 424-5.

17. **Jones FR, Christensen GR,** "Pullularia corneal ulcer", *Archives of Ophthalmology* , December 1974, vol. 92, no.6, 529-30.

18. **Osol A.** "The United States dispensatory". 27th Edition, J.B. Lippincott Co., Washington, 1967.

19. **Ahmad I, Ahmad T and Usmanghan K. "**Sulfacetamide". *Profiles of Drug Substances, Excipients and Related Methodology*, 1994, vol. 23, 471-509.

20. **Whelan S T,** "Sodium sulfacetamide for seborrheic dermatitis", *American Medical Association archives of dermatology*, 1955, vol. 71, no. 6, 724.

21. **Yontef R,** "Topical use of sodium sulfacetamide in selected dermatoses*", Journal of the Medical Society of New Jersey*, August 1955, vol. 52, no. 8, 416-418.

22. **Fanburg S J,** "Response of seborrheic dermatitis, dandruff, and pyodermas to a form of sodium sulfacetamide", *Journal of the Medical Society of New Jersey* , February 1956, vol. 53, no. 2, 78-82.

23. **Alvea EP, Parrish AA,** "Sulfacetamide and Sulfadiazine Therapy in Urinary Tract Infections". *Southern Medical Journal*, November 1943, vol. 36, no. 11, 719-723.

24. **Brown G M**, "Inhibition by sulfonamides of the biosynthesis of folic acid". *International Journal of Leprosy and Other Mycobacterial Diseases*, 1967, vol. 35, no. 4, 580-589.

25. Physician's Desk Reference, 50th Edition, May 1996, Medical Economics Company at Montvale, NJ 07645.

26. **Mastrolorenzo A and Supuran CT,** "Antifungal Activity of Ag(I) and Zn(II) Complexes of Sulfacetamide Derivatives". *Metal Based Drugs*, 2000, vol. 7, no. 1, 49–54.

27. **Lacy CF, Armstrong LL, Goldman MP,** "Drug information handbook: a comprehensive resource for all clinicians and healthcare professionals", Laxi-Comp inc, 12th Edition, Hudson, Ohio, page 1354.

28. http://www.solimide.eu/en/pharmapolymers/eudragit/quality/spezifikationen_neu.Par.0001.TRow.0010.TCell.0002.File.tmp/7.1.07_INFO7.7e_RL_RSPO_RL_RS100_200409.pdf

29. **Khan MZI, Prebeg Z, Kurjakovic N,** "A pH-dependent colon targeted oral drug delivery system using methacrylic acid copolymers. I. Manipulation of drug release using Eudragit® L100-55 and Eudragit® S100 combinations", *Journal of Controlled Release* , 1999, vol. 58, no. 2, 215-222.

30. **El-Malah Y and Nazzal S,** "Novel use of Eudragit® NE 30D/Eudragit® L 30D-55 blends as functional coating materials in time-delayed drug release applications", *International Journal of Pharmaceutics*, June 2008, vol. 357, no. 1-2, 219-227.

31. **Bucolo C, Maltese A, Puglisi G and Pignatello R,** "Enhanced ocular anti-inflammatory activity of ibuprofen carried by an Eudragit RS100 nanoparticle suspension", *Ophthalmic Reserch*, September- October 2002, vol. 34 no. 5, 319-23.

32. **Castelli F, Messina C, Sarpietro MG, Pignatello R and Puglisi G,** "Flurbiprofen Release From Eudragit RS and RL Aqueous Nanosuspensions: a Kinetic Study by DSC and Dialysis Experiments", *AAPS PharmSciTech*, 2002, vol. 3, no. 2, 9.

33. **Pignatello R, Bucolo C, Spedalieri G, Maltese A and Puglisi G,** "Flurbiprofen-loaded acrylate polymer nanosuspensions for ophthalmic application". *Biomaterials*, 2002, vol. 23, no. 15, 3247-3255.

34. **Adibkia K, Siahi Shadbad MR, Nokhodchi A, Javadzedeh A, Barzegar-Jalali M, Barar J, Mohammadi G and Omidi Y,** "Piroxicam nanoparticles for ocular delivery:physicochemical characterization and implementation in endotoxin-induced uveitis", *Journal of Drug Targeting*, July 2007, vol. 15, no. 6, 407-416.
35. **Pignatello R, Ricupero N, Bucolo C, Maugeri F, Maltese A and Puglisi G,** "Preparation and Characterization of Eudragit Retard Nanosuspensions for the Ocular Delivery of Cloricromene", *AAPS PharmSciTech*, March 2006, vol. 7, no. 1, 27.
36. **Das S, Sureshb PK and Desmukh R, "**Design of Eudragit® RL 100 nanoparticles by nanoprecipitation method for for ocular drug delivery", *Nanomedicine: Nanotechnology, Biology and Medicine*, Article in press, October 2009.
37. **Pignatello R, Bucolo C, Puglisi G,** "Ocular tolerability of Eudragit RS100® and RL100® nanosuspensions as carriers for ophthalmic controlled drug delivery", *Journal of Pharmaceutical Science*, September 2002, vol. 91, no. 12, 2636-2641
38. www2.basf.us/performancechemical/pdfs/Pluronic_F108.pdf
39. **Csaba N, Sanchez A, Alonso MJ,** "PLGA: Poloxamer and PLGA: Poloxamine blend nanostructures as carriers for nasal gene delivery", *Journal of Controlled Release*, June 2006, vol. 113, no. 2, 164-172.
40. **Mandal BB and Kundu SC,** "Self-assembled silk sericin/poloxamer nanoparticles as nanocarriers of hydrophobic and hydrophilic drugs for targeted delivery", *Nanotechnology* August 2009, vol.**20**, no 35, 355101.

41. **Csaba N, Caamaño P, Sánchez A, Domínguez F and Alonso MJ,** "PLGA:Poloxamer and PLGA:Poloxamine Blend Nanoparticles: New Carriers for Gene Delivery", *Biomacromolecules*, January 2005, vol. 6, no. 1, 271–278.

42. **Cappel MJ and Kreuter J,** "Effect of nonionic surfactants on transdermal drug delivery: II. Poloxamer and poloxamine surfactants". *International Journal of Pharmaceutics* , March 1991, vol. 69, no.2, 155-167.

43. **Gilbert P, Jones MV, Allison DG, Heys S, Maira T and Wood P,** "The use of poloxamer hydrogels for the assessment of biofilm susceptibility towards biocide treatments", *Journal of Applied Microbiolgy*, December 1998, vol. 85, no. 6, 985-990.

44. **Clutterbuck AL, Cochrane CA, Dolman J and Percival SL,** "Evaluating antibiotics for use in medicine using a poloxamer biofilm model", *Annals of Clinical Microbiology and Antimicrobials,* February 2007, vol. 6, no. 2.

45. http://www.sciencelab.com/xMSDS-Poloxamer_338_N_F_-9926615

46. www.mtholyoke.edu/.../acetone.structure.JPG

47. **Weiner ML and Kotkoskie LA**, *Excipient Toxicity and Safety* . Informa Healthcare, 2000, pp 32.

48. http://www.cosmeticsdatabase.com/ingredient.php?ingred06=700081

49. www.sciencelab.com/xMSDS-Acetone-9927062

50. **Fessi H, Puisieux F, Devissaguet JP, Ammoury N and Benita S.** "Nanocapsule formation by interfacial polymer deposition following solvent displacement", *International Journal of Pharmaceutics*, 1989, vol. 55:R1-R4.

51. **Bilati U, Allémann E and Doelker E.** "Development of a nanoprecipitation method intended for the entrapment of hydrophilic drugs into nanoparticles", *Europian Journal of Pharmaceutical Science*, January 2005, vol. 24, no. 1, 67-75.

52. **Galindo-Rodriguez S, Allémann E, Fessi H and Doelker E,** "Physicochemical Parameters Associated with Nanoparticle Formation in the Salting-Out, Emulsification-Diffusion, and Nanoprecipitation Methods", *Pharmceutical Research*, 2004, vol. 21, no. 8 , 1428-1439.

53. **Peltonen L, Aitta J, Hyvonen S, Karjalainen M and Hirvonen J,** "Improved Entrapment Efficiency of Hydrophilic Drug Substance During Nanoprecipitation of Poly(l)lactide Nanoparticles", *AAPS PharmSciTech*, March 2004, vol. 5, no. 1, article 16 .

54. **Hornig S, Heinze T, Becer CR and Schubert US,** "Synthetic polymeric nanoparticles by nanoprecipitation**",** *Journal of Materials Chemistry,* 2009, vol. 19**,** 3838 – 3840.

55. **Govender T, Stolnik S, Garnett MC, Illum L and Davis SS,** "PLGA nanoparticles prepared by nanoprecipitation: drug loading and release studies of a water soluble drug", *Journal of Controlled Release,* February 1999, vol. 57, no. 2, 171-185.

56. **Ribeiro HS, Chu B, Ichikawa S and Nakajima M,** "Preparation of nanodispersions containing b-carotene by solvent displacement method", *Food Hydrocolloids*, January 2008, vol. 22, no. 1, 12-17.

57. **Hadjiioannou TP, Christian GD and Koupparis MA,** "*Quantitative Calcula tions in Pharmaceutical Practice and Research* "', New York, NY: VCH Publishers Inc, 1993, 345-348.

58. **Wagner JG,** "Interpretation of percent dissolved-time plots derived from in vitro testing of conventional tablets and capsules", *Journal of Pharmaceutical Science* , October 1969, vol. 58, no.10, 1253-1257.

59. **Bourne DW,** "Pharmacokinetics". In: Banker GS, Rhodes CT, eds.", *Modern Pharmaceutics.* 4th ed. New York, NY: Marcel Dekker Inc; 2002, 67-92.

60. **Gibaldi M and Feldman S,** "Establishment of sink conditions in dissolution rate determinations: theoretical considerations and application to nondisintegrating dosage forms", *Journal of Pharmaceutical Science*, October 1967, vol. 56, no. 10, 1238-1242.

61. **Higuchi T,** "Mechanism of sustained action medication. Theoretical analysis of rate of release of solid drugs dispersed in solid matrices", *Journal of Pharmaceutical Science* , December 1963, vol. 52, 1145-1149.

62. **Higuchi T,** "Rate of release of medicaments from ointment bases containing drugs in suspension", *Journal of Pharmaceutical Science*, October 1961, vol. 50, 874-875.

63. **Cobby J, Mayersohn M and Walker GC,** "Influence of shape factors on kinetics of drug release from matrix tablets. II. Experimental", *Journal of Pharmaceutical Science* , May 1974, vol. 63, no. 5, 732-737.

64. **Hixson AW and Crowell JH,** "Dependence of reaction velocity upon surface and agitation: I-theoretical consideration", *Industrial & Engineerin g Chemistry Research* , 1931, vol. 23, 923-931.

65. **Korsmeyer RW, Gurny R, Doelker E, Buri P and Peppas NA,** "Mechanisms of solute release from porous hydrophilic polymers", *International Journal of Pharmaceutics* , May 1983, vol. 15, 25-35.

66. **Peppas NA,** "Analysis of Fickian and non-Fickian drug release from polymers", *Pharmaceutica Acta Helvetiae*, 1985, vol. 60, 110-111.
67. **Harland RS, Gazzaniga A, Sangalli ME, Colombo P and Peppas NA,** "Drug/polymer matrix swelling and dissolution", *Pharmaceutical Reseaerch* , August 1988, vol. 5, no. 8, 488-494.
68. **Siepmann J and Peppas NA,** "Modeling of drug release from delivery systems based on hydroxypropyl methylcellulose (HPMC)", *Advanced Drug Deliver y Reviews*, January 2001, vol. 48, no. 2-3, 139-157.

Chapter Twelve

1. **Fessi H., Puisieux F., Devissaguet J.P., Ammoury N., Benita S.** "Nanocapsule formation by interfacial polymer deposition following solvent displacement". *International Journal of Pharmaceutics*, October 1989, vol. 55, no. 1, r1-r4.
2. **Delair T.** "Colloidal particles: elaboration from preformed polymers". In A. Elaissari (ed.), Colloidal Biomolecules, Biomaterials and Biomedical Applications, Marcel Dekker, New York, 2004, pp. 329–347.
3. **Marangoni C.** "U¨ ber die Ausbreitung der Tropfen einer Flu¨ssigkeit auf der Oberfla¨che einer anderen". *Annalen der Physik und Chemie, 1871*, vol. 219, 337–354.
4. **Mecklenburg W,** "The relation between the Tyndall effect and the size of the particles of colloidal solutions". *Kolloid-Zeitschrift*, 1915, vol. 16, 97-103.
5. **Zimmer A., Kreuter J.** "Microspheres and nanoparticles used in ocular delivery systems". *Advanced Drug Delivery Reviews*, August 1995, vol. 16, no. 1, 61-73.

6. **Kelly J.W.** (PPI05) Parenteral Products- Industrial 05, USP 29-NF 24, Page 2729.

7. **Das S., Sureshb P.K., Desmukhc R.** "Design of Eudragit® RL 100 nanoparticles by nanoprecipitation method for ocular drug delivery". *Nanomedicine: Nanotechnology, Biology and Medicine ,* October 2009. (in press)

8. **Pignatello R, Bucolo C, Spedalieri G, Maltese A and Puglisi G,** "Flurbiprofen-loaded acrylate polymer nanosuspensions for ophthalmic application". *Biomaterials*, 2002, vol. 23, no. 15, 3247-3255

9. **Marchal-Heussler L, Maincent P, Hoffman M, Spittler J and Couvreur P.** "Antiglaucomatous activity of betaxolol chlorhydrate sorbed onto different isobutylcyanoacrylate nanoparticle preparations". *International journal of pharmaceutics* , January 1990, vol. 58, n. 2, 115-122

10. **Cairns D.** Essentials of pharmaceutical chemistry. Ed 2, Pharmaceutical Press, 2003, page 75.

11. **Ter VR, Fromell K and Caldwell KD,** "Shifts in polystyrene particle surface charge upon adsorption of the Pluronic F108 surfactant". *Journal of Colloid and Interface Science*, August 2005, vol. 288, no. 1, 124-128.

12. **Xu X, Fu Y, Hu H, Duan Y and Zhang Z,** "Quantitative determination of insulin entrapment efficiency in triblock copolymeric nanoparticles by high-performance liquid chromatography", *Journal of Pharmaceutical and Biomedical Analysis* , 2006, vol. 41, no. 1, 266-273.

13. **Peltonen L, Aitta J, Hyvönen S, Karjalainen M and Hirvonen J,** "Improved Entrapment Efficiency of Hydrophilic Drug Substance During Nanoprecipitation of Poly(l)lactide Nanoparticles". *AAPS PharmSciTech*. 2004, vol. 5, no. 1 article 16.
14. **Govender T, Stolnik S, Garnett MC, Illum L and Davis SS,** "PLGA nanoparticles prepared by nanoprecipitation: Drug loading and release studies of a water soluble drug", *Journal of Controlled Release*, 1999, vol. 57, no. 2, 171-185.
15. **Gupta VK, Beckert TE, Deusch NJ and Hariharan M,** "Price JC. Investigation of Potential Ionic Interactions between Anionic and Cationic Polymethacrylates of Multiple Coatings of Novel Colonic Delivery System". *Drug Development and Industrial Pharmacy*, March 2002, vol. 28, no. 2, 207-215.
16. **Passerini N, Albertini B, González-Rodríguez ML, Cavallari C and Rodriguez L,** "Preparation and characterisation of ibuprofen–poloxamer 188 granules obtained by melt granulation". *European Journal of Pharmaceutical Science* , February 2002, vol. 15, no. 1, 71-78.
17. **Pignatello R, Spadaro D, Vandelli MA, Forni F and Puglisi G,** "Characterization of the Mechanism of Interaction in Ibuprofen-Eudragit RL100® Coevaporates". *Drug Development & Industrial Pharmacy*, March 2004, vol. 30, no. 3, 277-288.
18. **Heun GN, Lambov N and Gröning R,** "Experimental and molecular modeling studies on interactions between drugs and Eudragit® RL/RS resins in aqueous environment". *Pharmaceutica Acta Helvetiae*, June 1998, vol. 73, no. 1, 57-62.

19. **Eerikainen H., Kauppinen EI and Kansikas J,** "Polymeric Drug Nanoparticles Prepared by an Aerosol Flow Reactor Method"**.** *Pharmaceutical Research*, January 2004, vol. 21, no. 1, 136-143.
20. **Nagendrappa G,** "An elegant example of chemoselective reaction". *Resonance*, October 2008, vol. 13, no. 10, 929-940.
21. **Hans ML and Lowman AM,** "Biodegradable nanoparticles for drug delivery and targeting". *Current Opinion in Solid State and Materials Science*, August 2002, vol. 6, no. 4, 319-327.
22. **Pignatello R, Consoli P and Puglisi G,** "In vitro release kinetics of Tolmetin from tabletted Eudragit microparticles". *Journal of Microencapsulation* , May-June 2000, vol. 17, no. 3, 373-83.